ORIGINAL ARTICLE

Aberrant expression and activity of histone deacetylases in sporadic idiopathic pulmonary fibrosis

Martina Korfei,[1,2] Sylwia Skwarna,[1,2] Ingrid Henneke,[1,2] BreAnne MacKenzie,[1,2] Oleksiy Klymenko,[1,2] Shigeki Saito,[3] Clemens Ruppert,[1,2,4] Daniel von der Beck,[1,2] Poornima Mahavadi,[1,2] Walter Klepetko,[5,11] Saverio Bellusci,[1,2,4] Bruno Crestani,[6,11] Soni Savai Pullamsetti,[1,2,7] Ludger Fink,[2,4,8] Werner Seeger,[1,2,4] Oliver Holger Krämer,[9] Andreas Guenther[1,2,4,10,11]

▶ Additional material is published online only. To view please visit the journal online (http://dx.doi.org/10.1136/thoraxjnl-2014-206411).

For numbered affiliations see end of article.

Correspondence to
Professor Andreas Guenther, Department of Internal Medicine II, Justus-Liebig-University Giessen, Klinikstrasse 36, Giessen D-35392, Germany; Andreas.Guenther@innere.med.uni-giessen.de

Received 6 October 2014
Revised 10 August 2015
Accepted 15 August 2015
Published Online First
10 September 2015

ABSTRACT

Background Activation and differentiation of fibroblasts into contractile protein-expressing myofibroblasts and their acquired apoptosis-resistant phenotype are critical factors towards the development of idiopathic pulmonary fibrosis (IPF), a fatal disease characterised by distorted pulmonary structure and excessive extracellular matrix (ECM) deposition. The molecular mechanisms underlying these processes in IPF remain incompletely understood. We investigated the possible implication of aberrant overexpression and activity of histone deacetylases (HDACs) in IPF.

Methods We analysed lung tissues from patients with sporadic IPF (n=26) and non-diseased control lungs (n=16) for expression of class I and II HDACs. Primary IPF fibroblasts were treated with HDAC inhibitors (HDACi) LBH589 or valproic acid (VPA).

Results Compared to control lungs, protein levels of class I (HDAC1, HDAC2, HDAC3, HDAC8) and class II HDACs (HDAC4, HDAC 5, HDAC 7, HDAC 9) were significantly elevated in IPF lungs. Using immunohistochemistry, strong induction of nearly all HDAC enzymes was observed in myofibroblasts of fibroblast foci and in abnormal bronchiolar basal cells at sites of aberrant re-epithelialisation in IPF lungs, but not in controls. Treatment of primary IPF fibroblasts with the pan-HDACi LBH589 resulted in significantly reduced expression of genes associated with ECM synthesis, proliferation and cell survival, as well as in suppression of HDAC7, and was paralleled by induction of endoplasmic reticulum stress and apoptosis. The profibrotic and apoptosis-resistant phenotype of IPF fibroblasts was also partly attenuated by the class I HDACi VPA.

Conclusions Aberrant overexpression of HDACs in basal cells of IPF lungs may contribute to the bronchiolisation process in this disease. Similarly, generation and apoptosis resistance of IPF fibroblasts are mediated by enhanced activity of HDAC enzymes. Therefore, pan-HDAC inhibition by LBH589 may present a novel therapeutic option for patients with IPF.

Key messages

What is the key question?

- Although altered activity and expression of histone deacetylases (HDACs) have been reported in various pathological conditions, such as cancer or COPD, no data are currently available about the regional expression patterns of HDAC enzymes in idiopathic pulmonary fibrosis (IPF), a fatal lung disease for which no cure exists to date.

What is the bottom line?

- This study shows for the first time that both myofibroblasts of fibroblast foci and bronchiolar basal cells of IPF lungs reveal 'cancer-like' overexpression of class I and class II HDAC enzymes, which may explain their progressive expansion as well as apoptosis resistance in this disease.

Why read on?

- This study demonstrates for the first time that the pan-HDAC inhibitor LBH589/panobinostat, which is a proven antitumour agent, is capable of significantly downregulating collagen I biosynthesis and antiapoptotic genes in IPF fibroblast populations, and may thus potentially stop fibrotic remodelling in IPF.

To cite: Korfei M, Skwarna S, Henneke I, *et al*. *Thorax* 2015;**70**:1022–1032.

INTRODUCTION

Idiopathic pulmonary fibrosis (IPF) is a fatal lung disease characterised by destruction of alveolar architecture, abnormal fibroblast proliferation and excessive collagen deposition. Myofibroblasts are the primary collagen-producing cells in IPF, and their accumulation within pathological lesions called fibroblast foci (FF) is a key feature of IPF lungs.[1] Moreover, it has been suggested that IPF fibroblasts and myofibroblasts possess a cancer-like, 'malignant' phenotype,[2] with enhanced resistance to apoptosis due to increased expression of antiapoptotic and survival-related proteins, such as phosphatidylinositol-3-kinase-γ[3] or survivin.[4] However, the precise mechanisms of such apoptosis resistance remain unclear.

Structural changes of the chromatin, including alterations in the histone acetylation/deacetylation balance, have been suggested to underlie altered gene expression patterns in various pathological conditions, including cancer,[5] cardiac hypertrophy[6] and COPD.[7] Histone deacetylases (HDACs) are enzymes that remove acetyl moieties from ε-*N*-acetylated lysine residues in histones, resulting in chromatin condensation and epigenetic repression of gene transcription. HDACs also catalyse deacetylation of many non-histone proteins, such as the tumour suppressor p53, resulting in inhibition of its (pro-apoptotic) transcriptional activity.[8 9] In line with their profound antiapoptotic activity, HDACs are upregulated in many types of cancer.[5 8 9] In contrast, patients with COPD undergo a progressive reduction in total HDAC activity in lung tissue as a result of oxidative stress,[7] which is associated with proteasomal degradation of many HDACs.[10] HDACs are classified into four groups: class I (HDAC1, HDAC2, HDAC3 and HDAC8) are located primarily in the nuclei; class II (HDAC4, HDAC5, HDAC6, HDAC7, HDAC9 and HDAC10) are located in the cytoplasm but can shuttle to the nucleus; class III are NAD^+-dependent enzymes and known as the sirtuins; class IV is represented by HDAC11 only.[9] Class I, II and IV HDACs are Zn^{2+}-dependent enzymes, and can thus be efficiently inhibited by chelating agents such as the hydroxamic acids vorinostat (SAHA) and panobinostat (LBH589).[9 11 12] Importantly, these HDAC inhibitors (HDACi) have been reported as successful anticancer agents as they induce cell cycle arrest and apoptosis in cancer cells by increasing the acetylation status of chromatin and other non-histone proteins.[9 11 12]

Despite some reports about the involvement of altered HDAC activity in fibrotic lung fibroblasts and IPF,[13–15] regulation and regional expression of HDACs have not been characterised in IPF. This study provides a comprehensive description of class I and class II HDAC expression patterns in the IPF lung. In addition, we can demonstrate that the profibrotic and 'malignant' phenotype of IPF fibroblasts can be greatly corrected by incubation with the pan-HDACi LBH589.

MATERIALS AND METHODS

Human lung tissue

Lung tissue samples were obtained from 26 patients with sporadic IPF (mean age±SD: 55.85±8.75 years; 5 females, 21 males), and 16 non-diseased control subjects (organ donors; mean age±SD: 48.92±15.84 years; 7 females, 8 males, 1 unknown). Explanted lungs were obtained from the Department of Thoracic Surgery, Vienna (W. Klepetko). All IPF diagnoses were made according to the American Thoracic Society/European Respiratory Society consensus criteria.[1] Four out of 26 patients with IPF were former smokers, 14 were never-smokers and from 8 patients the smoking status is unknown. With regard to control subjects, 3 out of 16 were former smokers, 7 were never-smokers and from 6 controls the smoking status is unknown.

Isolation of primary human lung fibroblasts

Primary human lung fibroblasts were isolated from explanted IPF (n=8) and control lungs (n=6) using an outgrowth technique as published.[3] Experiments were carried out with IPF/control fibroblasts between passages 3 and 4.

Cell culture experiments

At 95–99% confluency, IPF fibroblasts (n=6) were incubated for 30 h with the HDACi LBH589 (panobinostat, 85nM, Selleckchem) and valproic acid (VPA, 1.5 mM, Santa Cruz), and as control experiment with the respective solvents (vehicle control) in the concentration 0.1% ethanol and 0.03% dimethyl sulfoxide. The dosages of HDACi were chosen according to published[12 16] and own preliminary studies.

Methodology

Full details for quantitative immunoblotting, immunohistochemistry (IHC), semiquantitative RT-PCR and qRT-PCR (including primers) and statistics are available in the online supplementary material.

RESULTS

Upregulation of class I and class II HDACs in FF and abnormal bronchiolar epithelium in IPF lungs

Comparative immunoblot analysis of subpleural lung tissues from 26 patients with IPF versus 16 non-diseased control lungs revealed a significant upregulation of the class I HDACs HDAC1, HDAC2, HDAC3 and HDAC8 (see online supplementary figures S1A–D), as well as of the class IIa HDACs HDAC4, HDAC5, HDAC7 and HDAC9 (see online supplementary figures S2A–E), which comprises several isoforms (see online supplementary figures S2D, E). Protein expression of the class IIb HDAC10 was insignificantly upregulated (see online supplementary figure S2F). Though class IIb HDAC6 protein expression was not detectable by western blot, qRT-PCR indicated slightly increased *HDAC6* mRNA levels in subpleural IPF lung tissues compared with controls (see online supplementary figure S3).

Next, we employed IHC in order to identify the cellular distribution of these enzymes. A nuclear immunostaining for HDAC1 was observed in myofibroblasts of FF, which were identified by staining for alpha smooth muscle actin (α-SMA) (figure 1A, dashed arrows). Prominent nuclear expression of HDAC1 was also observed in overlying, hyperplastic bronchiolar basal cells (figure 1A, indicated by hashmark and cytoplasmic cytokeratin-5/KRT5 staining). Likewise, strong nuclear induction in FF and the overlying bronchiolar epithelium was encountered for the other class I members HDAC2/HDAC3 (see figure 1B and supplementary figures S4A/C). In addition, basal cell sheets of abnormal hyperplastic bronchioles in areas of bronchiolisation (indicated by KRT5 and nuclear p63 staining) showed strong nuclear expression of HDAC1 (figure 1C) and HDAC2/ HDAC3 (see online supplementary figure S5). HDAC2 and HDAC3 also revealed robust nuclear overexpression in ciliated bronchial cells in abnormal bronchiolar structures of IPF lungs (see online supplementary figures S4B and S6). Of note, neither HDAC1, HDAC2, nor HDAC3 showed a significant staining in type II alveolar epithelial cells (AECII) of IPF lungs (figure 1C, D, AECII indicated by arrows and proSP-C staining). In control lungs, HDAC1, HDAC2 and HDAC 3 expression was faint or nearly absent in AECII (figure 1E, indicated by arrows), and only weak expression of HDAC1, HDAC2 and HDAC3 could be encountered in basal and ciliated bronchial cells of normal bronchioles (see figure 1F and online supplementary figure S7).

Interestingly, robust cytoplasmic expression of HDAC3, but not of HDAC2, was detected in non-ciliated Clara cells of IPF and control lungs (see online supplementary figures S6 and S7B). The same observation was made in IHC for class I member HDAC8, which was expressed in general by bronchiolar epithelium in IPF and control lungs including basal, non-ciliated and ciliated bronchial cells as well as by vascular smooth muscle cells (see online supplementary figures S8B, C). Moreover, cytoplasmic overexpression of HDAC8 was observed

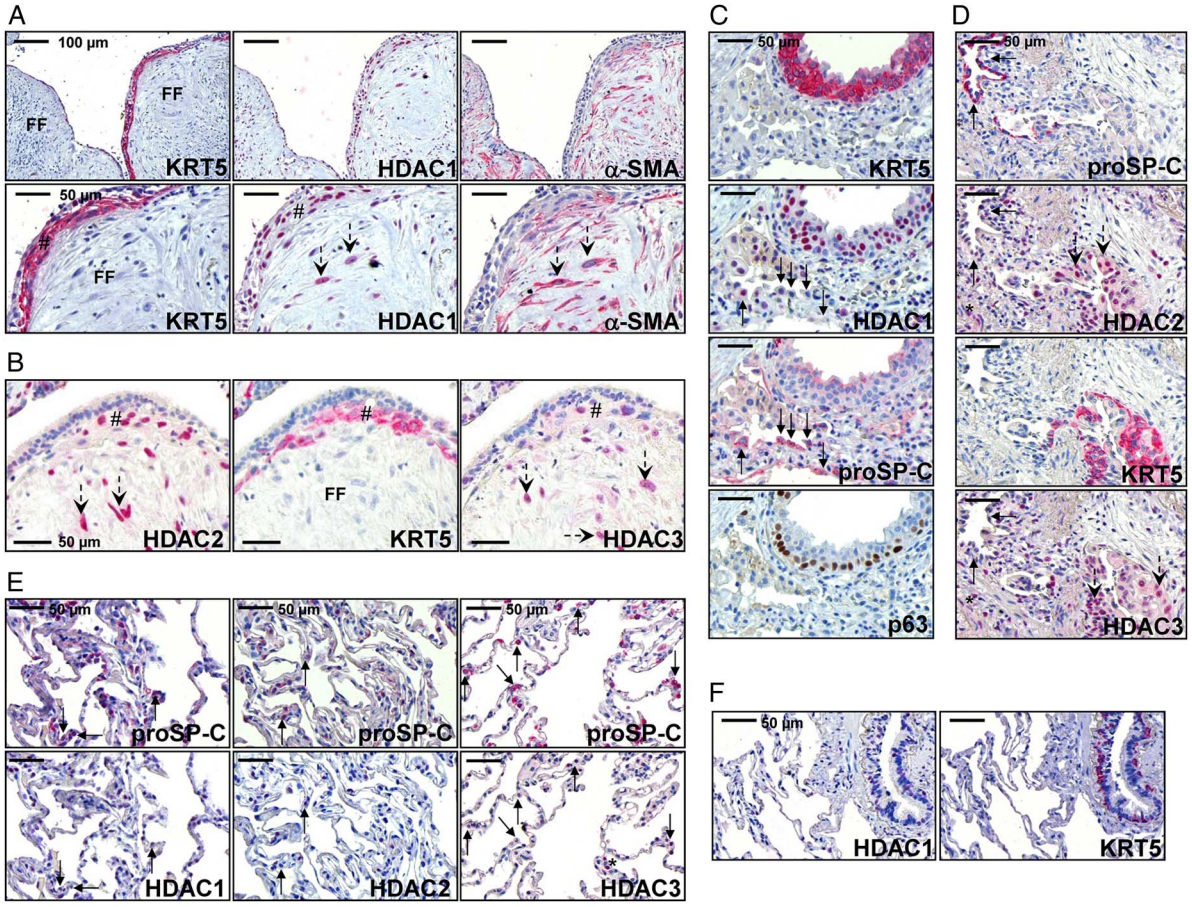

Figure 1 Induction of class I histone deacetylases in fibroblast foci (FF) and abnormal bronchiolar epithelium of idiopathic pulmonary fibrosis (IPF) lungs. (A) Representative immunohistochemistry for cytokeratin-5 (KRT5), histone deacetylase 1 (HDAC1) and alpha-smooth muscle actin (α-SMA) in serial sections of IPF lung tissue. Strong nuclear staining for HDAC1 was predominantly observed in myofibroblasts of FF (indicated by dashed arrows and α-SMA-staining of a serial section) as well as in overlying hyperplastic bronchiolar basal cells (indicated by hashmark and KRT5 staining) of IPF lungs. (B) Representative immunohistochemistry for HDAC2, HDAC3 and KRT5 in serial sections of IPF lung tissue. In IPF, FF as well as overlying abnormal bronchiolar basal cells (indicated by hashmark and KRT5 expression) revealed strong nuclear induction of HDAC2 and HDAC3. (C) Representative immunohistochemistry for KRT5, HDAC1, prosurfactant protein C (proSP-C) and p63 in serial sections of IPF lung tissue. In IPF, bronchiolar basal cell sheets of hyperplastic bronchioles (positive for KRT5 and p63) indicated robust nuclear induction of HDAC1, whereas type II alveolar epithelial cells (AECII, indicated by arrows) indicated no expression of HDAC1. Only in very rare cases an expression of HDAC1 was observed in the IPF-AECII. AECII are identified by proSP-C immunostaining. (D) Representative immunohistochemistry for proSP-C, HDAC2, HDAC3 and KRT5 in serial sections of IPF lung tissue. IPF-AECII (indicated by arrows and proSP-C staining) did neither express HDAC2 nor HDAC3, which were found in the nucleus of bronchiolar basal cells in abnormal epithelia (positive for KRT5) as well as in some interstitial inflammatory cells (indicated by asterisk) in the very same IPF lung section. (E) Representative immunohistochemistry for proSP-C, HDAC1, HDAC2 and HDAC3 in serial sections of control lung tissue. No or only faint staining for HDAC1, HDAC2 and HDAC3 was observed in AECII of normal lungs; interstitial inflammatory cells (indicated by asterisk) of control lungs showed nuclear HDAC3 expression. (F) Representative immunohistochemistry for HDAC1 and KRT5 in serial sections of control lung tissue. Basal cells of normal bronchioles in control lungs (indicated by KRT5 staining) revealed no notable HDAC1 expression.

in myofibroblasts of FF (see online supplementary figure S8A), which is in line with previous reports describing that cytoplasmic HDAC8 associates with α-SMA and acts as an essential regulator of smooth muscle cell contractility.[17]

Concerning the cellular distribution of class II HDACs, HDAC4 was abundantly expressed by myofibroblasts of FF (figure 2A, dashed arrows) and in the overlying hyperplastic bronchiolar epithelium (marked by KRT5 staining, figure 2A), as well as in basal cell sheets of abnormal bronchiolar structures in IPF lungs (see online supplementary figure S9A), thereby indicating predominantly cytoplasmic localisation. A similar expression pattern was observed for class IIb HDAC10 (figure 2A, dashed arrows). Furthermore, HDAC4 was robustly expressed in the mature smooth muscle in areas of established fibrosis (indicated by α-SMA staining in figure 2B and online supplementary figure S10B), and co-localised with nuclear HDAC2 and survivin expression (figure 2B). Interestingly, ciliated bronchial cells of IPF lungs indicated strong nuclear expression of HDAC4 (indicated by arrowheads and FOXJ1 staining, figure 2C and supplementary figures S9B and S10C), which appeared to be weak in ciliated epithelium of normal bronchioles in control lungs (figure 2D). Notably, IPF-AECII did not indicate a significant expression of HDAC4 (figure 2C, arrows), whereas robust nuclear expression of HDAC4 was detected in the AECII of control lungs (figure 2D, arrows, and online supplementary figure S11A).

With regard to other class IIa HDAC members, HDAC7 immunostaining was strikingly pronounced in FF and bronchiolar epithelial cells of IPF lungs (figure 2E, F), but was faint in both IPF and donor AECIIs (see figure 2F, arrows, and online supplementary figure S11B). As expected, the expression of the other class IIa HDACs HDAC5 and HDAC9 isoform histone deacetylase-related protein (HDRP) was similarly distributed in IPF and control lungs (see online supplementary figures S12–S18).

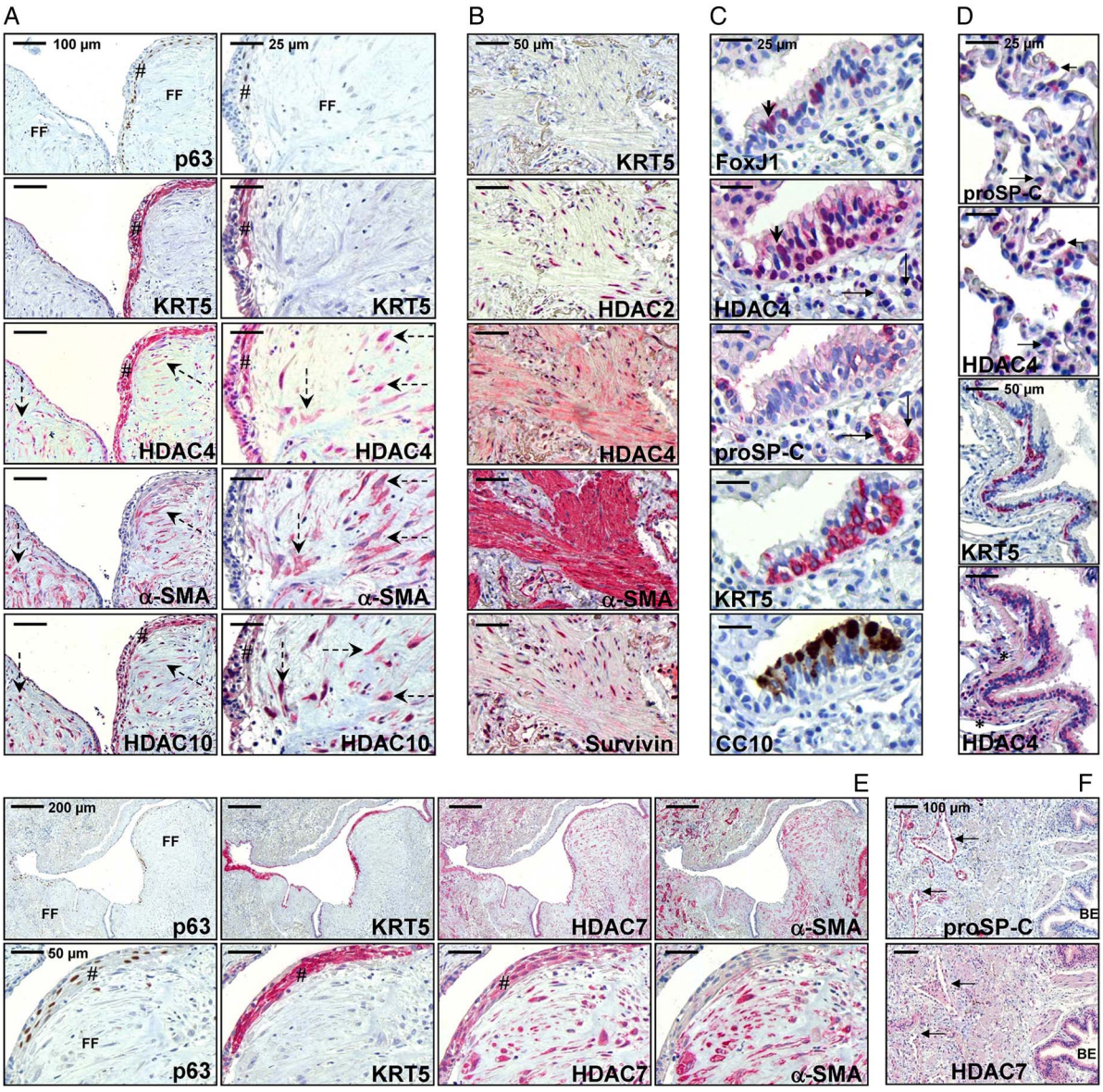

Figure 2 Overexpression of class II histone deacetylases (HDACs) in fibroblast foci and abnormal bronchiolar epithelium of idiopathic pulmonary fibrosis (IPF) lungs. (A) Representative immunohistochemistry for p63, KRT5, HDAC4, alpha smooth muscle actin (α-SMA) and HDAC10 in serial sections of IPF lung tissue. In IPF, immunostaining for HDAC4 (cytoplasmic) and HDAC10 (nuclear and cytoplasmic) was observed in myofibroblasts of fibroblast foci (FF) (indicated by dashed arrows and α-SMA staining of serial sections) as well as in overlying hyperplastic bronchiolar basal cells (indicated by hashmarks, positive for p63 and KRT5). (B) Representative immunohistochemistry for KRT5, HDAC2, HDAC4, α-SMA and survivin in serial sections of IPF lung tissue. Established smooth muscle (indicated by α-SMA staining) in areas of dense 'older' fibrosis in IPF revealed cytoplasmic expression of HDAC4, with concomitant nuclear expression of HDAC2 and survivin. (C) Representative immunohistochemistry for KRT5, proSP-C, HDAC4, Forkhead box protein J1 (FOXJ1) and Clara cell protein 10 (CC10) in serial sections of IPF lung tissue. In IPF, strong nuclear staining for HDAC4 is observed in ciliated bronchial cells (indicated by arrowheads and FOXJ1 staining) and basal cells (positive for KRT5) of abnormal hyperplastic bronchioles. Type II alveolar epithelial cells (AECII, indicated by arrows and proSP-C staining) and Clara cells (positive for CC10) in IPF lungs did not express HDAC4. (D) Representative immunohistochemistry for proSP-C, HDAC4 and KRT5 in serial sections of control lung tissue. In the normal lung, HDAC4 was found to be expressed in the nucleus of AECII (indicated by arrows and proSP-C-staining), and basal cytoplasmic expression of HDAC4 was observed in bronchioles of control lungs. (E) Representative immunohistochemistry for p63, KRT5, HDAC7 and α-SMA in serial sections of IPF lung tissue. In IPF, the antibody for HDAC7 revealed strong cytoplasmic staining of myofibroblasts in FF as well as in overlying hyperplastic bronchiolar basal cells (indicated by hashmarks, positive for p63 and KRT5). (F) Representative immunohistochemistry for proSP-C and HDAC7 in serial sections of IPF lung tissue. AECII in areas of dense fibrotic tissue (indicated by arrows and proSP-C-staining) in IPF showed no or only faint immunostaining for HDAC7, whereas bronchial epithelium (BE) indicated robust cytoplasmic HDAC7 expression.

Next, cellular localisation of class IIb member HDAC6 was characterised in IPF and control lungs. HDAC6, which has been reported to function in aggresome-autophagy pathway,[18] was the only HDAC with pronounced expression in AECII of IPF lungs. Moreover, HDAC6 cytoplasmic expression was upregulated in IPF-AECII compared with control-AECIIs (see online supplementary figures S19A,C, indicated by arrows). In addition, HDAC6 expression was increased in proSP-C-negative, AECII-like (or AECI-like) cells (see online supplementary figure S20). Compared to HDAC7 expression, HDAC6 expression in

myofibroblasts was mild (see online supplementary figure S19B). Notably, the ciliated epithelium in IPF and control lungs exhibited abundant cytoplasmic expression of HDAC6 (indicated by hashmarks in online supplementary figures S19A–C).

The IHC expression patterns for all described HDAC enzymes are summarised in table 1.

HDAC expression is upregulated in primary IPF fibroblasts

In accordance with previous reports showing persistence of a profibrotic phenotype of IPF-originating fibroblasts through several passages, we were able to detect a robust and significant upregulation of transcripts for the extracellular matrix (ECM)-associated genes *COL1A1*, *COL3A1* and *P4HTM* in IPF (n=8) versus control (n=6) fibroblasts (see online supplementary figures S22A–D). *ACTA2* appeared only slightly upregulated on mRNA level in IPF (see online supplementary figures S22A/E). In line with mRNA expression, protein biosynthesis of procollagen I was significantly upregulated in IPF versus control fibroblasts (see online supplementary figure S22F). Moreover, primary IPF fibroblasts indicated a significant downregulation of CD90/Thy-1 antigen versus non-diseased controls (see online supplementary figure S22G), which is in line with many previous studies reporting loss of this cell surface glycoprotein in fibroblast populations of IPF lungs, especially in the myofibroblasts of FF.[19]

Furthermore, RT-PCR indicated similar expression of *HDAC2* mRNA in IPF and control fibroblasts (figure 3A), but significant upregulation of mRNA transcripts for *HDAC3* (figure 3B), *HDAC4* (figure 3C), *HDAC5* (figure 3D), *HDAC7* (figure 3E) and *HDAC11* (figure 3F) in IPF fibroblasts. As anticipated by IHC analysis, quantitative immunoblotting revealed significant elevated protein expression of HDAC2 (figure 3G), HDAC3 (figure 3H), HDAC4 and HDAC7 (figure 3I), HDAC8 (figure 3J) and HDAC10 (figure 3K) in IPF versus control fibroblasts. HDAC9 protein expression was equal in IPF and control fibroblasts (see online supplementary figure S24). Additionally, IPF fibroblasts indicated reduced tubulin acetylation, which is indicative of increased expression of class IIb HDAC6 and HDAC10 (figure 3L).

Impact of HDACi treatment on survival and ECM production of IPF fibroblasts

Primary IPF fibroblasts (n=6) were treated with the pan-HDACi LBH589 (85nM) or the class I HDACi VPA (1.5 mM) or vehicle (Veh.) for 30 h, and analysed for cellular consequences. In LBH589 versus vehicle-treated IPF fibroblasts, mRNA expression of the matrix components *ACTA2* (figure 4A), *COL1A1* (figure 4B), *COL3A1* (figure 4C) and *FN* (figure 4D) were significantly decreased. Likewise, expression of the proliferation marker *CCND1* (figure 4E) and the

Table 1 IHC expression pattern of HDAC enzymes in IPF and control lungs

Cell type	HDAC expression pattern in IPF	HDAC expression pattern in control
Fibroblast foci	+++ HDAC1, HDAC2, HDAC3 (nucleus) +++ HDAC8, HDAC4, HDAC5, HDRP (cytoplasm) + HDAC6 (cytoplasm)* ++++ HDAC7 (cytoplasm) +++ HDAC10 (cytoplasm and nucleus)	–
Basal cell	+++ HDAC1, HDAC2, HDAC3 (nucleus) ++++ HDAC4 (cytoplasm and nucleus) +++ HDAC8, HDAC6 (cytoplasm) ++++ HDAC7 ++ HDAC5, HDRP (cytoplasm) +++ HDAC10 (cytoplasm and nucleus)	+ HDAC1 (nucleus) ++ HDAC4 (cytoplasm and nucleus) + HDAC7, HDRP (cytoplasm)
Ciliated bronchial cell	+++ HDAC2, HDAC3 (nucleus) +++ HDAC8, HDAC5 (cytoplasm) ++++ HDAC6*, HDAC7 (cytoplasm) ++++ HDAC4 (nucleus) ++ HDAC10 (cytoplasm)†	+ HDAC2, HDAC3 (nucleus) +++ HDAC8 (cytoplasm) + HDAC5, HDAC7, HDRP (cytoplasm) ++++ HDAC6 (cytoplasm)* ++ HDAC10 (cytoplasm)†
Clara cell	+++ HDAC3, HDAC8 (cytoplasm) ++ HDAC10 (cytoplasm)†	+++ HDAC3, HDAC8 (cytoplasm) ++ HDAC10 (cytoplasm)†
Unknown bronchial epithelial cell type	++++ HDRP (cytoplasm)‡	–
AECII	+ HDAC1 (nucleus) + HDAC5 (cytoplasm) +++ HDAC6 (cytoplasm)*	+ HDAC2, HDAC3 (nucleus) +++ HDAC4 (nucleus and cytoplasm) + HDAC5, HDAC7 (cytoplasm)
SMC	+++ HDAC2, HDAC3 (nucleus) +++ HDAC4 (cytoplasm) ++ HDAC7, HDAC8 (cytoplasm) + HDAC5 (cytoplasm)	+ HDAC4, HDAC7 (cytoplasm)
VSMC	++ HDAC1 (nucleus) +++ HDAC2, (nucleus) ++++ HDAC3 (nucleus+cytoplasm) +++ HDAC4, HDAC7, HDAC9, HDAC10 (cytoplasm) ++++ HDAC5 (cytoplasm) +++ HDAC8 (cytoplasm)	+ HDAC1, HDAC2, HDAC3 (nucleus) ++ HDAC4, HDAC5, HDAC7, HDAC9 (cytoplasm) ++ HDAC8 (cytoplasm) + HDAC10 (cytoplasm and nucleus)

++++, very strong expression; +++, strong expression; +, very weak/faint expression; ++, weak-to-moderate expression; AECII, type II alveolar epithelial cell; HDAC, histone deacetylase; HDRP, histone deacetylase-related protein; IHC, immunohistochemistry; IPF, idiopathic pulmonary fibrosis; SMC, smooth muscle cell; VSMC, vascular smooth muscle cell.
*See supplementary figures S19 and S20.
†See supplementary figure S21.
‡See supplementary-figures S16 and S17.

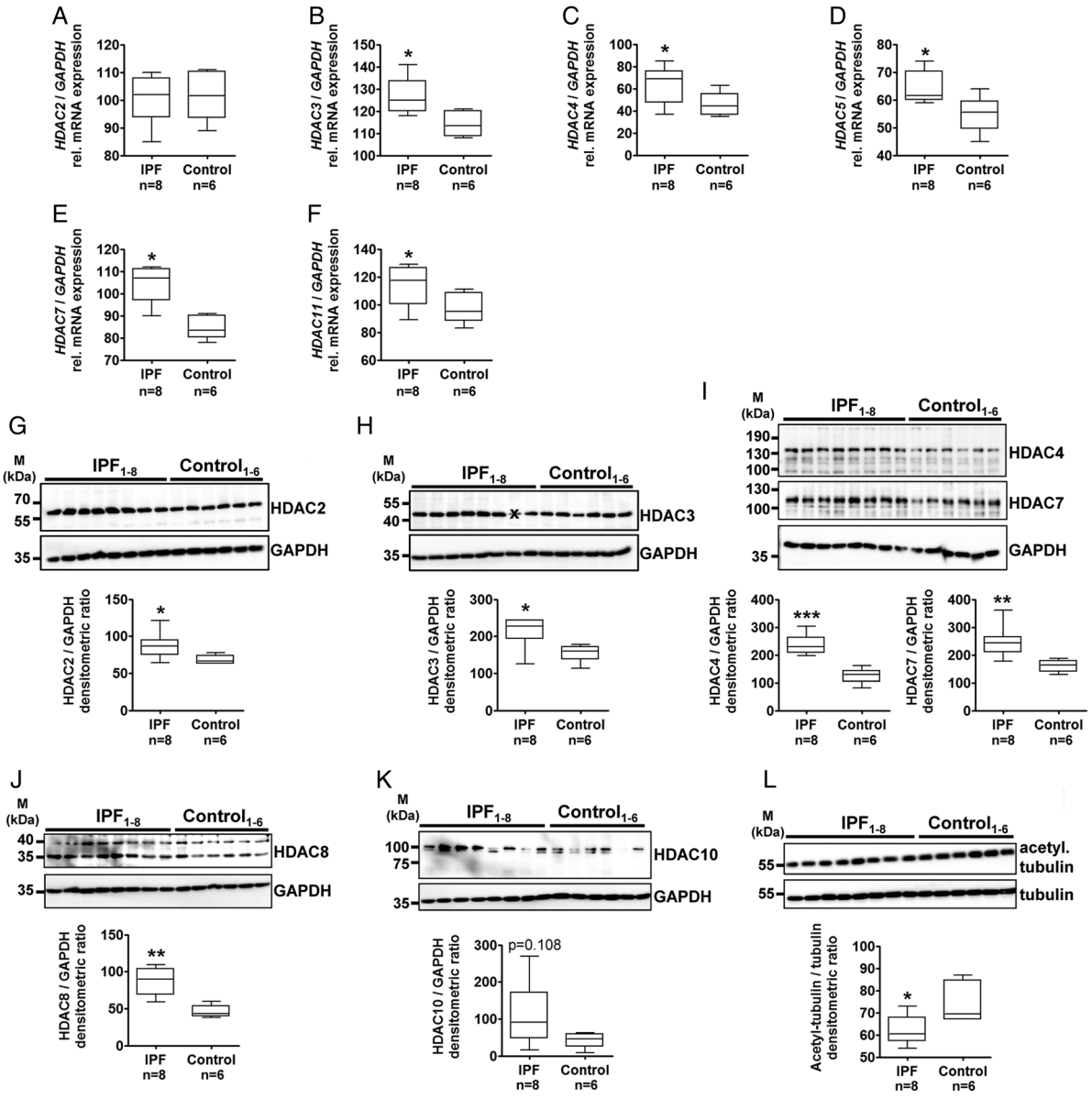

Figure 3 Expression analysis of histone deacetylases (HDACs) in primary fibroblasts isolated from idiopathic pulmonary fibrosis (IPF)–and non-diseased control lungs. (A–F) Reverse transcription-PCRs (RT-PCR) for *HDAC2* (A), *HDAC3* (B), *HDAC4* (C), *HDAC5* (D), *HDAC7* (E) and *HDAC11* (F) of human fibroblasts isolated from peripheral explanted lung tissue of patients with IPF (n=8) and non-diseased control lungs (control, n=6). Each PCR reaction was performed with 100 ng reverse-transcribed complementary DNA, followed by electrophoresis through a 2% (w/v) agarose gel containing ethidium bromide. Scanned agarose gels of indicated genes are shown in online supplementary figure S23. Band intensities of PCR products were densitometrically quantified, and mRNA expression of *HDAC* genes was normalised to the expression of glyceraldehyde 3-phosphate dehydrogenase (*GAPDH*). *p<0.05. (G–L) Representative immunoblots and quantitative immunoblot analysis of human fibroblasts isolated from peripheral lung tissue of patients with sporadic IPF (n=8) and non-diseased control lungs (control, n=6) for HDAC2 (G), HDAC3 (H), HDAC4 and HDAC7 (I), HDAC8 (J), HDAC10 (K), acetylated tubulin (L) and GAPDH or tubulin as loading controls. *p<0.05, **p<0.01, ***p<0.001. Densitometric ratios of the respective gene to *GAPDH*, as well as of the respective protein to GAPDH or tubulin, are depicted as a box-and-whisker diagram (*box* indicates 25th and 75th, *horizontal line* indicates the 50th percentile (median), and extensions above and below reflect extreme values); statistics were performed by Mann–Whitney test. x indicates this sample was not included for statistical analysis due to artefact.

survival gene *BIRC5* (figure 4F) was reduced, whereas mRNA levels for the proapoptotic genes *CIP1* (figure 4G) and *PUMA* (figure 4I) were increased. Notably, significant impairment of survival signalling was also observed in VPA-treated cells (figure 4E–G, I). However, a significant reduction of *P53* mRNA in response to LBH589 or VPA treatment (figure 4H) was observed, despite increases of p53 target genes *CIP1* and *PUMA* in both conditions. In line with apoptotic signalling, significant induction of the endoplasmic reticulum (ER) stress-associated proapoptotic transcription factor *CHOP* was observed in LBH589 versus vehicle-treated cells, but not in VPA treatments (figure 4K). The mRNA expression of the ER stress marker ATF6 was slightly elevated in response to LBH589 treatment (figure 4J). Finally, VPA treatment leads to elevated transcription of the E2 conjugase *UBE2L6* (figure 4L) that has been described as part of the ubiquitination machinery for HDAC2, which is selectively degraded by the proteasome in response to VPA.[16]

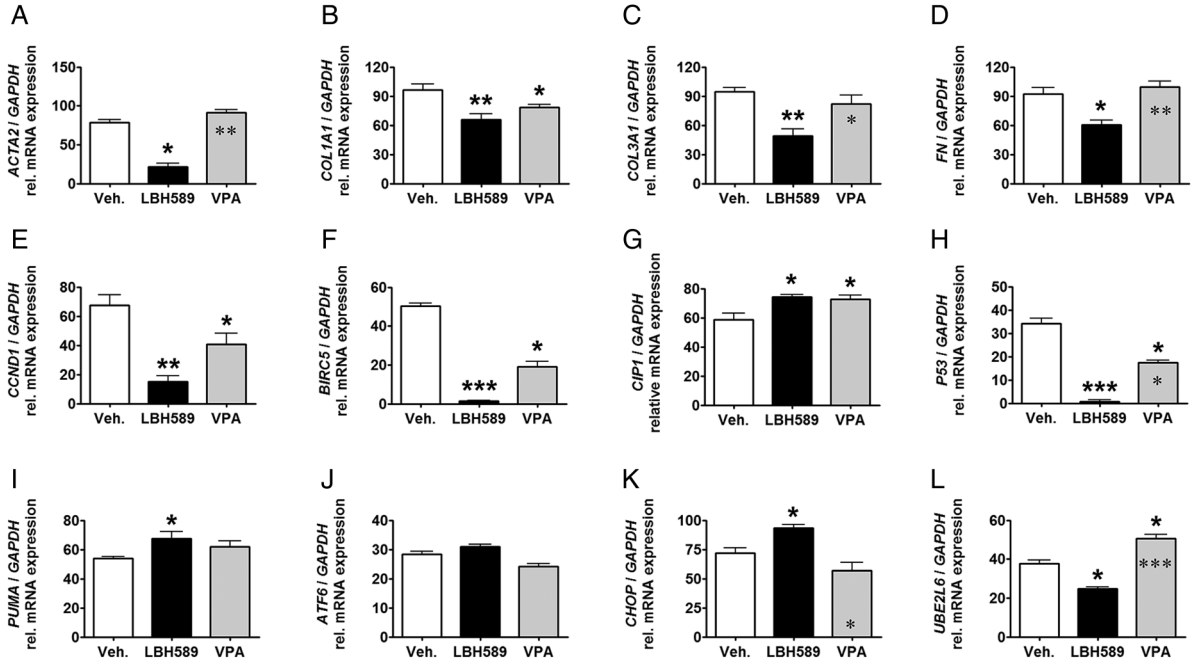

Figure 4 Cellular signalling in primary idiopathic pulmonary fibrosis (IPF) fibroblasts in response to treatment with panobinostat or valproic acid (VPA). Primary IPF fibroblasts (n=6) were incubated for 30 h with vehicle (0.03% dimethyl sulfoxide, 0.1% ethanol), panobinostat (LBH589, 85 nmol) or VPA (1.5 mM). The effects of vehicle and histone deacetylase (HDACs) inhibitor treatments were analysed by semiquantitative reverse transcription-PCR (RT-PCR) for indicated genes. (A) *ACTA2*, (B) *COL1A1*, (C) *COL3A1*, (D) *FN*, (E) *CCND1*, (F) *BIRC5*, (G) *CIP1*, (H) *P53*, (I) *PUMA*, (J) *ATF6*, (K) *CHOP* and (L) *UBE2L6*. Each PCR reaction was performed with 100 ng reverse-transcribed complementary DNA, followed by electrophoresis through a 2% (w/v) agarose gel containing ethidium bromide. Scanned agarose gels of indicated genes are shown in online supplementary figure S25. Band intensities of PCR products were densitometrically quantified, and mRNA expression of indicated genes was normalised to the expression of glyceraldehyde 3-phosphate dehydrogenase (*GAPDH*). Data are presented as mean±SEM of the individual values of different treatments. *p<0.05, **p<0.01, ***p<0.001, LBH589 or VPA vs vehicle; *p<0.05, **p<0.01, ***p<0.001 VPA vs LBH589; by Dunn's multiple comparison test.

Next, gene expression of HDAC enzymes in response to HDACi treatment was analysed (see online supplementary figures S26A–N). Compared to vehicle-treated cells, LBH589 treatment resulted in reduced *HDAC11* expression (see online supplementary figure S9L) and to marked suppression of *HDAC7* (see online supplementary figure S9H), paralleled by a significant increase in *HDAC3* (see online supplementary figure S9D) and *SIRT2* transcripts (see online supplementary figureS9N).

On protein level (see figure 5 and online supplementary figure S27), IPF fibroblast lysates (n=4) indicated a significant increase of total acetylated histone H3 after treatment with LBH589 or VPA versus vehicle (figure 5A), whereas significant tubulin-acetylation was detected only in LBH589-treated cells (figure 5B) due to efficient inhibition of class IIb HDAC6 and HDAC10. In line with mRNA expression analysis, p21 protein was significantly increased (despite reduction of p53) in LBH589-treated IPF fibroblasts compared with vehicle control (figure 5C, D). Furthermore, western blot analyses displayed a decrease in proliferation marker phospho-histone H3 in LBH589-treated as well as VPA-treated IPF fibroblasts (figure 5E). Cyclin D1 was reduced only in LBH589-treated cells (figure 5F). Concomitantly, antiapoptotic proteins survivin (figure 5G) and Bcl-XL (figure 5H) were reduced, with parallel induction of the proapoptotic ER stress marker CHOP (figure 5I) and caspase-3 activation (figure 5J), in LBH589-treated, but not VPA-treated IPF fibroblasts. It has been already shown in cancer cells that ER stress plays a pivotal role in cell death mediated by LBH589, independent of p53.[20]

In accordance with suppression of *HDAC7* gene expression in response to LBH589 treatment, protein expression of HDAC7 was almost absent under these conditions, but also reduced in VPA-treated IPF fibroblasts in comparison to vehicle control (see figure 5K and online supplementary figure S28; two different antibodies were tested for HDAC7 expression). In line with this interesting observation, the pan-HDACi SAHA has been shown to selectively suppress expression of *HDAC7* in several cell lines.[21]

Furthermore, VPA, but not LBH589 treatment, resulted in a significant downregulation of HDAC2 protein expression (figure 5L), presumably through E2-conjugase *UBE2L6*-mediated polyubiquitination and proteasomal degradation of HDAC2, a process that has been observed in several cell lines in response to VPA.[16] In contrast, protein expression of HDAC3 was not altered by VPA, but was significantly upregulated in LBH589-treated versus vehicle-treated IPF fibroblasts (figure 5M).

Finally, all these changes were accompanied by significant reduction of collagen I biosynthesis in both LBH589-treated and VPA-treated IPF fibroblasts versus vehicle treatment, as assessed by immunoblotting for pro-forms (figure 5O) and mature forms of collagen I (figure 5P). Of note, VPA treatment did not reduce α-SMA expression in IPF fibroblasts (figure 5N).

DISCUSSION

The development, growth and aggressiveness of cancer cells have been associated with upregulated HDAC expression. Class I HDACs such as HDAC2 appear to be crucial for the regulation of proliferation and apoptosis resistance of cancer cells, in part

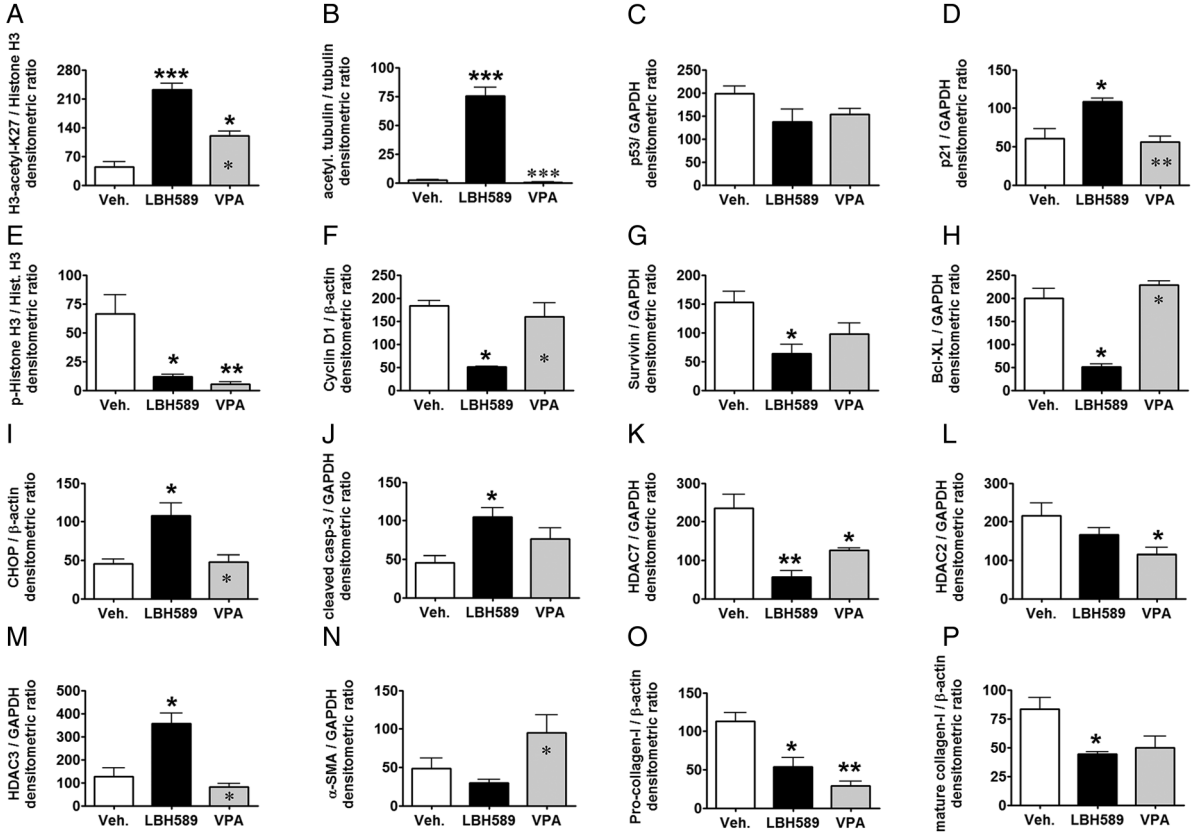

Figure 5 Analysis of acetylation status, apoptotic signalling and profibrotic protein expression in primary idiopathic pulmonary fibrosis (IPF) fibroblasts in response to treatment with panobinostat or valproic acid (VPA). Primary IPF fibroblasts (n=4) were incubated for 30 h with vehicle (0.03% dimethyl sulfoxide, 0.1% ethanol), panobinostat (LBH589, 85 nmol) or VPA (1.5 mM). Status of acetylation, apoptosis, histone deacetylase (HDAC) protein expression and profibrotic protein expression was analysed by quantitative immunoblotting. Representative immunoblots of indicated research targets are shown in online supplementary figure S27. In dependency of research target, histone H3, glyceraldehyde 3-phosphate dehydrogenase (GAPDH), β-actin or tubulin served as loading control. (A) Histone H3-acetyl K27, (B) acetylated tubulin, (C) p53, (D) p21, (E) phospho-histone H3, (F) cyclin-D1, (G) survivin, (H) Bcl-Xl, (I) CHOP, (J) caspase-3, (K) HDAC7, (L) HDAC2, (M) HDAC3, (N) alpha-smooth muscle actin (α-SMA), (O) COL1A1 (pro-form) and (P) COL1A1 (mature form). Data are presented as mean±SEM of the individual values of different treatments. *p<0.05, **p<0.01, ***p<0.001, LBH589 or VPA vs vehicle; *p<0.05, **p<0.01, ***p<0.001 VPA vs LBH589; by Dunn's multiple comparison test.

through their ability to inhibit the tumour suppressor p53 and to promote expression of the proto-oncogene c-Myc.[8] Several publications have also implicated many roles of class II HDACs in tumourigenesis: HDAC4 promotes growth of colon cancer cells via repression of p21.[22] HDAC5 strongly interacts with the tumour suppressor RUNX3 and induces its degradation through deacetylation.[23] HDAC7 has been shown to protect from apoptosis by inhibiting c-Jun expression[24] and contributes to carcinogenesis by transcriptional activation of c-Myc.[25] However, little was known about expression and function of HDACs in IPF. In this paper, we show for the first time that nearly all class I and II HDAC enzymes are overexpressed and upregulated in IPF lung tissue. In detail, upregulation of HDACs was predominantly observed in myofibroblasts of FF as well as in abnormal bronchiolar basal cells in areas of bronchiolisation in IPF lungs, and co-localised with expression of survivin. These results are not surprising as key features in the pathogenesis of IPF include expansion of the population of fibroblasts and their differentiation into apoptosis-resistant myofibroblasts, which consecutively produce large amounts of ECM components.[1] While class I HDACs revealed strong nuclear induction in FF, class IIa HDACs HDAC4, HDAC5, HDAC7 and HDAC9 were predominantly expressed in the cytoplasm of myofibroblasts. The translocation of class IIa HDACs from the nucleus to the cytoplasm is associated with activation of transcription factors myocyte-enhancer factor-2 and serum response factor, which activate myogenic genes such as *ACTA2*, and which are repressed by nuclear localisation of class IIa HDACs.[14] Additional studies using RNAi technology identified HDAC4 as an HDAC that mediates transforming growth factor (TGF)-β1-induced differentiation of normal lung fibroblasts into myofibroblasts. Also here, the cytoplasmic localisation of HDAC4 was required for activation of AKT signalling pathway, which is necessary for *ACTA2* expression in response to TGF-β1.[14] We suggest that 'cancer-like' upregulation of class I and II HDACs in IPF fibroblasts is associated with (i) increased fibroblast proliferation, (ii) fibroblast-to-myofibroblast differentiation and (iii) with the apoptosis-resistant phenotype of myofibroblasts. Another striking hallmark of IPF is the so-called 'bronchiolisation-process' that describes the aberrant progressive re-epithelialisation of damaged alveolar epithelium by proliferating bronchiolar basal cells.[1 26] Based on our data, we suggest that the exaggerated, proliferative character of basal cells in IPF may be in part due to overexpression of HDACs and that HDACs may govern the process of aberrant bronchiolisation in this disease. In line with this, luminal ciliated bronchial cells (which stem from the progenitor basal cells) indicated also robust overexpression of class I (especially HDAC2 and

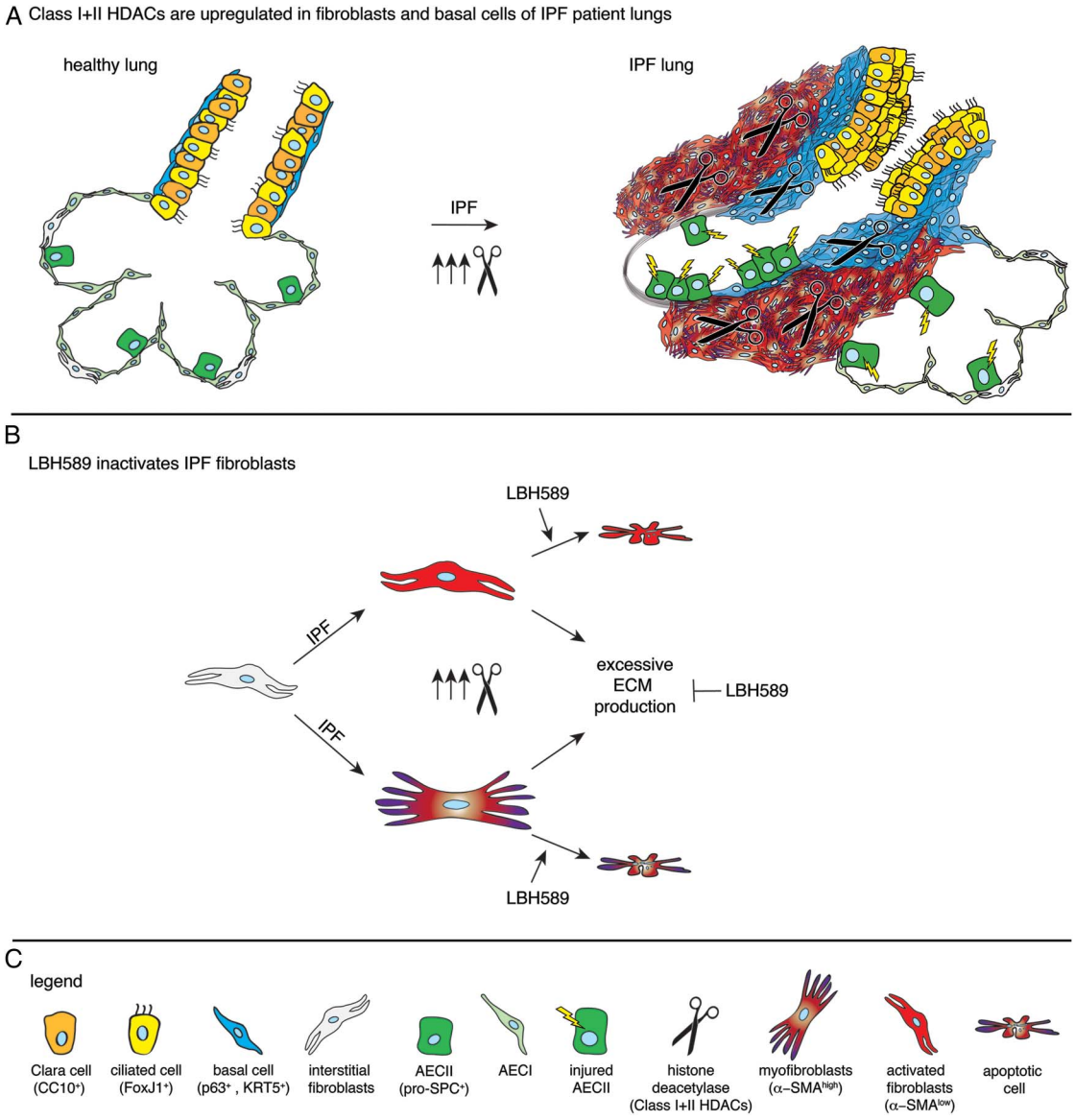

Figure 6 Aberrant histone deacetylase (HDAC) overexpression likely contributes to idiopathic pulmonary fibrosis (IPF) pathogenesis. (A) In the healthy lung with normal alveolar architecture, histone acetylation and deacetylation is balanced and contributes to appropriate gene transcription of pivotal cellular signalling pathways. The triggering event for IPF is alveolar epithelial cell (AEC) injury and death. AECII cells become hyperplastic and depleted of HDACs (except for HDAC6); endoplasmic reticulum stress and apoptosis are also present. In parallel, an aberrant upregulation of class I/II HDACs is observed in different fibroblast populations including myofibroblasts and bronchiolar basal cells. The contribution of injured IPF-AECIIs to the malignant HDAC overexpression in fibroblasts and basal cells in IPF remains to be elucidated. As a result of class I HDAC overexpression, we hypothesise that transcription of repressors of fibrosis is reduced in both fibroblast and basal cell populations of IPF lungs, thereby leading to aberrant activation of proliferative, profibrotic and apoptosis-resistant genes. Class II HDACs contribute to profibrotic gene expression by activating and maintaining cytoplasmic AKT phosphorylation. All together, this leads to abnormal fibroblast proliferation and myofibroblast generation. Alveolar spaces are infiltrated by myofibroblasts and activated resident fibroblasts, which begin to form fibroblast foci. Basal cells proliferate and migrate distally. As IPF progresses, alveolar spaces are progressively replaced by fibrotic tissue, smooth muscle and abnormal bronchiolar epithelium ('bronchiolisation'). (B) In vitro, pan-HDAC inhibition by LBH589/panobinostat efficiently inactivates primary profibrotic fibroblasts and myofibroblasts through downregulation of extracellular matrix (ECM) production on the one side and induction of apoptosis on the other side, and which thus may have a significant benefit for patients with IPF. (C) Legend.

HDAC3) and of all class II HDACs, whereas only faint or moderate expression was observed in the ciliated epithelium of non-diseased control lungs. Moreover, basal and luminal epithelial cells near areas of active fibrotic remodelling and aberrant bronchiolar proliferation or of abnormal IPF bronchioles that often appear hyperplastic and larger in size are suspected to contribute to the abnormal, exaggerated production of profibrotic signals in IPF[26] and that thus may require enhanced overexpression of 'cancer-like' HDACs. Of note, expression of many HDAC enzymes seemed to be virtually absent or was only faint in normal bronchiolar structures as well as AECII (or rather in the whole lung tissue) of non-diseased control lungs, presumably due to their crucial intrinsic activity in cell proliferation and apoptosis inhibition,[5 8 9] which justifies an only low and basal expression in normal, healthy cells.

The class IIa HDACs HDAC4 and HDAC7 were the only HDACs with moderate to robust expression in ciliated epithelium and AECII of non-diseased control lungs. However, we

can only speculate about the function of both these HDACs in the normal AECII. HDAC4 and HDAC7 have been both reported to regulate the functional activity of HIF-1α in various cell types in vitro because loss of each of them resulted in reduced HIF-1α transcriptional activity of adaptive responses to hypoxia.[27 28] For alveolar-epithelial expressed HIF-1α, a surprising role in lung protection during acute lung injury (ALI) has recently been reported in which normoxic HIF-1α stabilisation and HIF-1α-dependent control of alveolar-epithelial glucose metabolism attenuated lung inflammation during ALI induced by stretch conditions in vitro or by ventilator-induced lung injury in vivo.[29] Additionally, HIF-1α has been reported to be essential for proper lung maturation and surfactant production in the newborn lung of mice.[30] Based on these studies, we can presume that HDAC4 and HDAC7 might play a crucial role in maintaining AECII homeostasis through regulation of HIF-1α.

Though, and in marked contrast to bronchiolar epithelial cells in IPF, AECII of IPF lungs did not reveal significant expression of class I and II HDACs (which were in part significantly expressed in AECII of normal lungs, such as HDAC4 and HDAC7 as described above), possibly due to pro-apoptotic ER and oxidative stress in IPF-AECII,[31–33] which in turn lead to proteasomal degradation of many HDACs. Moreover, HDAC4 is a death substrate, cleaved by caspase-3 during apoptotic cell death,[34] and HDAC7 is the best caspase-8 substrate described to date.[35]

Importantly, the class IIb member HDAC6 was the only HDAC expressed in IPF-AECII, but not in AECII of normal lungs. As a tubulin deacetylase, HDAC6 is involved in aggresome formation and autophagic clearance of protein aggregates in response to increased misfolding,[18] and its induction in AECII can be due to severe alveolar epithelial ER stress in IPF.[31–33] Additionally, HDAC6 deacetylates antioxidants PRDX1 and PRDX2, which impairs their function to reduce H_2O_2, thereby promoting apoptosis.[36] Despite its reported pro-apoptotic and pathological function, it seemed to be an intrinsic normality of ciliated bronchial cells of IPF as well as non-diseased control lungs to robustly express HDAC6 in the cytoplasm, as shown by our IHC studies. Of note, autophagy is also critical for cell survival because unwanted intracellular materials are degraded, and HDAC6 controls autophagosome maturation through its deacetylase activity.[37] Indeed, it was shown that cells deficient in HDAC6 failed to form autophagosomes and to clear misfolded protein aggregates, and were hypersensitive to the accumulation of malfolded proteins.[37] On the other hand, inhibition of HDAC6 deacetylase activity by pan-HDACi such as SAHA or trichostatin-A has been shown to ameliorate disease progression and neurodegeneration in rodent models of Huntington's disease and amyotrophic lateral sclerosis.[38 39] Anyway, the exact role of HDAC6 in the ciliated lung epithelium and the impact of its induction in IPF-AECII remain still elusive and have to be further investigated.

More than 10 HDACi have already been examined in clinical trials as cancer drugs and only minor side effects have been observed.[9] HDACi possess the ability to selectively induce apoptosis in tumour cells, whereas normal cells are relatively resistant to HDACi-induced cell death.[9 11 40] In addition to antitumour activities, HDACi have been shown to exert beneficial effects on several diseases such as cardiac hypertrophy,[6] inflammatory bowel disease[41] and above-mentioned neurodegenerative diseases.[38 39] The present study suggests that HDACi such as LBH589 may also be useful for the treatment of IPF. Interfering with the generation of myofibroblast foci to decrease production of ECM components is important in treating IPF because the increase in the number of these fibrotic foci has been associated with disease progression and a worsened prognosis.[42] We demonstrated that LBH589 downregulated significantly the mRNA expression of *ACTA2* and ECM genes *COL1A1*, *COL3A1* and *FN* in primary IPF fibroblasts and thus interfered with fibroblast-to-myofibroblast differentiation. In addition, LBH589 efficiently reduced the protein biosynthesis of the large collagen α-1 chains (*COL1A1*) in IPF fibroblasts. The reduction in ECM synthesis was accompanied by growth inhibition as shown by immunoblotting for p-histone H3 and cyclin-D1. In parallel, LBH589 suppressed expression of the survival-related *HDAC7* gene and downregulated expression of antiapoptotic genes *BCL2L1*/Bcl-XL and *BIRC5*/survivin in IPF fibroblasts, and led to induction of ER stress and apoptosis, thereby resulting in efficient inactivation of ECM producing and 'malignant appearing' IPF fibroblasts. Moreover, in renal fibrosis, it was demonstrated in a murine model of unilateral ureteral obstruction that trichostatin-A led simultaneously to inactivation of renal interstitial fibroblasts and inhibition of renal tubular epithelial cell death,[43] thus adding further experimental proof to use pan-HDACi for the treatment of IPF. Furthermore, it should be noted that the treatment of IPF fibroblasts with VPA, which has been described as a weak class I HDACi, led also to a significant reduction in collagen I biosynthesis. Additionally, VPA treatment induced significant downregulation of HDAC2 protein levels in IPF fibroblasts, presumably through *UBE2L6*-mediated polyubiquitination and proteasomal degradation of HDAC2.[16] Because overexpression of HDAC2 is a classical 'cancer condition', drugs that interfere with HDAC2 protein turnover in myofibroblasts are of great importance.

The exact targets of HDACs in the setting of fibrosis are yet not clear. Similar to cancer cells, in which 'aberrant transcriptional repression' has been described as a result of class I HDAC overexpression,[5 8 11 16] we suggest that target genes of class I HDACs in lung fibroblasts might be repressors of antiapoptotic and profibrotic gene expression (which are silenced in the setting of fibrosis due to class I HDAC upregulation). The contribution of class IIa HDACs to lung fibrosis is presumably antiapoptosis[22–25] as well as maintaining of cytoplasmic AKT phosphorylation/activation and consequent promotion of profibrotic gene expression.[14]

In conclusion, based on the results of our study, HDACs are novel molecular targets for IPF therapy, and pan-HDACi such as LBH589 are promising therapeutic agents for the treatment of IPF, even though their exact targets and mechanisms of action in the setting of IPF must be further investigated. The main observations and suggestions from this study are summarised in figure 6.

Author affiliations
[1]Department of Internal Medicine, Justus-Liebig-University Giessen, Giessen, Germany
[2]Universities of Giessen and Marburg Lung Center (UGMLC), Member of the German Center for Lung Research (DZL)
[3]Department of Medicine, Section of Pulmonary Diseases, Critical Care and Environmental Medicine, Tulane University Health Science Center, New Orleans, Louisiana, USA
[4]Excellence Cluster Cardio-Pulmonary System (ECCPS), Giessen, Germany
[5]Department of Thoracic Surgery, Vienna General Hospital, Vienna, Austria
[6]CHU Paris Nord-Val de Seine, Hôpital Xavier Bichat-Claude Bernard, Paris, France
[7]Department of Lung Development and Remodeling, Max-Planck-Institute for Heart and Lung Research, Bad Nauheim, Germany
[8]Institute of Pathology and Cytology, Wetzlar, Germany
[9]Department of Toxicology, University Medical Center, Mainz, Germany
[10]Agaplesion Lung Clinic Waldhof Elgershausen, Greifenstein, Germany
[11]European IPF Network and European IPF Registry

Acknowledgements We thank Gabriele Dahlem and Susanna Ziegler for isolation of primary fibroblasts from explanted IPF and non-diseased control lungs.

Contributors MK, OHK and AG designed experiments and wrote the manuscript. MK, SS, IH, BAMK, OK, ShS, LF, CR, DvdB, PM, and WK carried out the experimental work. BAMK, SB, BC, SSP and WS served as key advisors and critically read the manuscript. OHK and AG equally contributed to this manuscript.

Competing interests None declared.

Patient consent Obtained.

Ethics approval The study protocol was approved by the Ethics Committee of the Justus-Liebig-University School of Medicine (no. 31/93, 29/01, and no. 111/08: European IPF Registry).

Provenance and peer review Not commissioned; externally peer reviewed.

REFERENCES

1 American Thoracic Society. Idiopathic pulmonary fibrosis: diagnosis and treatment. International consensus statement. American Thoracic Society (ATS), and the European Respiratory Society (ERS). *Am J Respir Crit Care Med* 2000;161:646–64.
2 Vancheri C. Common pathways in idiopathic pulmonary fibrosis and cancer. *Eur Respir Rev* 2013;22:265–72.
3 Conte E, Gili E, Fruciano M, *et al*. PI3K p110gamma overexpression in idiopathic pulmonary fibrosis lung tissue and fibroblast cells: in vitro effects of its inhibition. *Lab Invest* 2013;93:566–76.
4 Sisson TH, Maher TM, Ajayi IO, *et al*. Increased survivin expression contributes to apoptosis-resistance in IPF-fibroblasts. *Adv Biosci Biotechnol* 2012;3:657–64.
5 Lafon-Hughes L, Di Tomaso MV, Mendez-Acuna L, *et al*. Chromatin-remodelling mechanisms in cancer. *Mutat Res* 2008;658:191–214.
6 Backs J, Olson EN. Control of cardiac growth by histone acetylation/deacetylation. *Circ Res* 2006;98:15–24.
7 Ito K, Ito M, Elliott WM, *et al*. Decreased histone deacetylase activity in chronic obstructive pulmonary disease. *New Engl J Med* 2005;352:1967–76.
8 Brandl A, Wagner T, Uhlig KM, *et al*. Dynamically regulated sumoylation of HDAC2 controls p53 deacetylation and restricts apoptosis following genotoxic stress. *J Mol Cell Biol* 2012;4:284–93.
9 Xu WS, Parmigiani RB, Marks PA. Histone deacetylase inhibitors: Molecular mechanisms of action. *Oncogene* 2007;26:5541–52.
10 Sundar IK, Yao H, Rahman I. Oxidative stress and chromatin remodelling in chronic obstructive pulmonary disease and smoking-related diseases. *Antioxid Redox Signal* 2013;18:1956–71.
11 Richon VM, Garcia-Vargas J, Hardwick JS. Development of vorinostat: current applications and future perspectives for cancer therapy. *Cancer Lett* 2009;280:201–10.
12 Anne M, Sammartino D, Barginear MF, *et al*. Profile of panobinostat and its potential for treatment in solid tumors: an update. *Onco Targets Ther* 2013;6:1613–24.
13 Coward WR, Watts K, Feghali-Bostwick CA, *et al*. Defective histone acetylation is responsible for the diminished expression of cyclooxygenase 2 in idiopathic pulmonary fibrosis. *Mol Cell Biol* 2009;29:4325–39.
14 Guo W, Shan B, Klingsberg RC, *et al*. Abrogation of TGF-beta1-induced fibroblast-myofibroblast differentiation by histone deacetylase inhibition. *Am J Physiol Lung Cell Mol Physiol* 2009;297:L864–870.
15 Sanders YY, Hagood JS, Liu H, *et al*. Histone deacetylase inhibition promotes fibroblast apoptosis and ameliorates pulmonary fibrosis in mice. *Eur Respir J* 2014;43:1448–58.
16 Krämer OH, Zhu P, Ostendorff HP, *et al*. The histone deacetylase inhibitor valproic acid selectively induces proteasomal degradation of HDAC2. *EMBO J* 2003;22:3411–20.
17 Waltregny D, Glenisson W, Tran SL, *et al*. Histone deacetylase HDAC8 associates with smooth muscle alpha-actin and is essential for smooth muscle cell contractility. *FASEB J* 2005;19:966–8.
18 Lam HC, Cloonan SM, Bhashyam AR, *et al*. Histone deacetylase 6-mediated selective autophagy regulates COPD-associated cilia dysfunction. *J Clin Invest* 2013;123:5212–30.
19 Hagood JS, Prabhakaran P, Kumbla P, *et al*. Loss of fibroblast Thy-1 expression correlates with lung fibrogenesis. *Am J Pathol* 2005;167:365–79.
20 Montalbano R, Waldegger P, Quint K, *et al*. Endoplasmic reticulum stress plays a pivotal role in cell death mediated by the pan-deacetylase inhibitor panobinostat in human hepatocellular cancer cells. *Transl Cncol* 2013;6:143–57.
21 Dokmanovic M, Perez G, Xu W, *et al*. Histone deacetylase inhibitors selectively suppress expression of HDAC7. *Mol Cancer Ther* 2007;6:2525–34.
22 Wilson AJ, Byun DS, Nasser S, *et al*. HDAC4 promotes growth of colon cancer cells via repression of p21. *Mol Biol Cell* 2008;19:4062–75.
23 Jin YH, Jeon EJ, Li QL, *et al*. Transforming growth factor-beta stimulates p300-dependent RUNX3 acetylation, which inhibits ubiquitination-mediated degradation. *J Biol Chem* 2004;279:29409–17.
24 Ma C, D'Mello SR. Neuroprotection by histone deacetylase-7 (HDAC7) occurs by inhibition of c-jun expression through a deacetylase-independent mechanism. *J Biol Chem* 2011;286:4819–28.
25 Zhu C, Chen Q, Xie Z, *et al*. The role of histone deacetylase 7 (HDAC7) in cancer cell proliferation: Regulation on c-myc. *J Mol Med* 2011;89:279–89.
26 Chilosi M, Poletti V, Murer B, *et al*. Abnormal re-epithelialization and lung remodelling in idiopathic pulmonary fibrosis: the role of deltaN-p63. *Lab Invest* 2002;82:1335–45.
27 Wang Z, Qin G, Zhao TC. HDAC4: mechanism of regulation and biological functions. *Epigenomics* 2014;6:139–50.
28 Witt O, Deubzer HE, Milde T, *et al*. HDAC family: what are the cancer relevant targets? *Cancer Lett* 2009;277:8–21.
29 Eckle T, Brodsky K, Bonney M, *et al*. HIF1A reduces acute lung injury by optimizing carbohydrate metabolism in the alveolar epithelium. *PLoS Biol* 2013;11:e1001665.
30 Saini Y, Harkema JR, LaPres JJ. HIF1alpha is essential for normal intrauterine differentiation of alveolar epithelium and surfactant production in the newborn lung of mice. *J Biol Chem* 2008;283:33650–7.
31 Lawson WE, Crossno PF, Polosukhin VV, *et al*. Endoplasmic reticulum stress in alveolar epithelial cells is prominent in IPF: association with altered surfactant protein processing and herpesvirus infection. *Am J Physiol Lung Cell Mol Physiol* 2008;294:L1119–26.
32 Korfei M, Ruppert C, Mahavadi P, *et al*. Epithelial endoplasmic reticulum stress and apoptosis in sporadic idiopathic pulmonary fibrosis. *Am J Respir Crit Care Med* 2008;178:838–46.
33 Cha SI, Ryerson CJ, Lee JS, *et al*. Cleaved cytokeratin-18 is a mechanistically informative biomarker in idiopathic pulmonary fibrosis. *Respir Res* 2012;13:105.
34 Paroni G, Mizzau M, Henderson C, *et al*. Caspase-dependent regulation of histone deacetylase 4 nuclear-cytoplasmic shuttling promotes apoptosis. *Mol Biol Cell* 2004;15:2804–18.
35 Scott FL, Fuchs GJ, Boyd SE, *et al*. Caspase-8 cleaves histone deacetylase 7 and abolishes its transcription repressor function. *J Biol Chem* 2008;283:19499–510.
36 Parmigiani RB, Xu WS, Venta-Perez G, *et al*. HDAC6 is a specific deacetylase of peroxiredoxins and is involved in redox regulation. *Proc Natl Acad Sci USA* 2008;105:9633–8.
37 Lee JY, Koga H, Kawaguchi Y, *et al*. HDAC6 controls autophagosome maturation essential for ubiquitin-selective quality-control autophagy. *EMBO Journal* 2010;29:969–80.
38 Hockly E, Richon VM, Woodman B, *et al*. Suberoylanilide hydroxamic acid, a histone deacetylase inhibitor, ameliorates motor deficits in a mouse model of Huntington's disease. *Proc Natl Acad Sci USA* 2003;100:2041–6.
39 Petri S, Kiaei M, Kipiani K, *et al*. Additive neuroprotective effects of a histone deacetylase inhibitor and a catalytic antioxidant in a transgenic mouse model of amyotrophic lateral sclerosis. *Neurobiol Dis* 2006;22:40–9.
40 Qiu L, Burgess A, Fairlie DP, *et al*. Histone deacetylase inhibitors trigger a G2 checkpoint in normal cells that is defective in tumor cells. *Mol Biol Cell* 2000;11:2069–83.
41 Tao R, de Zoeten EF, Ozkaynak E, *et al*. Deacetylase inhibition promotes the generation and function of regulatory T cells. *Nat Med* 2007;13:1299–307.
42 King TE Jr, Schwarz MI, Brown K, *et al*. Idiopathic pulmonary fibrosis: relationship between histopathologic features and mortality. *Am J Respir Crit Care Med* 2001;164:1025–32.
43 Pang M, Kothapally J, Mao H, *et al*. Inhibition of histone deacetylase activity attenuates renal fibroblast activation and interstitial fibrosis in obstructive nephropathy. *Am J Physiol Renal Physiol* 2009;297:F996–F1005.

Aberrant expression and activity of histone deacetylases (HDACs) in lungs of patients with sporadic idiopathic pulmonary fibrosis (IPF)

Martina Korfei[1,2]; Sylwia Skwarna[1,2]; Ingrid Henneke[1,2]; BreAnne MacKenzie[1,2]; Oleksiy Klymenko[1,2]; Shigeki Saito[3]; Clemens Ruppert[1,2,4]; Daniel von der Beck[1,2]; Poornima Mahavadi[1,2]; Walter Klepetko[5,11]; Saverio Bellusci[1,2,4]; Bruno Crestani[6,11]; Soni Savai Pullamsetti[1,2,7]; Ludger Fink[2,4,8]; Werner Seeger[1,2,4]; Oliver Holger Krämer[9]* and Andreas Guenther[1,2,4,10,11]*#.

* both authors have contributed equally to the manuscript

#Corresponding Author
Andreas Guenther, M.D.
Department of Internal Medicine II, Justus-Liebig-University Giessen
Klinikstrasse 36, 35392 Giessen Germany
E-mail: Andreas.Guenther@innere.med.uni-giessen.de
Tel.: +49 641 98542502
Fax: +49 641 98542508

Affiliation of co-authors:

[1]Department of Internal Medicine, Justus-Liebig-University Giessen, D-35392 Giessen, Germany.

[2]Universities of Giessen and Marburg Lung Center (UGMLC), Member of the German Center for Lung Research (DZL).

[3]Department of Medicine, Section of Pulmonary Diseases, Critical Care and Environmental Medicine, Tulane University Health Science Center, New Orleans, LA 70112, USA.

[4]Excellence Cluster Cardio-Pulmonary System (ECCPS), D-35392 Giessen, Germany.

[5]Department of Thoracic Surgery, Vienna General Hospital, A-1090 Vienna, Austria.

[6]CHU Paris Nord-Val de Seine, Hôpital Xavier Bichat-Claude Bernard, F-75018 Paris, France.

[7]Max-Planck-Institute for Heart and Lung Research, Department of Lung Development and Remodeling, D-61231 Bad Nauheim.

[8]Institute of Pathology and Cytology, D-35578 Wetzlar, Germany.

[9]Department of Toxicology, University Medical Center, D-55131 Mainz, Germany.

[10]Agaplesion Lung Clinic Waldhof Elgershausen, D-35753 Greifenstein, Germany.

[11]European IPF Network and European IPF Registry.

Supporting Information: Materials and Methods/Supplementary-Figures

Handling of human lung tissue

Explanted lungs or lobes were obtained from the Dept. of Thoracic Surgery, Vienna (W. Klepetko). Already at the surgical theatre, peripheral lung tissue samples were snap-frozen or placed in 4% (w/v) paraformaldehyde immediately after explantation. Thereafter, the remaining lung lobes were placed on ice, and shipped (together with the other samples) to our institute immediately. Upon arrival, lung lobes were sectioned under the hood on ice according to a predefined algorithm; and additional lung tissue samples from subpleural and hilar regions were placed in 4% (w/v) PFA or snap-frozen in liquid nitrogen. The latter samples were stored at -80°C until used.

Isolation of primary human lung fibroblasts

Primary human lung fibroblast cells were derived from subpleural lung tissue of explanted lungs at the time of transplantation from patients with sporadic IPF (n=8, 44.63 $\pm$ 12.14 years; 5 females, 3 males) and non-diseased control-lungs (organ donors, n=4, 46.50 $\pm$ 4.80 years; 3 females, one male), or from histologically normal areas of surgical lung specimens from patients undergoing resective surgery for benign or malignant tumors (n=2, 66.00 $\pm$ 8.48 years; 2 females).

Primary fibroblastic lines were established by using an outgrowth-technique from explants according to the method by Jordana and coworkers [S1,S2]. In brief, the peripheral lung tissue (size: ~1-2 $\times$ 3-4 cm) was washed with RPMI medium; and the pleural margin and vessels were removed from the lung tissue. Thereafter, the lung tissue was chopped/minced into very small pieces (~ 1 mm^3), which were placed on a cell culture dish in PBS containing 200 U/mL penicillin and 200 µg/mL streptomycin. Then the pieces were transferred into a 50 mL Falcon-tube and

incubated for 10 min (for further washing) in a volume of 40 mL PBS containing antibiotics at RT, followed by centrifugation (5 min, 248 rcf, RT) and repeated washings in PBS containing antibiotics until the supernatants were clear. After centrifugation, small lung tissue pieces were put into culture medium [MCDB 131 medium (PAN Biotech) containing 10% (v/v) FBS (PAA Laboratories), 100 U/mL penicillin, 100 µg/mL streptomycin, 2 mM L-glutamine (all from Invitrogen), and 2 ng/mL basic-FGF (Invitrogen), 0.5 ng/mL EGF (Sigma) and 5 µg/mL insulin (Invitrogen)] and cultured à 5 mL in four T75 cell culture flasks in a humidified atmosphere of 37°C and 5% CO_2 (with medium change twice weekly). Upon follow up, fibroblastic cells appeared to be growing either out of the tissue pieces or as islets. After 3-4 weeks, the fibroblast layer was nearly confluent (first passage). The small lung tissue pieces were removed, and fibroblastic cells were harvested by trypsination and centrifugation, and pooled and replated on five T75 cell culture flasks at 37°C and 5% CO_2. After one week, fibroblasts were confluent (passage 2) and harvested resulting in 5 $\times$ 2 cell pellets. One cell pellet was replated on a 10 cm tissue culture dish with 10 mL medium (this corresponds to a splitting 1:2), the other nine fibroblast aliquots were frozen and stored in liquid nitrogen. The fibroblasts from a 10 cm-dish could then be split 1:6-1:7 at confluency (passage 3), and fibroblasts were then cultured for phenotyping/biochemical characterization for a time period of four days. Fibroblast aliquots at each passage were frozen and stored in liquid nitrogen.

In general, the purity of isolated IPF-fibroblasts was verified by positive immunostaining for collagen I (mesenchymal marker), and negative staining for MNF-116 (detects an epitope common to many cytokeratins [Moll's numbers 5, 6, 8, 17 and 19]) and vWF (von Willebrand factor, marker for blood vessels). All experiments

were carried out with IPF-fibroblasts and normal fibroblasts between passages 3 and 4.

Cell Culture experiments

Primary fibroblasts of patients with IPF (n=6) were seeded in normal culture medium on 10 cm tissue culture dishes and cultured for 3 days. At 95-99% confluency, IPF-fibroblasts were incubated for 30h with the HDAC inhibitors (HDACi) panobinostat (LBH589, 85nM, from Selleckchem) and valproic acid (VPA, 1.5mM, from Santa Cruz), and as control experiment with the respective solvents (vehicle-control) in the concentration 0.1% (v/v) ethanol and 0.03% (v/v) DMSO.

The pan-HDACi LBH589 has an efficient inhibitory activity at nanomolar concentrations (14-200 nM) and appears to be the most potent clinically available HDAC inhibitor (S3). Valproic acid is a weak class-I-HDACi and efficient in the milli-molar range (0.5 – 5.0 mM) (S4,S5). The dosages of HDACi (S3-S5) were chosen according to published - and own preliminary studies. HDACi experiments were performed using culture medium containing 2% (v/v) FBS.

After incubation, fibroblastic cells from each plate were harvested by trypsination and divided in two equal volume parts, and centrifuged using two Falcon-tubes (5 min, 1000 rpm, RT) resulting in two pellets. One pellet was subjected to protein isolation, the other to RNA isolation.

Semiquantitative Reverse Transcription-Polymerase Chain Reaction (RT-PCR)

Total cellular RNA was prepared from treated IPF-fibroblasts using the RNeasy® Plus Mini-Kit (Qiagen) and 600 µL RLT Plus-lysis buffer according to the protocol of the manufacturer. The great advantage of the kit is the efficient removal of genomic DNA during the isolation procedure with use of the ″gDNA eliminator column″. The purity

and quantity of the isolated RNA was determined by spectrophotometry at 260/280 nm using NanoDrop 2000c photometer (PeqLab).

Reverse transcription (RT) and PCR were performed sequentially in two separate steps. Complementary DNA (cDNA, 2 µg) was first synthesized by reverse transcription (RT) using 2 µg total RNA, and with use of oligo-dT-primers and the Omniscript-RT-Kit (Qiagen). An aliquot of the finished RT reaction/cDNA (100 ng) was then used for PCR amplification employing gene-specific primers for transcripts. The complete list of primers used is given in **Table S1**.

Each 40-µL RT reaction contained (final concentration): 2 µg total RNA, 1 µM oligo-dT-primers, 10 units RNAse inhibitor (both Applied Biosystems), 500 µM of each dNTP and 4 units Omniscript Reverse Transcriptase (both Qiagen). The RT reactions were incubated for 65 min at 37°C, directly followed by PCR using gene-specific primers. Each 20-µL PCR reaction contained (final concentration): 2 µL finished RT reaction (= 100 ng template cDNA), 0.2 µM each forward and reverse primer (metabion, Martinsried, Germany), 200 µM of each dNTP (Thermo Scientific) and 0.4 µL Phire-Hot-Start-II-DNA-Polymerase (Thermo Scientific), which is a novel PCR enzyme and significantly faster than *Taq*-based polymerases. For amplification of all described mRNA´s/genes, a special cycling protocol according to the manufacturer´s protocol was performed: ″Hot-Start″ (initial activation step: 98°C for 30 sec) followed by 3-step-cycling (20-35 cycles of amplification): denaturation: 98°C for 5 s; annealing: 59-65°C for 5 s (the annealing temperatures of each primer pair is given in **Table S1**), extension: 72°C for 15 sec (and 60 sec in the final extension). The thermal cycler used was from Bio-Rad (model: PTC-1148).

As control experiment, PCR reactions of RNA samples without reverse transcriptase were performed (to exclude amplification of genomic DNA contaminations).

Equal aliquots of the PCR products were electrophoresed through a 2% (w/v) agarose gel containing ethidium bromide in 1× tris-acetate-EDTA (TAE) buffer, and documented by scanning using an UV imager (Gel-Doc XR$^+$, Bio-Rad). Thereafter, band intensities of PCR products were quantified using Image Lab-Software (version 4.1, Bio-Rad), and mRNA expression of genes of interest were normalized to the expression of *GAPDH*.

Quantitative Real-Time- Polymerase Chain Reaction (qRT-PCR)

For mRNA expression analysis of HDAC6 in IPF- (n=31) and control-lung tissues (n=12), qRT-PCR was performed. RNA was reverse-transcribed using QuantiTect Reverse Transcription Kit (Qiagen). cDNA was diluted to a concentration between 20 ng/µL. Primers were designed using Roche Applied Sciences online Assay Design Tool. All primers were designed to span introns and blasted using NCBI software for specificity. Sybr Green Master Mix (Applied Biosciences) was used for RT-PCR with a Roche LightCycler 480 machine. Samples were run in triplicates using hydroxymethylbilane synthase (*HMBS*) as a reference gene for human samples.

Human Primers	**Forward**	**Reverse**
HMBS	5´-AGCTATGAAGGATGGGCAAC-3´	5´-TTGTATGCTATCTGAGCCGTCTA-3´
HDAC6	5´-AACTGAGACCGTGGAGAG-3´	5´-CCTGTGCGAGACTGTAGC-3´

Western Blot analysis

For analysis of HDAC protein expression, peripheral lung tissue samples from the lower lobe, from the subpleural region of the lung was used. Lung homogenates were

prepared of frozen lung tissue samples (size 1 cm^3) from IPF patients (n=26) and controls (n=16) according to the protocol previously described [S6].

For preparation of protein extracts from lung fibroblasts, frozen cell pellets were lysed with 100-200 µL cold extraction buffer [50 mmol/L tris-HCl [pH 7.5], 150 mmol/L NaCl, 1% (w/v) triton X-100, 0.5% (w/v) sodium-deoxycholate, 5 mmol/L EDTA, 1 µmol/L trichostatin-A (TSA, Selleckchem), and 1× Halt™ Protease & Phosphatase Cocktail (Thermo Scientific)], and subjected to 3× repeated freezings (in liquid nitrogen) and thawings for efficient cell disruption. Cell lysates were then incubated one ice for 1h, followed by centrifugation (10 min, 13000 rpm, 4°C) to remove cell debris. The resulting supernatants were then stored at -80°C until further use. In general, the protein concentration in lung homogenates and fibroblastic cell extracts was determined according to the Pierce® BCA protein assay from Thermo Scientific.

For one-dimensional SDS-PAGE, lung homogenates or cell lysates were then diluted (1:3) in 4×SDS-sample buffer [leading to a final concentration 2% (w/v) SDS, 2.5% (v/v) β-mercaptoethanol, 10% (v/v) glycerol, 12.5 mmol/L tris-HCl [pH 6.8], 0.1% (w/v) bromophenol blue in samples] and heated for denaturation at 99°C for 15 min. Denaturated proteins from each sample (50 µg/lane in case of lung homogenates, 15 µg/lane in case of fibroblastic cell lysates) were then separated by 8%, 9%, 10%, 12% or 15% Laemmli-SDS-PAGE. Thereafter, the separated proteins were transferred to a PVDF membrane (GE Healthcare) in a semi-dry blotting chamber according to the manufacturer´s protocol (Bio-Rad, Munich, Germany). Obtained immunoblots were then blocked by incubating at room temperature for 1 h in blocking buffer [1 × tris-buffered saline (TBS; 50 mmol/L tris-HCl, pH 7.5, 50 mmol/L NaCl) containing 5% (w/v) nonfat dried milk and 0.1 % (w/v) tween 20], followed by immunostaining for proteins of interest. In the following, the primary antibodies used for western blotting are listed, including the sources and dilutions: mouse monoclonal

for HDAC1 (1:500, Abcam, ab46985), rabbit monoclonal for human HDAC2 (1:2000, Abcam, ab32117), rabbit polyclonal for human HDAC3 (1:1000, Santa Cruz B. I., sc-11417), rabbit monoclonal for human HDAC3 (1:2000, Abcam, ab32369), rabbit polyclonal for human HDAC4 (1:500, Santa Cruz B. I., sc-11418), rabbit polyclonal for human HDAC5 (1:500, Abcam, ab55403, non-reducing SDS-PAGE), rabbit polyclonal for human HDAC7 (1:1000, Abcam, ab137366), rabbit polyclonal for human HDAC7 (1:500, Santa Cruz B. I., sc-11421), rabbit polyclonal for human HDAC8 (1:500, Santa Cruz B. I., sc-11405), rabbit polyclonal for human HDAC9/HDRP (1:2000, Abcam, ab59718), rabbit polyclonal for human HDAC9 (1:300, Santa Cruz B. I., sc-28732), rabbit polyclonal for human HDAC10 (1:1000, Abcam, ab53096), sheep polyclonal for human CD90/Thy-1 (1:500, R&D Systems, #AF2067), rabbit polyclonal for human histone H3 [acetyl K27] (1:15000, Abcam, ab4729), rabbit polyclonal for histone H3 (1:10000, Abcam, ab1791), mouse monoclonal for acetylated tubulin [from the outer arm of *Strongylocentrotus purpuratus* (sea urchin)] (1:50000, Sigma, T7451), mouse monoclonal for human p53 (1:250, Santa Cruz B. I., sc-263), mouse monoclonal for human p21 (1:250, Abcam, ab16767), mouse monoclonal for human cyclin D1 (1:250, Abcam, ab10540), rabbit polyclonal for human survivin (1:750, Abcam, ab24479), rabbit polyclonal for human phospho-histone H3 (1:500, Abcam, ab5176), rabbit polyclonal for human Bcl-XL (1:750, Abcam, ab32370), rabbit polyclonal for human CHOP/GADD153 (1:500, Santa Cruz B. I., sc-793), mouse monoclonal for human α-SMA (1:15000, Abcam, ab119952), rabbit polyclonal for collagen α1-type I [COL1A1] (1:300, Santa Cruz B. I., sc-28657), and rabbit polyclonal for collagen type-I (1:3000, Rockland, #600-401-103). Blots were incubated with primary antibody (diluted in blocking buffer) overnight at 4°C with gentle shaking. The blots were then washed four times in 1 ×

TBS containing 0.1 % (w/v) tween 20, and incubated with respective horseradish peroxidase-conjugated secondary antibodies (DakoCytomation, Hamburg, Germany; rabbit anti-mouse-IgG, rabbit anti-goat-IgG, rabbit anti-sheep IgG, or swine anti-rabbit IgG, all diluted 1:2000 in blocking buffer) for 2 hours at room temparature. After four washes, blot membranes were developed with the Pierce® ECL Plus chemiluminescent detection system (Thermo Scientific), and emitted signals were detected with a chemiluminescence imager (Intas ChemoStar, Intas, Göttingen, Germany). Thereafter, blots were stripped using ″stripping buffer″ [2% (w/v) SDS and 50 mmol/L dithiothreitol in tris-buffered saline (TBS)] under gentle shaking at 70°C for 1h, followed by reprobing the blots using antibodies against the loading control proteins β-actin (ab8226, abcam, diluted 1:3000), GAPDH (sc-20357, Santa Cruz, diluted 1:1000) or tubulin (#T0198, Sigma, diluted 1:2000).

For quantification, band intensities in acquired TIFF/JPEG-images were analyzed by densitometric scanning and quantified using ImageJ software (Version 1.46r, NIH). The band densities were normalized to β-actin, GAPDH or tubulin.

Immunohistochemistry (IHC)

Human lungs were placed in 4% (w/v) paraformaldehyde after explantation (fixation was done for 12 – 24 h), and processed for paraffin embedding. Sections (3 µm) were cut and mounted on positively charged glass slides (Super Frost Plus, Langenbrinck). Paraffin-embedded tissue sections of normal donor and IPF-lungs were deparaffinized in xylene and rehydrated in graded alcohol. Antigens were retrieved by cooking the sections for 5 min in 10 mmol/L citrate buffer (pH 6.0) using microwave irradiation (800 W). Thereafter, sections had to cool down for 20 min at RT, followed by repeated cookings (800 W, 5 min) and coolings (20 min at RT). This

procedure was performed three times. Importantly, the citrate buffer was freshly prepared by mixing 18 mL 100mmol/L citric acid monohydrate and 82 mL 100mmol/L sodium citrate tribasic dihydrate with 900 mL distilled water.

For immunostaining, the streptavidin-biotin-alkaline phosphatase (AP) - or the streptavidin-biotin- horse radish peroxidase (HRP) method with use of the ZytoChem-Plus AP Kit (Fast Red), Broad Spectrum or the ZytoChem-Plus HRP Kit (DAB-staining, brown dye), Broad Spectrum (Zytomed Systems, Berlin, Germany) according to the manufacturer´s protocol were employed.

In the following, the primary antibodies used for IHC are listed, including the sources and dilutions: rabbit polyclonal for human proSP-C (1:750, Millipore, AB3786), rabbit monoclonal for human cytokeratin-5 [KRT5] (1:200, Abcam, ab75869), rabbit polyclonal for human smooth muscle actin [α-SMA] (1:200, Abcam, ab5694), mouse monoclonal for human p63 (1:150, Abcam, ab3239), rat monoclonal for human clara cell-protein 10 [CC10] (1:75, R&D Systems), mouse monoclonal for human FoxJ1/HFH4 (1:75, Abcam), mouse monoclonal for HDAC1 (1:50, Abcam, ab46985), rabbit polyclonal for human HDAC2 (1:50, Santa Cruz Biotechnology Inc., sc-7899), rabbit monoclonal for human HDAC2 (1:200, Abcam, ab32117), rabbit polyclonal for human HDAC3 (1:100, Santa Cruz B. I., sc-11417), rabbit polyclonal for human HDAC4 (1:50, Santa Cruz B. I., sc-11418), rabbit polyclonal for human HDAC5 (1:100, Abcam, ab55403), rabbit monoclonal for human HDAC6 (1:100, Abcam, ab133493), rabbit polyclonal for human HDAC7 (1:100, Abcam, ab137366), rabbit polyclonal for human HDAC8 (1:50, Santa Cruz B. I., sc-11405), rabbit polyclonal for human HDAC9/HDRP (1:100, Abcam, ab59718), rabbit polyclonal for human HDAC10 (1:100, Abcam, ab53096) and rabbit polyclonal for human survivin (1:200, Abcam, ab24479). In general, sections were incubated for 2h with primary antibodies, which were diluted in PBS containing 2% (w/v) BSA.

Detection was performed with a polyvalent secondary biotinylated antibody (rabbit, mouse, rat, guinea pig, provided by the ZytoChem-Plus AP Kit/or ZytoChem-Plus HRP Kit, 20 min incubation) followed by incubation with AP/or HRP conjugated streptavidin (20 min). Sections were then developed with Fast Red/or DAB substrate solution, and the reaction was terminated by washing in distilled water. The stained sections were counterstained with hemalaun (Mayers hemalaun solution, WALDECK Division CHROMA GmbH & CO KG, Münster, Germany) and mounted in Glycergel (DakoCytomation).

Control sections were treated with PBS-2%BSA alone or with rabbit or mouse primary antibody isotype control (#NB810-56910 and #AM03096PU-N, both Acris Antibodies GmbH, Germany) to determine the specificity of the staining.

Lung tissue sections were scanned with a Mirax Desk slide scanning device (Mirax Desk, Zeiss, Germany), and examined histopathologically at 100×, 200×, 400× and 800× original magnification. IHC for mentioned antibodies was undertaken in 10 IPF- and 5 control-lung samples.

Statistics

For the statistical comparison of differences between two groups (IPF vs. control), the Mann Whitney-test was applied. For the statistical comparison of differences between three groups (LBH589-treatment vs. vehicle-treatment, VPA-treatment vs. vehicle-treatment, VPA-treatment vs. LBH589-treatment) the Kruskal-Wallis test with the Dunn´s multiple comparison test as post-test was applied. For statistics, the software GraphPad Prism version 5.02 was employed. A p-value < 0.05 was considered statistically significant.

Supplementary References

[S1] Jordana M, Newhouse MT, Gauldie J. Alveolar macrophage/peripheral blood monocyte-derived factors modulate proliferation of primary lines of human lung fibroblasts. *J Leukoc Biol* 1987;42:51-60.

[S2] Jordana M, Befus AD, Newhouse MT, et al. Effect of histamine on proliferation of normal human adult lung fibroblasts. *Thorax* 1988;43:552-558.

[S3] Anne M, Sammartino D, Barginear MF, et al. Profile of panobinostat and its potential for treatment in solid tumors: An update. *Onco Targets Ther* 2013;6:1613-1624.

[S4] Xu WS, Parmigiani RB, Marks PA. Histone deacetylase inhibitors: Molecular mechanisms of action. *Oncogene* 2007;26:5541-5552.

[S5] Kramer OH, Zhu P, Ostendorff HP, et al. The histone deacetylase inhibitor valproic acid selectively induces proteasomal degradation of HDAC2. *EMBO J* 2003;22:3411-3420.

[S6] Korfei M, Schmitt S, Ruppert C, et al. Comparative proteomic analysis of lung tissue from patients with idiopathic pulmonary fibrosis (IPF) and lung transplant donor lungs. *J Proteome Res* 2011;10:2185-2205.

Table E1: Primers used in semiquantitative RT-PCR (homo sapiens)

Gene/Name of primer	Primer-Sequence	Annealing Temp.(T_A)	Size of PCR product	No. of Cycles
HDAC1 forward	5´- GCC GCA AGA ACT CTT CCA AC - 3´	63°C	140 bp	28
HDAC1 reverse	5´- CTT GAC CCC TTT GGC TTC TG - 3´			
HDAC2 forward	5´- CAG GAG ACT TGA GGG ATA TTG G - 3´	65°C	320 bp	25
HDAC2 reverse	5´- ATG TGT CCA ACA TCG AGC AAC - 3´			
HDAC3 forward	5´- CCG GTT ATC AAC CAG GTA GTG - 3´	64°C	321 bp	25-26
HDAC3 reverse	5´- GGT GCT GAC ATC TGG ATG AAG - 3´			
HDAC4 forward	5´- CTT CTG CAG CAG AGG TTG AG - 3´	63°C	267 bp	28
HDAC4 reverse	5´- TCT GAA GGC CGC CAA GTA C - 3´			
HDAC5 forward	5´- TCA ACC GGC AGA AGC TAG AC - 3´	63°C	319 bp	28
HDAC5 reverse	5´- TTG CCC ACG TTC AAC TTC TG - 3´			
HDAC6 forward	5´- CCC AGC ACA GTC TTA TGG - 3´	63°C	320 bp	29
HDAC6 reverse	5´- AGG AAA GCA GCA ATG TAG - 3´			
HDAC7 forward	5´- CTC AAA CTG GAC AAC GGG AAG - 3´	63°C	270 bp	27
HDAC7 reverse	5´- GGC CAC TGA GTT GAA GAA GC - 3´			
HDAC8 forward	5´- GTC CCG AGT ATG TCA GTA TGT G - 3´	65°C	222 bp	27
HDAC8 reverse	5´- CTA TGG AGT CCG GAT GAT CAT C - 3´			
HDAC9 forward	5´- GAA AGG GCA GTG GCA AGT AC - 3´	63°C	222 bp	30
HDAC9 reverse	5´- ATC TTG TGC TCC TGG TAA TGT G - 3´			
HDAC10 forward	5´- GCA GGT GAA CAG TGG TAT AGC - 3´	63°C	220 bp	28
HDAC10 reverse	5´- CGT GGA GAC ATG GAA CAT GG - 3´			
HDAC11 forward	5´- AGG GCT ACC ATC ATT GAT CTT G - 3´	63°C	222 bp	28
HDAC11 reverse	5´- CTG GAG GGA TTT CTT GAT GTT C - 3´			
SIRT1 forward	5´- CAA GCT CTA GTG ACT GGA CTC - 3´	64°C	321 bp	30
SIRT1 reverse	5´- CAT CCC TTG ACC TGA AGT CAG- 3´			
SIRT2 forward	5´- CGG TAC ATG CAG AGC GAA C - 3´	60°C	221 bp	27
SIRT2 reverse	5´- TGC CCA GGA TAG AGT TCC TTG - 3´			
GAPDH forward	5´- ACC CAG AAG ACT GTG GAT GG - 3´	59°C	320 bp	24
GAPDH reverse	5´- GTG TCG CTG TTG AAG TCA GAG - 3´			
ACTB forward	5´- ACC CTG AAG TAC CCC ATC G - 3´	60°C	220 bp	25
ACTB reverse	5´- CAG CCT GGA TAG CAA CGT AC - 3´			
P53 forward	5´- CCT CAG CAT CTT ATC CGA GTG - 3´	64°C	223 bp	25
P53 reverse	5´- GTA GAT TAC CAC TGG AGT CTT CC – 3´			
CIP1 forward	5´- GAT GGA ACT TCG ACT TTG TCA C – 3´	61°C	220 bp	22
CIP1 reverse	5´- GGC ACA AGG GTA CAA GAC AG – 3´			
PUMA forward	5´- ATG GCG GAC GAC CTC AAC – 3´	58°C	119 bp	28
PUMA reverse	5´- CTG GGT AAG GGC AGG AGT C – 3´			
ACTA2 forward	5´- GAG ATC TCA CTG ACT ACC TCA TG – 3´	60°C	269 bp	26
ACTA2 reverse	5´- AGC AGA CTC CAT CCC GAT G - 3´			
COL1A1 forward	5´- TGC CAC TCT GAC TGG AAG AG – 3´	60°C	320 bp	20
COL1A1 reverse	5´- TTG CAG TGG TAG GTG ATG TTC- 3´			
COL3A1 forward	5´- TTA CAA GGC TTA CCT GGT ACA G - 3´	59°C	269 bp	25
COL3A1 reverse	5´- CCA GGC ATT CCT TGC AGA C - 3´			
FN forward	5´- CAT ACC ACG TAG GAG AAC AGT G - 3´	62°C	221 bp	20
FN reverse	5´- AGG CAT GAA GCA CTC AAT TGG - 3´			
CNN1 forward	5´- GAG TGA AGT ACG CAG AGA AGC - 3´	59°C	269 bp	26
CNN1 reverse	5´- CTC GAA GAT CTG CCG CTT G - 3´			

Table E1 continued: Primers used in semiquantitative RT-PCR (homo sapiens)

Gene/Name of primer	Primer-Sequence	Annealing Temp.(T_A) *	Size of PCR product	No. of Cycles
P4HTM forward	5´- TGG ATT ACC TGC CAG AGA GAC - 3´	64°C	272 bp	26
P4HTM reverse	5´- AGT CTC AGG GTC ATG TAC TGT AG - 3´			
VIM forward	5´- AAG CAG GAG TCC ACT GAG TAC -3´	64°C	270 bp	25
VIM reverse	5´- CTT CCT GTA GGT GGC AAT CTC - 3´			
CCND1 forward	5´- CGA GAA GCT GTG CAT CTA CAC - 3´	62°C	221 bp	26
CCND1 reverse	5´- ACT TCA CAT CTG TGG CAC AAG - 3´			
BIRC5 forward	5´- AAA GCA TTC GTC CGG TTG C - 3´	57°C	161 bp	25-26
BIRC5 reverse	5´- GCA CTT TCT TCG CAG TTT CC - 3´			
UBE2L6 forward	5´- CGT TCA AGC CTC CCA TGA TC - 3´	60°C	220 bp	25
UBE2L6 reverse	5´- AGC TCC GGA TTC TGT GTC AG - 3´			
ATF6 forward	5´- ACT CAG GGA GTG AGC TAC AAG - 3´	63°C	270 bp	25
ATF6 reverse	5´- GGA GGA TCC TGG TGT CCA TC - 3´			
CHOP forward	5´- ACT CTC CAG ATT CCA GTC AGA G - 3´	61°C	220 bp	24
CHOP reverse	5´- GCC TCT ACT TCC CTG GTC AG - 3´			

*It has to be noted that the annealing temperature (T_A) for listed primers is only valid for Phire-Hot-Start-II-DNA-Polymerase. The annealing rules for Phire II are different from many common DNA polymerases (such as *Taq* DNA polymerases). As a basic rule, for primers > 20 nt, the T_A is T_m +3°C of the lower T_m primer. For primers ≤ 20 nt, the T_A has to be equal to the T_m of the lower T_m primer.
T_m = melting temperature.

Primers were designed using “GeneFisher/GeneFisher2“-Software - interactive PCR primer design. (http://bibiserv.techfak.unibielefeld.de/genefisher2/).
GeneFisher - software support for the detection of postulated genes. *Robert Giegerich, Folker Meyer and Chris Schleiermacher.* Proc Int Conf Intell Syst Mol Biol. 1996;4:68-77.
In the majority, intron-spanning primers were chosen.

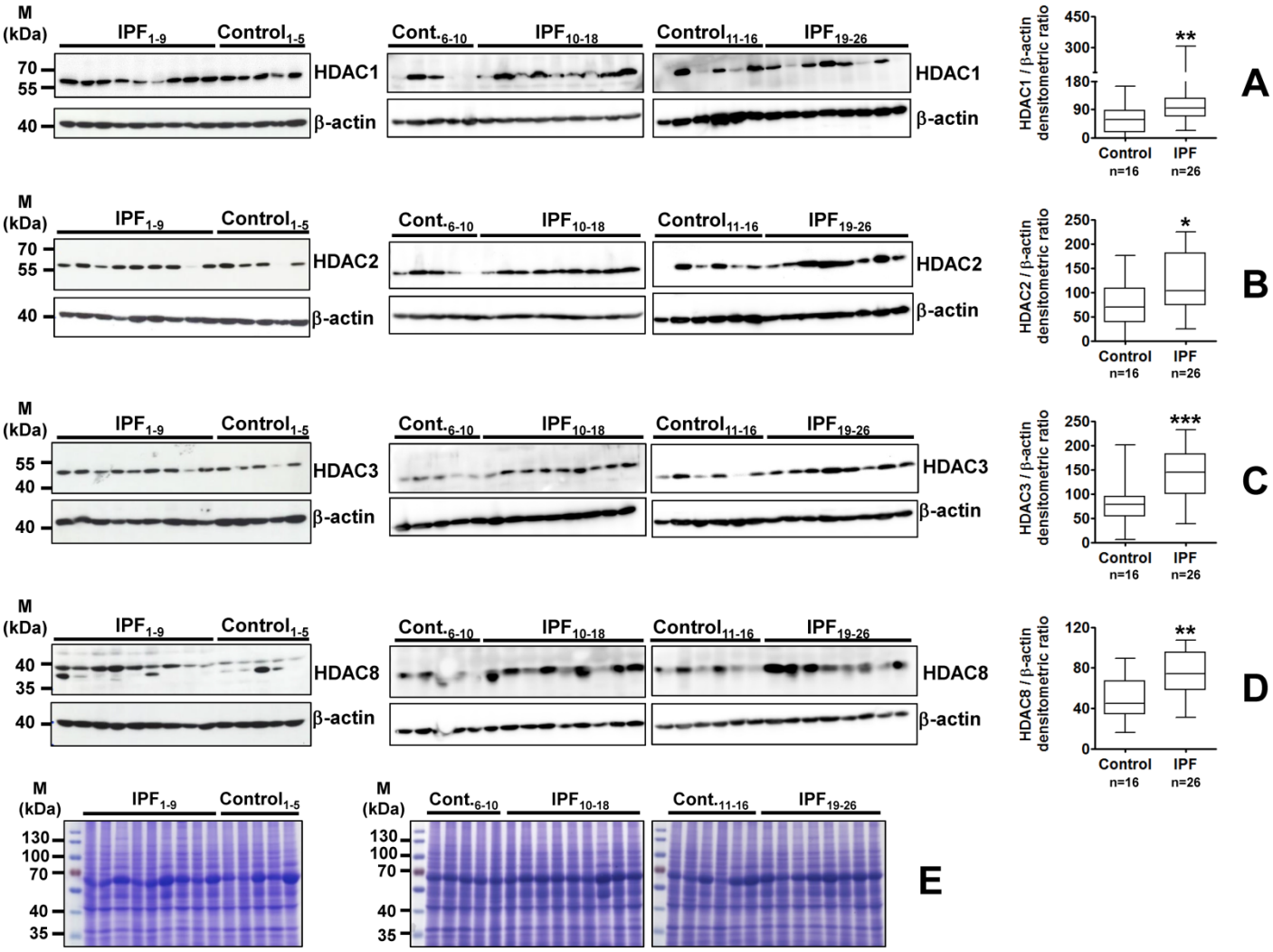

Supplementary-Figure S1: Upregulation of class-I-histone deacetylases in lung tissue from patients with idiopathic pulmonary fibrosis (IPF).

Representative immunoblots (left) and quantitative immunoblot analysis (right) of subpleural lung tissue from patients with sporadic IPF (n=26) and non-diseased control-lungs (control, n=16) using specific antibodies against HDAC1 (**A**), HDAC2 (**B**), HDAC3 (**C**), HDAC8 (**D**), and β-actin as loading control. Representative Coomassie stained gels of 50 µg proteins extracted from IPF- and control-lungs are shown in (**E**). Densitometric ratios of the respective protein to β-actin are depicted as a box-and whisker diagram (*box* indicates 25th and 75th, *horizontal line* indicates the 50th percentile [median], and extensions above and below reflect extreme values). *p < 0.05, **p < 0.01, ***p < 0.001; by Mann Whitney-test.

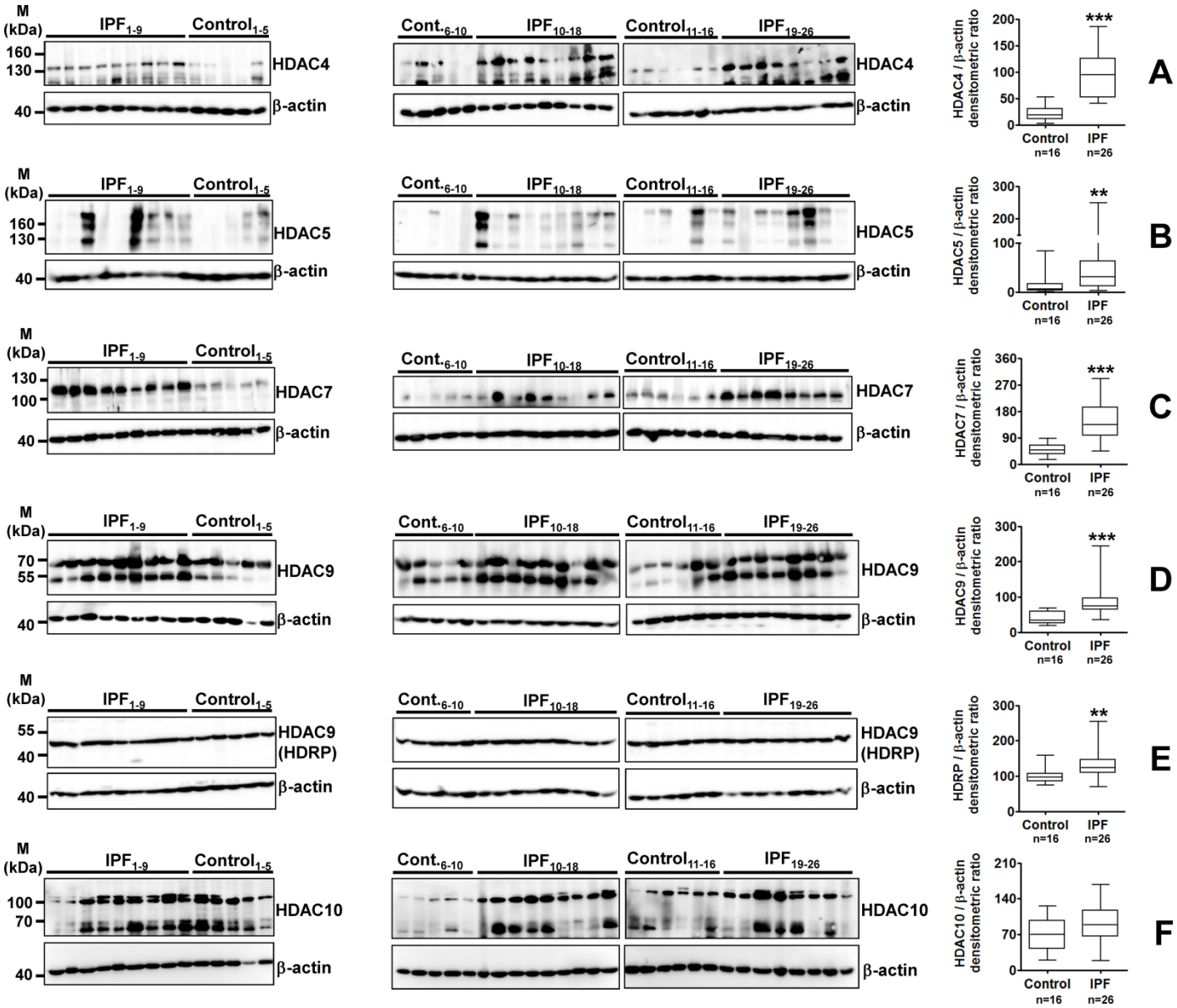

Supplementary-Figure S2: Upregulation of class-II-histone deacetylases in lung tissue from patients with idiopathic pulmonary fibrosis (IPF).
Representative immunoblots (left) and quantitative immunoblot analysis (right) of subpleural lung tissue from patients with sporadic IPF (n=26) and non-diseased control-lungs (control, n=16) using specific antibodies against HDAC4 (**A**), HDAC5 (**B**), HDAC7 (**C**), HDAC9 (**D**), HDAC9 isoform HDRP (**E**), HDAC10 (**F**), and β-actin as loading control. Densitometric ratios of the respective protein to β-actin are depicted as a box- and whisker diagram (*box* indicates 25th and 75th, *horizontal line* indicates the 50th percentile [median], and extensions above and below reflect extreme values). **p < 0.01, ***p < 0.001; by Mann Whitney-test.

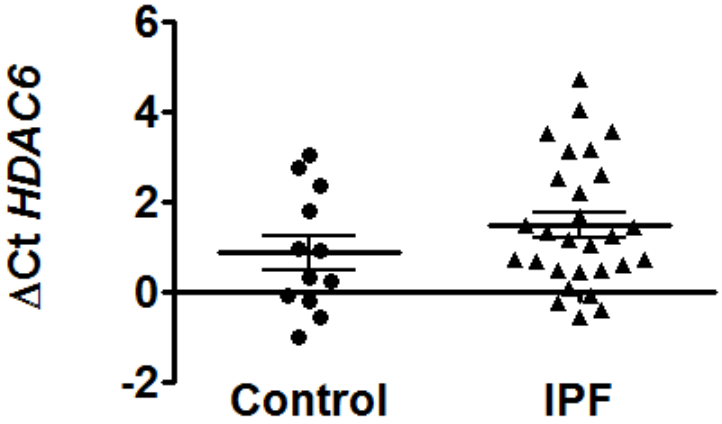

Supplementary-Figure S3: Gene expression analysis for class-IIb-histone deacetylase HDAC6 in control- (n=12) and IPF- (n=31) lung tissues by qRT-PCR.

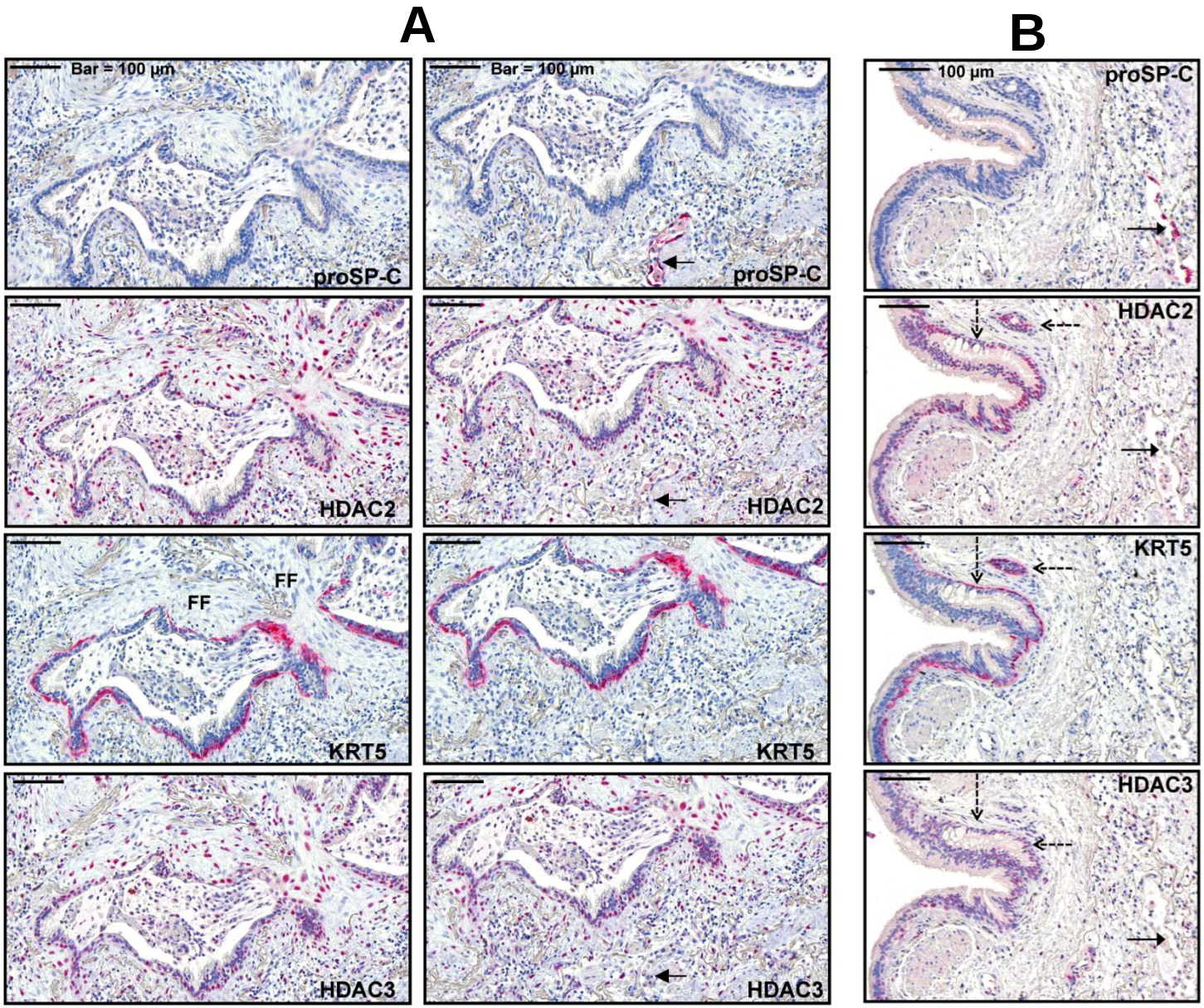

Supplementary-Figure S4: Induction of class-I-histone deacetylases HDAC2 and HDAC3 in fibroblast foci and abnormal bronchiolar epithelium of idiopathic pulmonary fibrosis (IPF)-lungs.

(**A**) Representative immunohistochemistry for prosurfactant protein-C (proSP-C), HDAC2, HDAC3 and cytokeratin-5 (KRT5) in serial sections of IPF-lung tissue. In IPF, fibroblast foci (FF) as well as overlying abnormal bronchiolar basal cells (positive for KRT5) indicated strong nuclear induction of HDAC2 and HDAC3. IPF-AECII (indicated by arrows and proSP-C-staining) did neither express HDAC2 nor HDAC3.

(**B**) Representative immunohistochemistry for proSP-C, HDAC2, HDAC3 and KRT5 in serial sections of IPF-lung tissue. IPF-AECII (indicated by arrows and proSP-C staining) did neither express HDAC2 nor HDAC3, which were observed to be expressed in the nucleus of ciliated bronchial cells in the very same IPF-lung section. Furthermore, ″normal-sized″, small bronchiolar basal cells (indicated by dashed arrows and KRT5-staining) in IPF-lungs did neither express HDAC2 nor HDAC3.

Korfei et al_Supplementary-Figure S4C

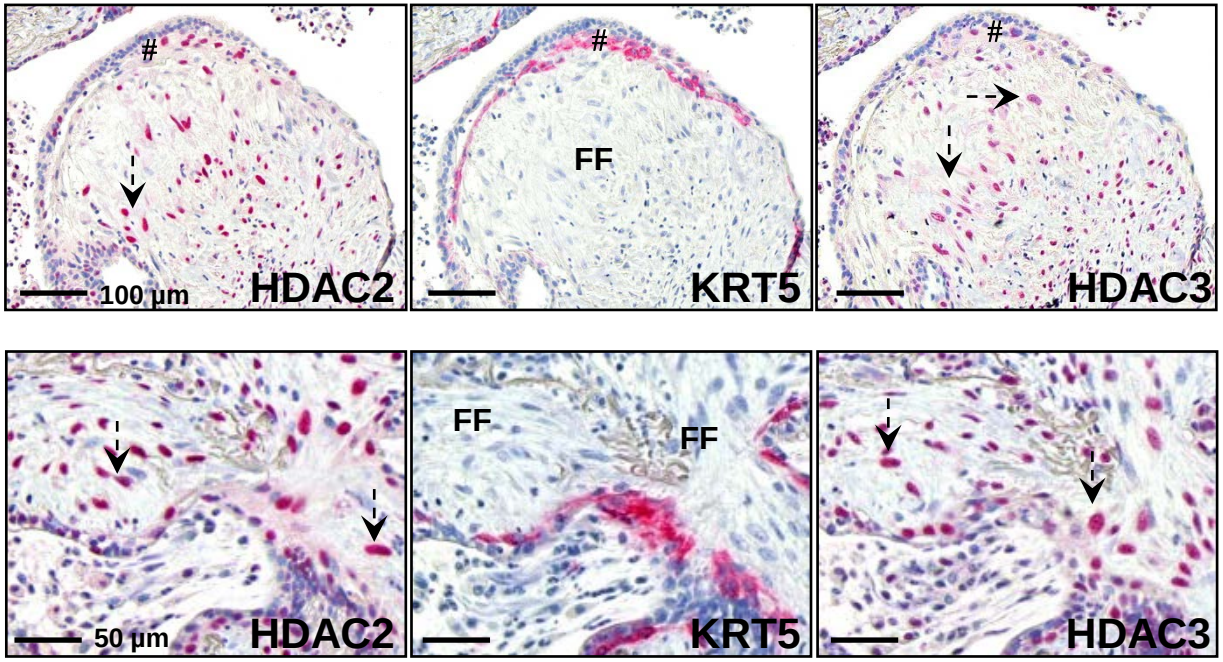

Supplementary-Figure S4C: Nuclear induction of class-I-histone deacetylases HDAC2 and HDAC3 in fibroblast foci and abnormal bronchiolar epithelium of idiopathic pulmonary fibrosis (IPF)-lungs.
Representative immunohistochemistry for HDAC2, HDAC3 and cytokeratin-5 (KRT5) in serial sections of IPF-lung tissue. In IPF, fibroblast foci (FF) as well as overlying abnormal bronchiolar basal cells (positive for KRT5) indicated strong nuclear induction of HDAC2 and HDAC3. The figures in the lower panel represent higher resolution images of supplementary figure S4A.

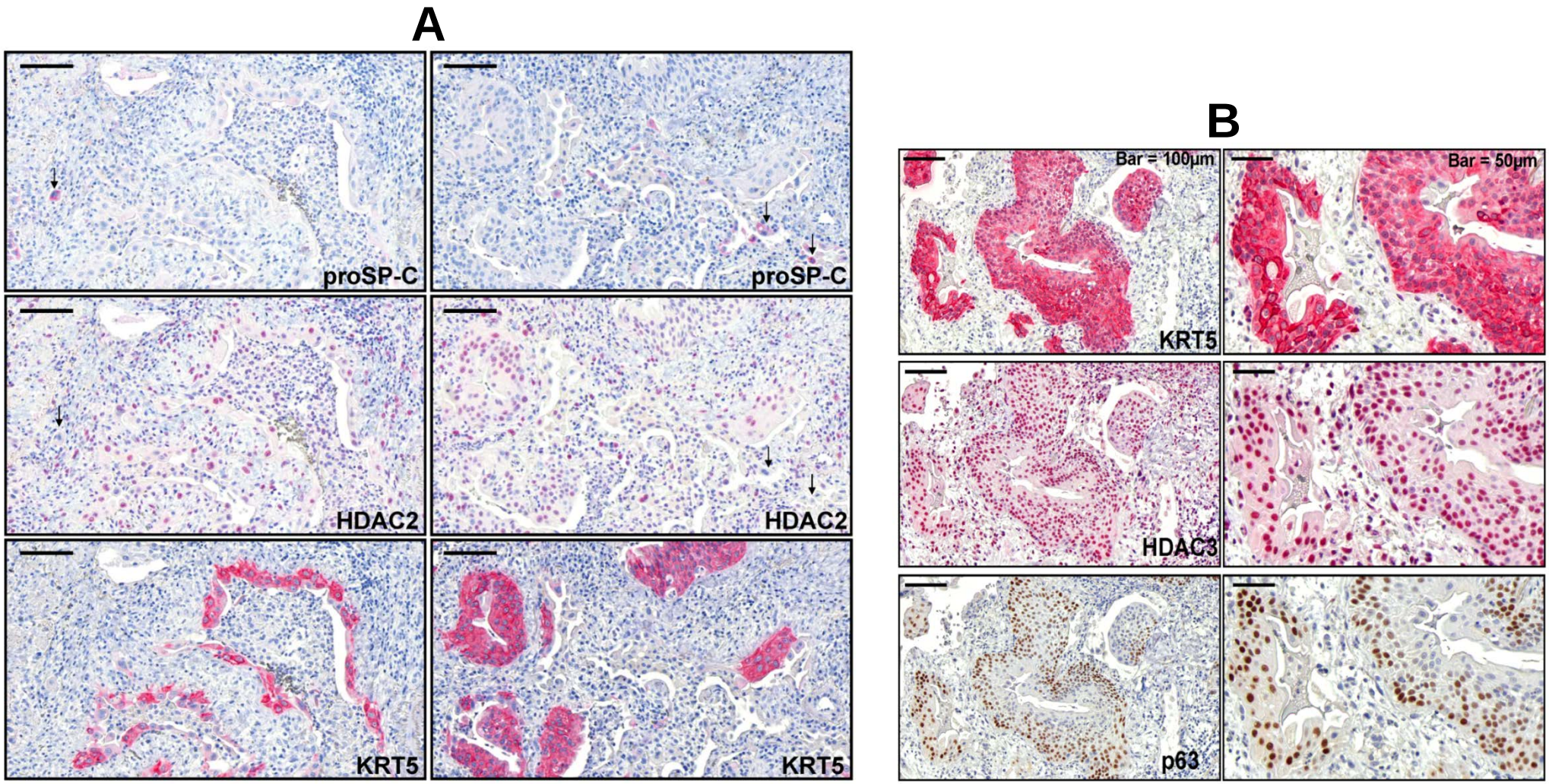

Supplementary-Figure S5: Induction of class-I-histone deacetylases HDAC2 and HDAC3 in hyperplastic bronchiolar basal cells in abnormal bronchiolar structures of idiopathic pulmonary fibrosis (IPF)-lungs.

(**A**) Representative immunohistochemistry for proSP-C, HDAC2, and KRT5 in serial sections of IPF-lung tissue. In IPF, induction of nuclear HDAC2 expression was observed in ″hyperplastic″ bronchiolar basal cells as well as in basal cell layers of squamous metaplasia (indicated by KRT5-staining) in areas of advanced bronchiolization. IPF-AECII (indicated by arrows and proSP-C-staining) did not express HDAC2.

(**B**) Representative immunohistochemistry for HDAC3, KRT5 and p63 in serial sections of IPF-lung tissue. In IPF, strong nuclear induction of HDAC3 was observed in bronchiolar basal cell sheets of squamous metaplasia (indicated by KRT5 - and nuclear p63-staining) in areas of advanced bronchiolization.

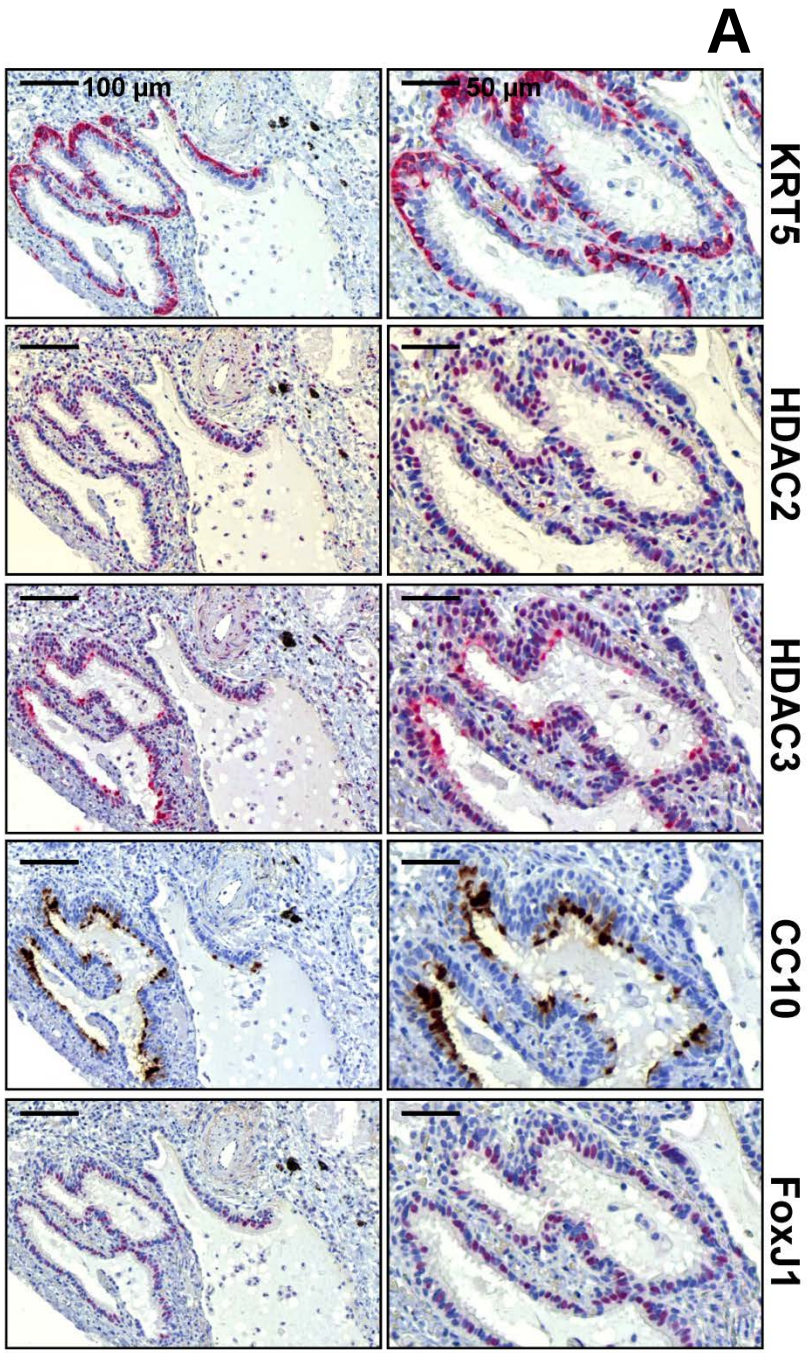

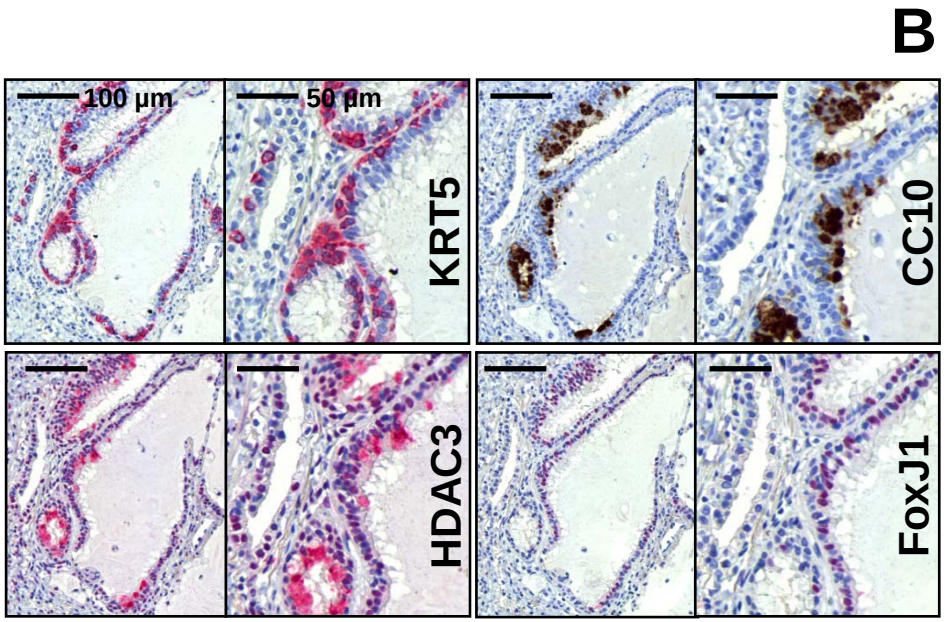

Supplementary-Figure S6: Overexpression of class-I-histone deacetylases HDAC2 and HDAC3 in ciliated bronchial cells in idiopathic pulmonary fibrosis (IPF) lungs. Cytoplasmic expression of HDAC3 in Clara cells of idiopathic pulmonary fibrosis (IPF)-lungs.

(**A**) Representative immunohistochemistry for KRT5, HDAC2, HDAC3, Clara Cell-protein 10 (CC10), and Forkhead box protein J1 (FoxJ1) in serial sections of IPF-lung tissue. Ciliated bronchial cells in IPF-lungs (indicated by FoxJ1-staining) revealed strong nuclear expression of HDAC2 and HDAC3. Additionally, non-ciliated Clara cells (positive for CC10) revealed strong cytoplasmic expression of HDAC3, but not of HDAC2.

(**B**) Representative immunohistochemistry for KRT5, HDAC3, CC10, and FoxJ1 in serial sections of IPF-lung tissue.

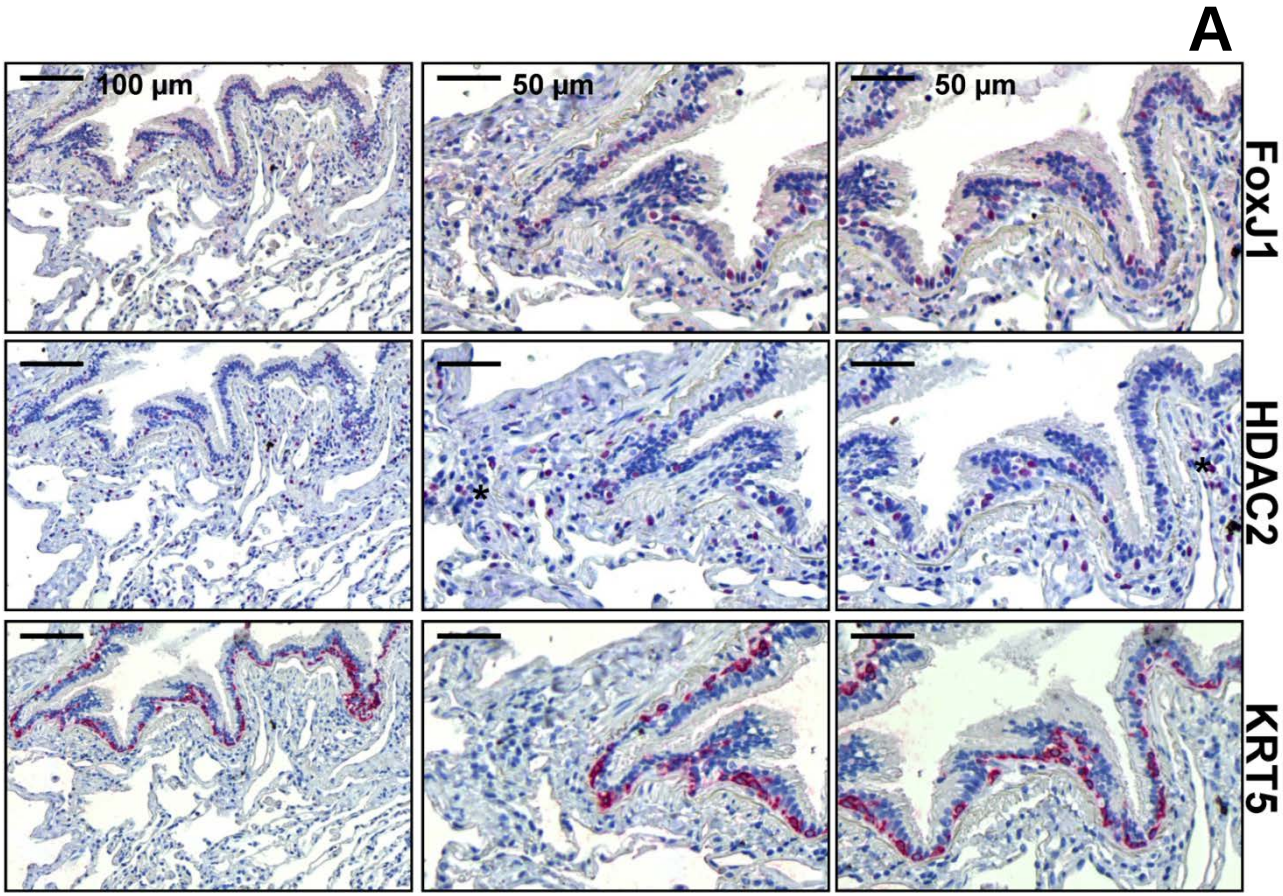

Supplementary-Figure S7: Expression of class-I-histone deacetylases HDAC2 and HDAC3 in normal control-lungs.
(**A**) Representative immunohistochemistry for proSP-C, HDAC2 and KRT5 in serial sections of control-lung tissue. ″Normal-sized″, small basal cells in normal bronchioles of control-lungs indicated no staining for HDAC2 and HDAC3 (not shown). Similarly, ciliated bronchial cells of normal control-lungs indicated no or only faint expression of HDAC2 and HDAC3 (not shown). Only few cells in the interstitium (presumably interstitial inflammatory cells, indicated by asterisks) of control-lungs expressed HDAC2 in the nucleus. (**B**) Representative immunohistochemistry for HDAC3 and proSP-C in serial sections of control-lung tissue. Clara Cells of control-lungs indicated robust cytoplasmic expression of HDAC3 (left panel), whereas type-II alveolar epithelial cells (AECII, indicated by arrows and proSP-C staining) did not express HDAC3 (right panel). Single interstitial cells in normal lungs (presumably interstitial inflammatory cells, indicated by asterisks) revealed strong nuclear expression of HDAC3.

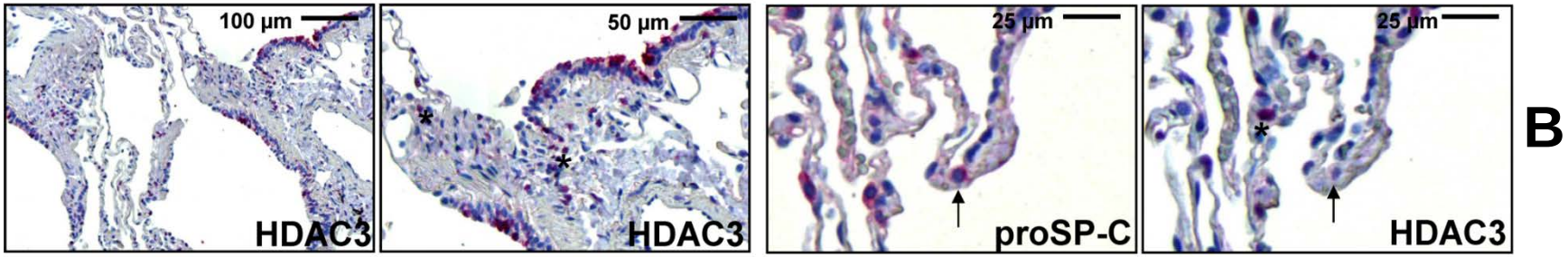

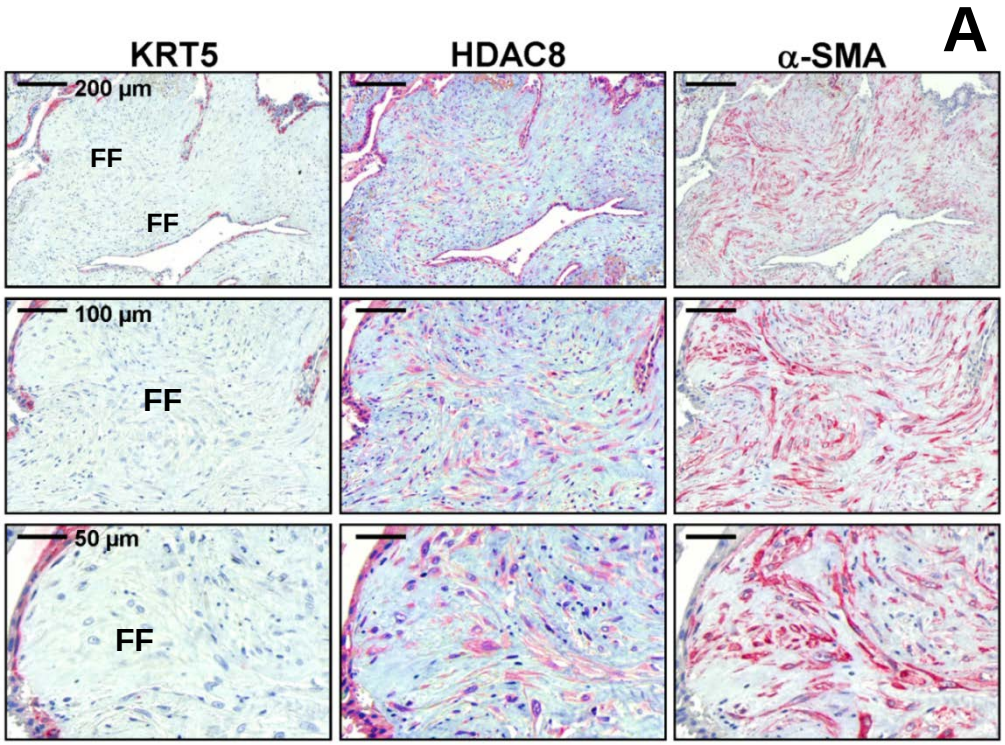

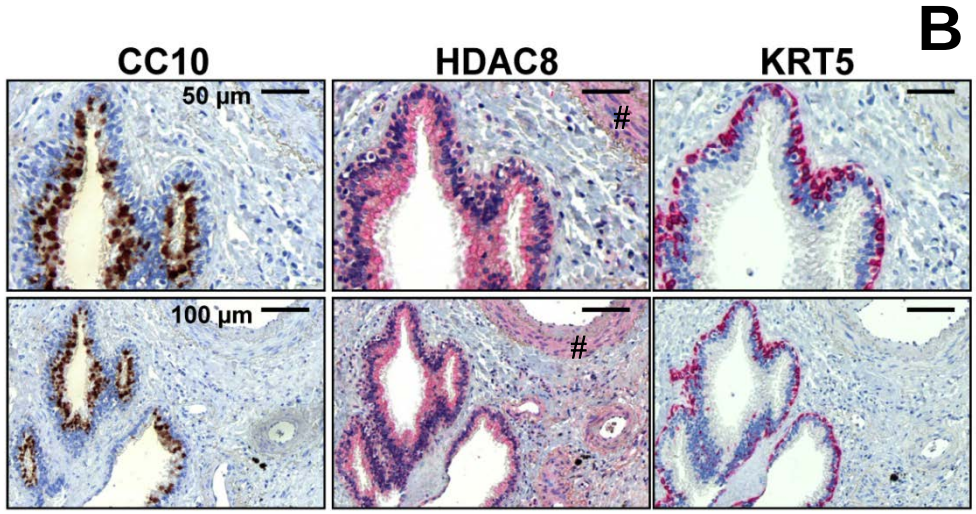

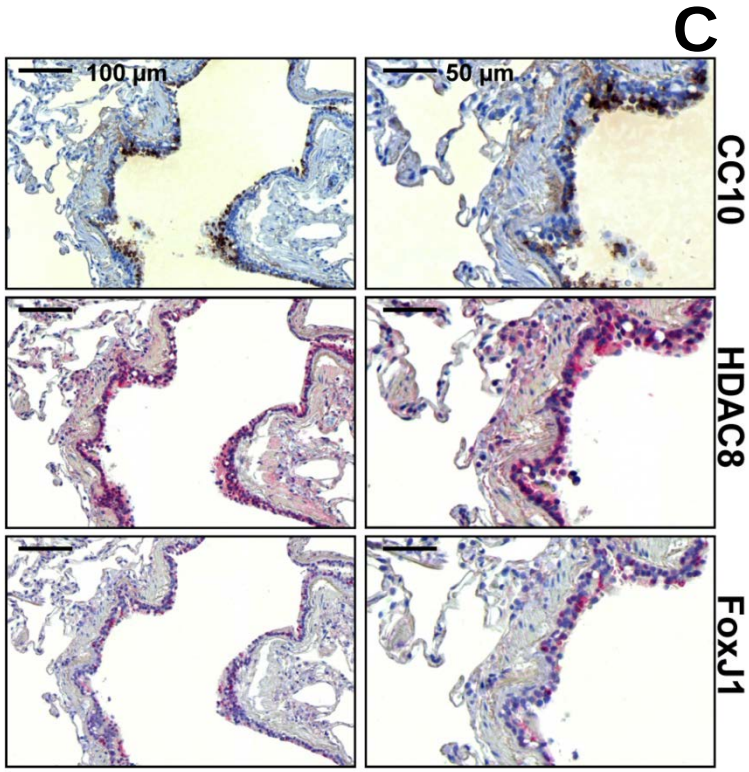

Supplementary-Figure S8: Expression of class-I-histone deacetylase HDAC8 in idiopathic pulmonary fibrosis (IPF)- and control-lungs.

(**A**) Representative immunohistochemistry for KRT5, HDAC8 and α-SMA in serial sections of IPF-lung tissue. In IPF, fibroblast foci (FF) as well as overlying abnormal bronchiolar basal cells (positive for KRT5) indicated cytoplasmic expression of HDAC8. (**B**) Representative immunohistochemistry for CC10, HDAC8 and KRT5 in serial sections of IPF-lung tissue. In IPF, cytoplasmic expression of HDAC8 was observed in bronchiolar basal cells (positive for KRT5), Clara cells (positive for CC10) as well as in ciliated bronchial cells. In addition, vascular smooth muscle cells (VSMCs, indicated by hashmark) showed also cytoplasmic staining for HDAC8. (**C**) Representative immunohistochemistry for CC10, HDAC8 and FoxJ1 in serial sections of control-lung tissue. Robust expression of HDAC8 was observed in Clara cells (positive for CC10) as well as in ciliated bronchial cells (positive for FoxJ1) of control-lungs.

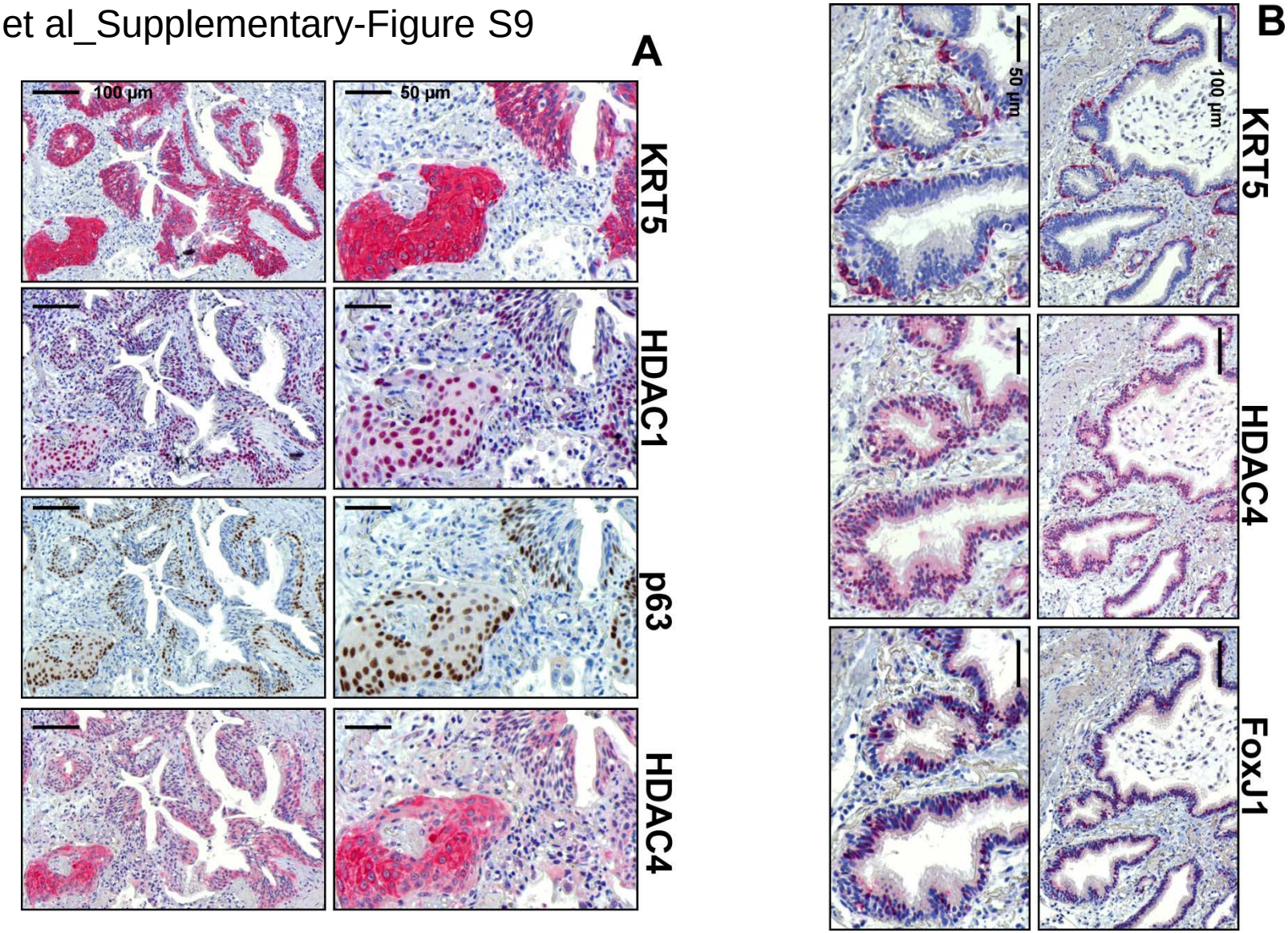

Supplementary-Figure S9: Expression and localization of class-I-histone deacetylase HDAC1 and Class-IIa-histone deacetylase HDAC4 in idiopathic pulmonary fibrosis (IPF)-lungs.

(**A**) Representative immunohistochemistry for KRT5, HDAC1, p63 and HDAC4 in serial sections of IPF-lung tissue. Bronchiolar basal cell layers of squamous metaplasia (indicated by KRT5- and nuclear p63-staining) in areas of advanced bronchiolization of IPF-lungs indicated a predominantly cytoplasmic expression of HDAC4, and a nuclear expression of HDAC1.

(**B**) Representative immunohistochemistry for KRT5, HDAC4 and FoxJ1 in serial sections of IPF-lung tissue. Ciliated bronchial cells in abnormal bronchioles of IPF-lungs (marked by FoxJ1-staining) indicated strong nuclear (and weak cytoplasmic) staining for HDAC4.

Supplementary-Figure S10: Expression and localization of Class-IIa-histone deacetylase HDAC4 in idiopathic pulmonary fibrosis (IPF)-lungs.

(**A**) Representative immunohistochemistry for p63, KRT5, HDAC4, α-SMA and HDAC10 in serial sections of IPF-lung tissue. Myofibroblastic cells of fibroblast foci (indicated by dashed arrows) as well as overlying abnormal bronchiolar basal cells (indicated by KRT5- and nuclear p63-staining) showed a predominantly cytoplasmic expression of HDAC4. In addition, HDAC10 was expressed in the nucleus and cytoplasm of myofibroblasts.

(**B**) Representative immunohistochemistry for KRT5, HDAC2, HDAC4, α-SMA and survivin in serial sections of IPF-lung tissue. HDAC4 indicated a marked cytoplasmic expression in the ″mature″ smooth muscle in areas of dense, older fibrosis, thereby co-localizing with nuclear HDAC2- and survivin expression.

(**C**) Representative immunohistochemistry for KRT5, proSP-C, HDAC4, Forkhead box protein J1 (FOXJ1) and Clara cell-protein-10 (CC10) in serial sections of IPF-lung tissue. In IPF, strong nuclear staining for HDAC4 is observed in ciliated bronchial cells (indicated by arrowheads and FOXJ1 staining) and basal cells (positive for KRT5) of abnormal hyperplastic bronchioles. Type-II alveolar epithelial cells (AECII, indicated by arrows and proSP-C-staining) and Clara cells (positive for CC10) in IPF-lungs did not express HDAC4.

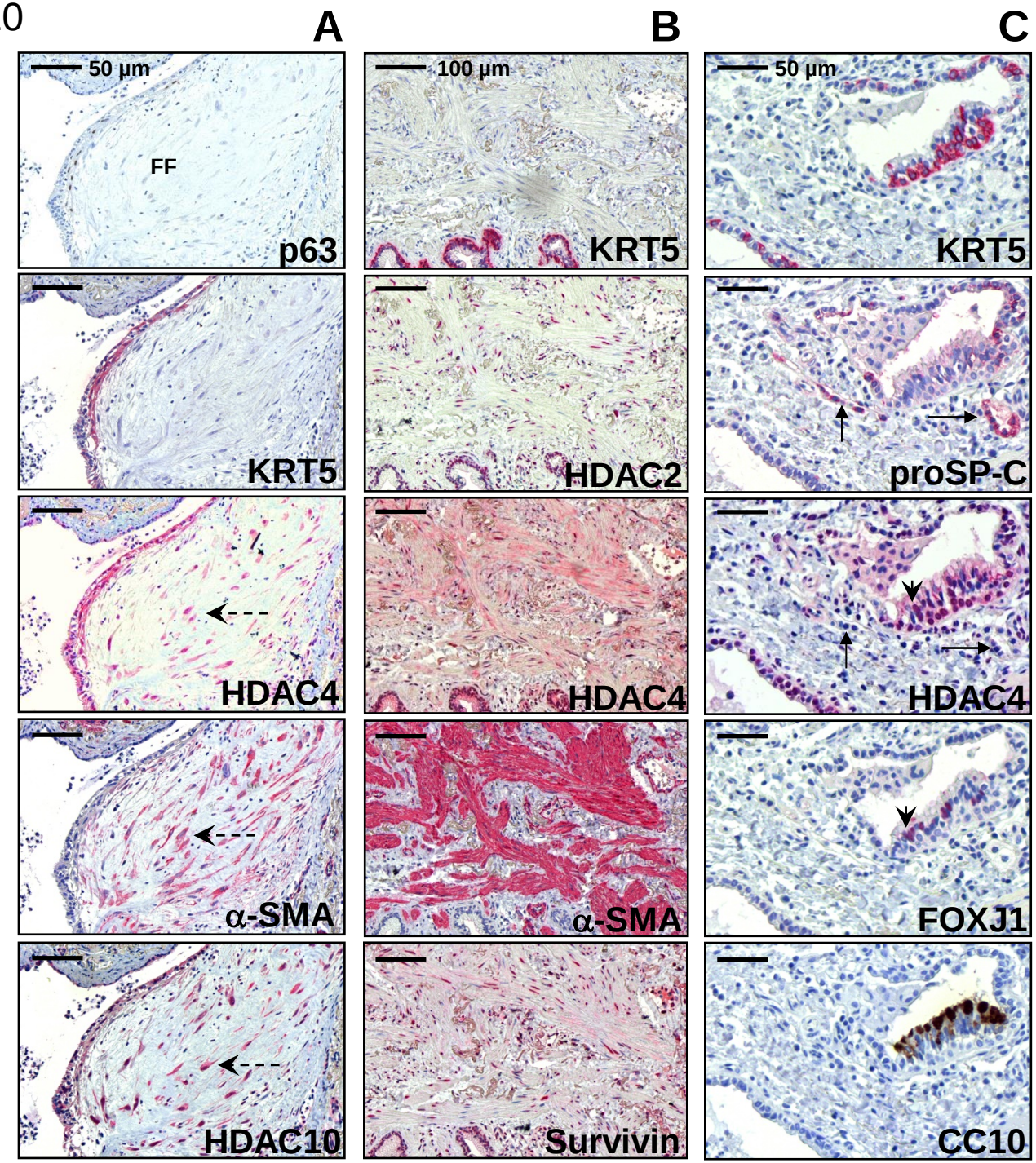

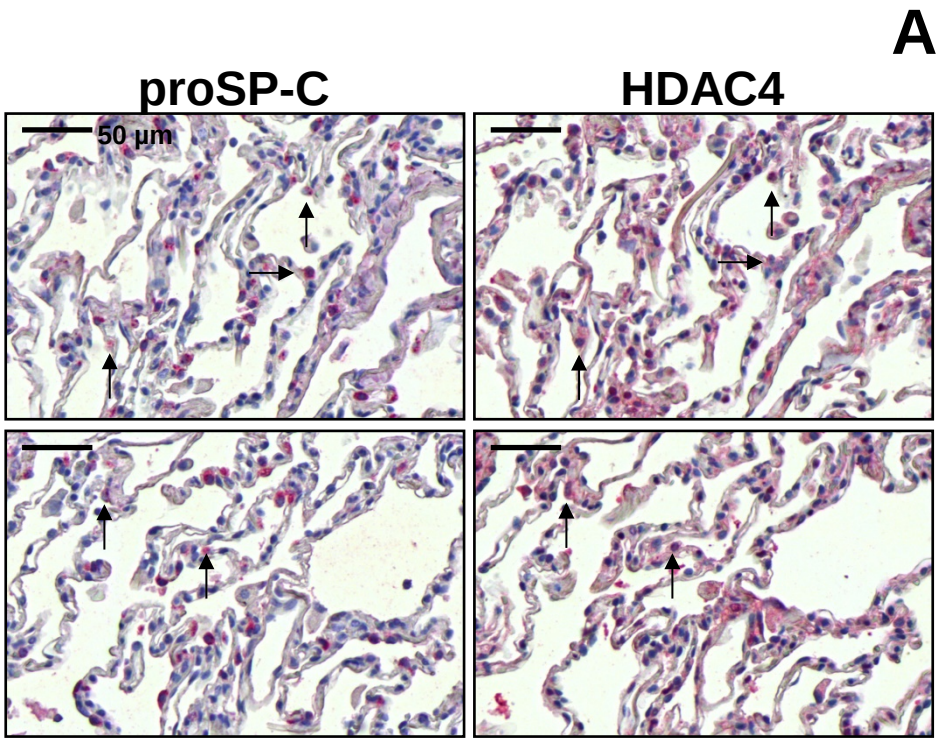

Supplementary-Figure S11: Expression and localization of class-IIa-histone deacetylases HDAC4 and HDAC7 in normal control-lungs.

(**A**) Representative immunohistochemistry for HDAC4 and proSP-C in serial sections of control donor-lungs. In the normal lung, HDAC4 is expressed in the nucleus of type-II alveolar epithelial cells (AECII, indicated by arrows and proSP-C staining). (**B**) Representative immunohistochemistry for KRT5, HDAC7, and proSP-C in serial sections of control-lung tissue. In control-lungs, moderate expression for HDAC7 is observed in bronchial epithelium (BE); AECII in normal lungs (indicated by arrows and proSP-C staining) revealed faint cytoplasmic HDAC7 expression.

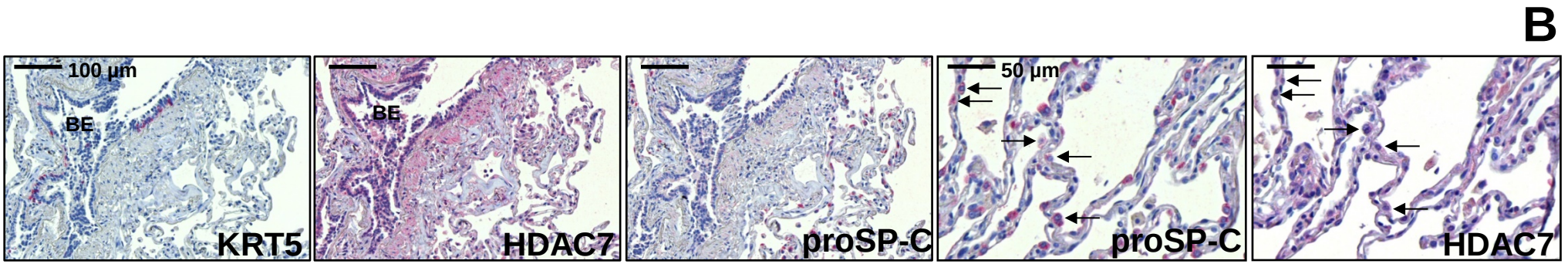

Korfei et al_Supplementary-Figure S12

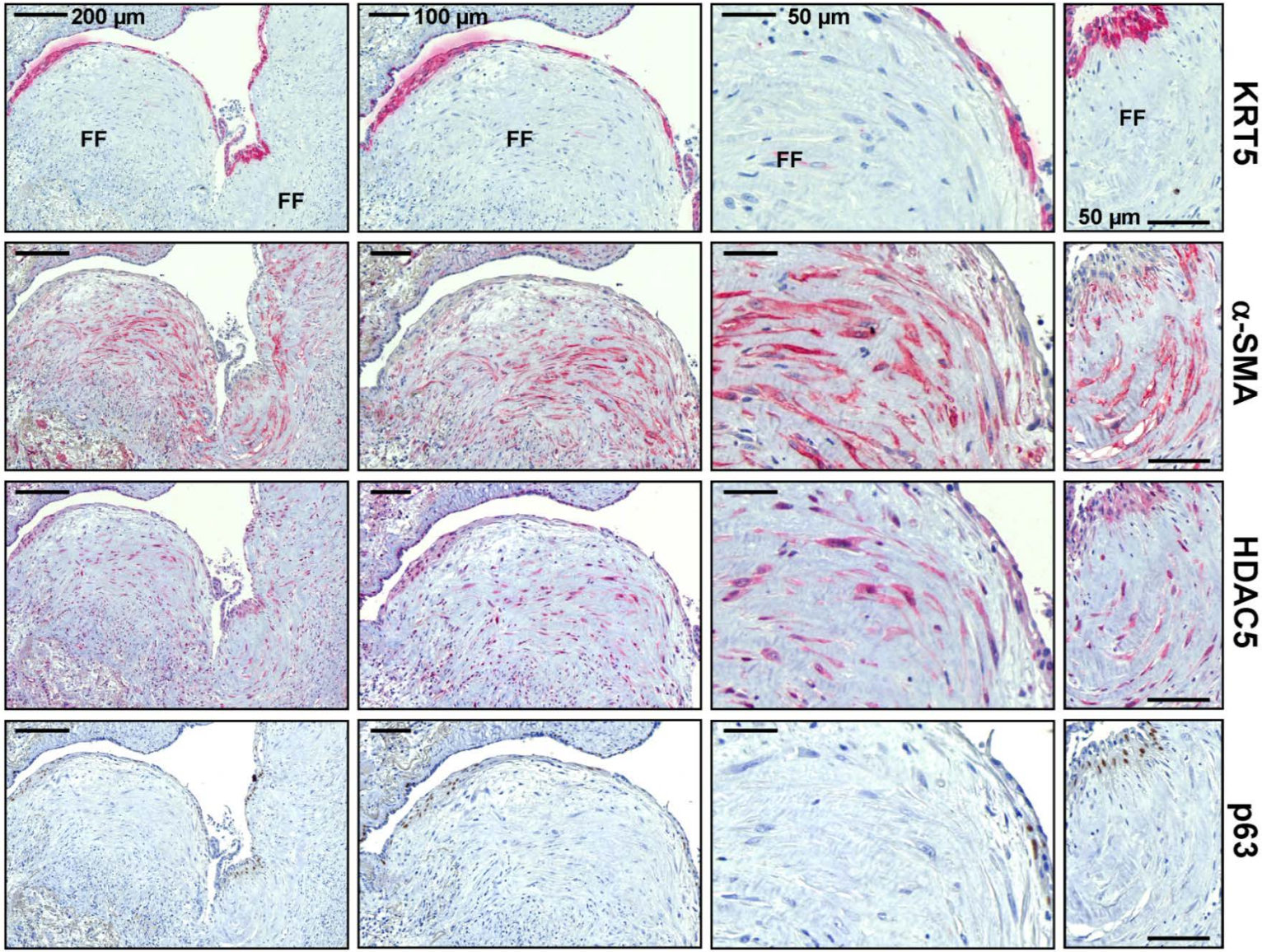

Supplementary-Figure S12: Induction of class-IIa-histone deacetylase HDAC5 in fibroblast foci and abnormal bronchiolar epithelium of idiopathic pulmonary fibrosis (IPF)-lungs.

Representative immunohistochemistry for KRT5, α-SMA, HDAC5 and p63 in serial sections of IPF-lung tissue. In IPF, the antibody for HDAC5 revealed cytoplasmic staining of myofibroblasts in fibroblast foci [FF] (indicated by α-SMA-staining of serial sections) and in overlying hyperplastic bronchiolar basal cells (positive for KRT5 and p63).

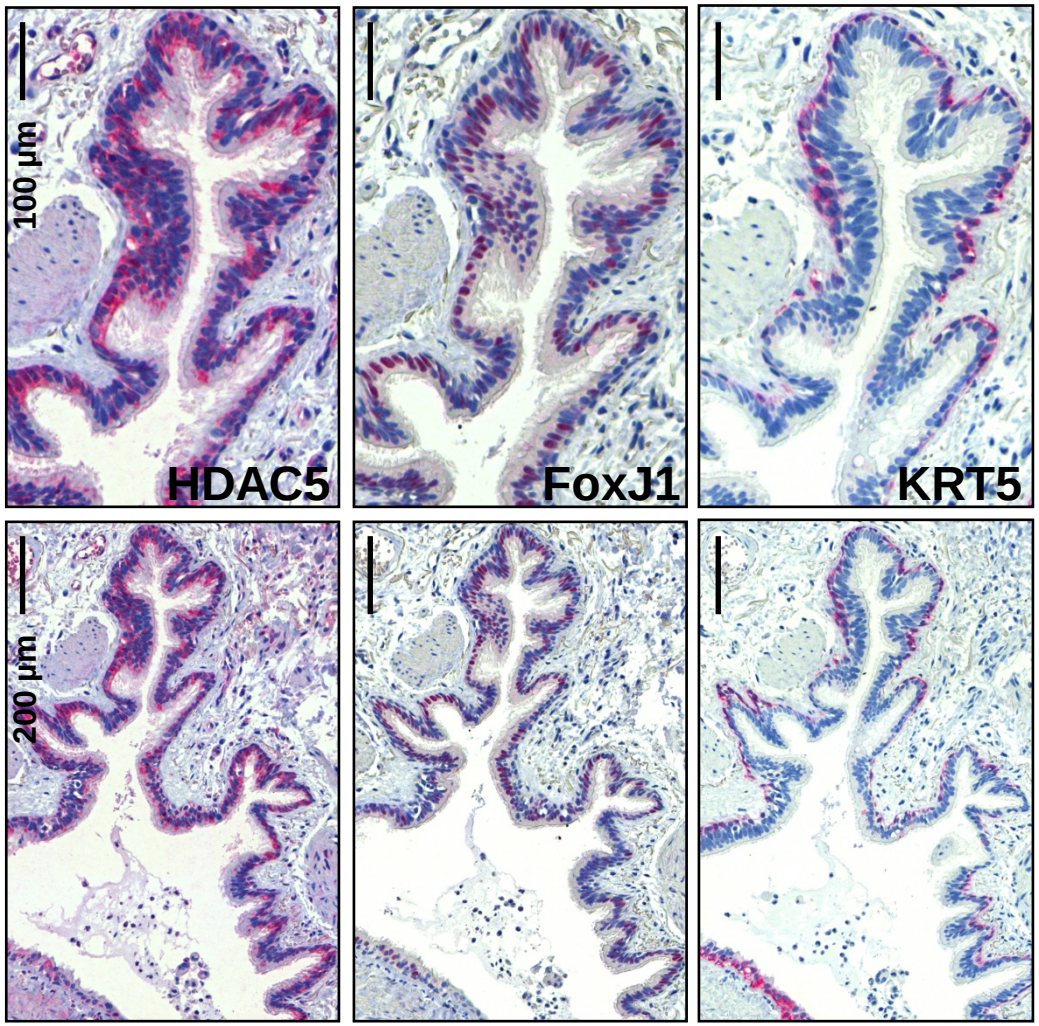

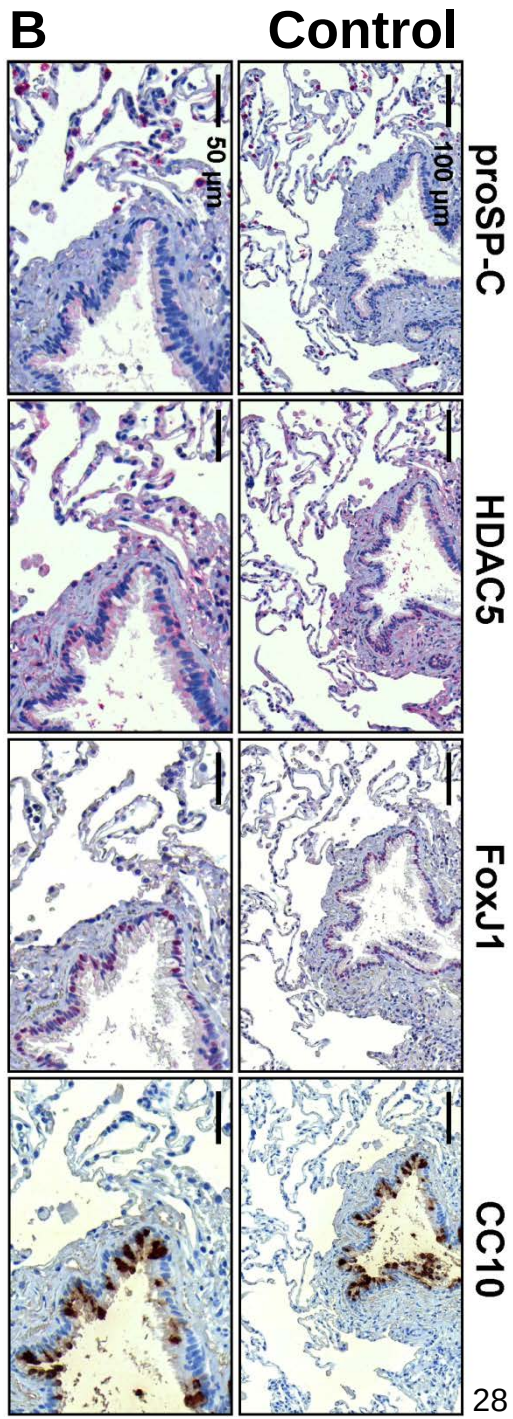

Supplementary-Figure S13: Induction and upregulation of class-IIa-histone deacetylase HDAC5 in ciliated bronchial epithelium of idiopathic pulmonary fibrosis (IPF)-lungs.

(**A**) Representative immunohistochemistry for HDAC5, FoxJ1 and KRT5 in serial sections of IPF-lung tissue. Strong cytoplasmic expression of HDAC5 was observed in ciliated bronchial cells (indicated by nuclear FoxJ1-staining) of abnormal bronchioles in IPF-lungs.

(**B**) Representative immunohistochemistry for proSP-C, HDAC5, FoxJ1 and CC10 in serial sections of control-lung tissue. Ciliated bronchial cells of normal bronchioles in control-lungs (indicated by nuclear FoxJ1-staining) revealed faint cytoplasmic expression of HDAC5. Type-II alveolar epithelial cells (indicated by proSP-C-staining) and Clara cells (positive for CC10) revealed no notable expression of HDAC5.

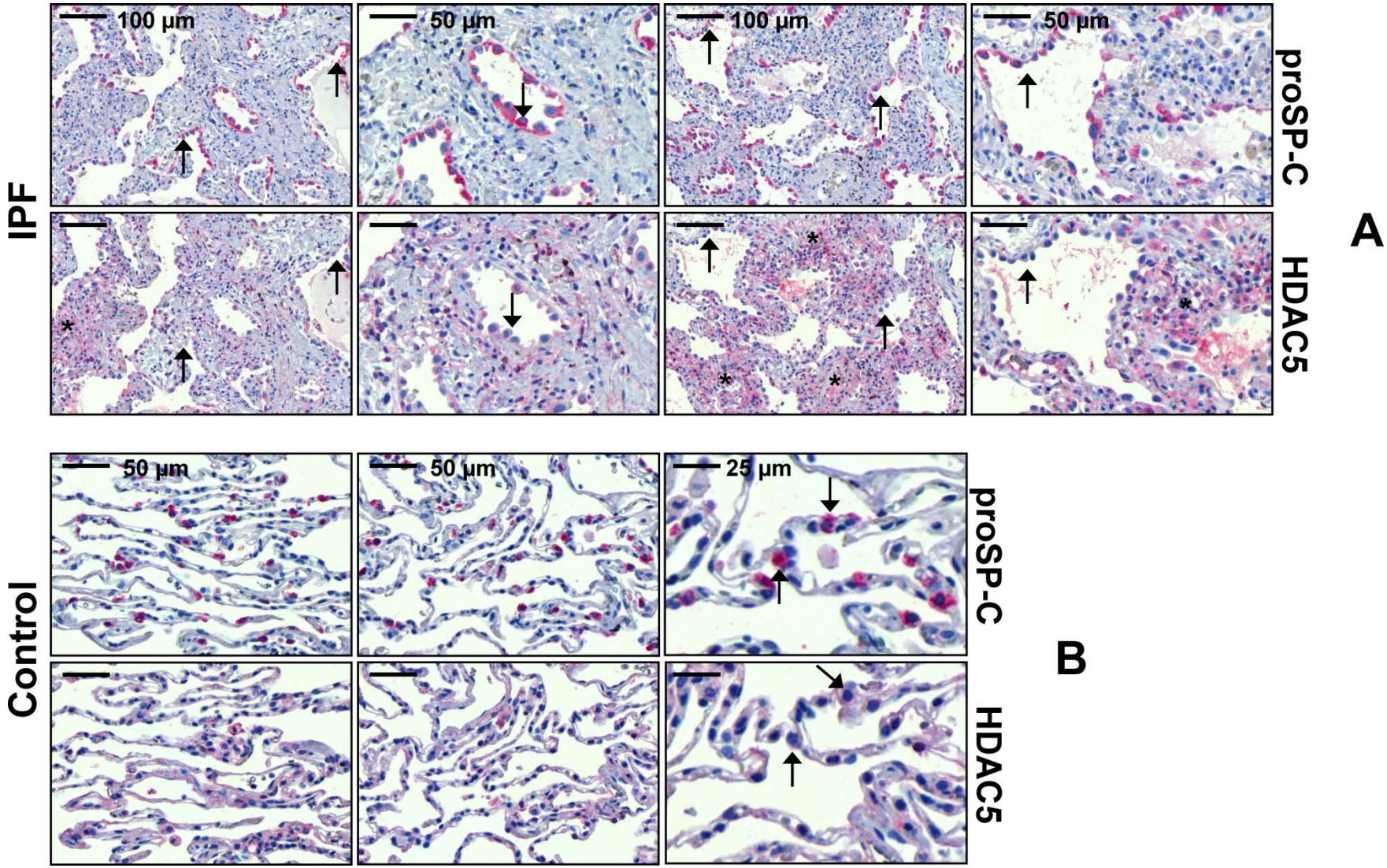

Supplementary-Figure S14: Class-IIa-histone deacetylase HDAC5 is not significantly expressed in type-II alveolar epithelial cells of idiopathic pulmonary fibrosis (IPF)- and control-lungs.

(**A**) Representative immunohistochemistry for proSP-C and HDAC5 in serial sections of IPF-lung tissue. Type-II alveolar epithelial cells (AECII) of IPF-lungs (indicated by arrows and proSP-C-staining) did not reveal a significant immunostaining for HDAC5. (**B**) Representative immunohistochemistry for proSP-C and HDAC5 in serial sections of control-lung tissue. AECII of normal lungs (indicated by arrows and proSP-C-staining) did not express HDAC5.

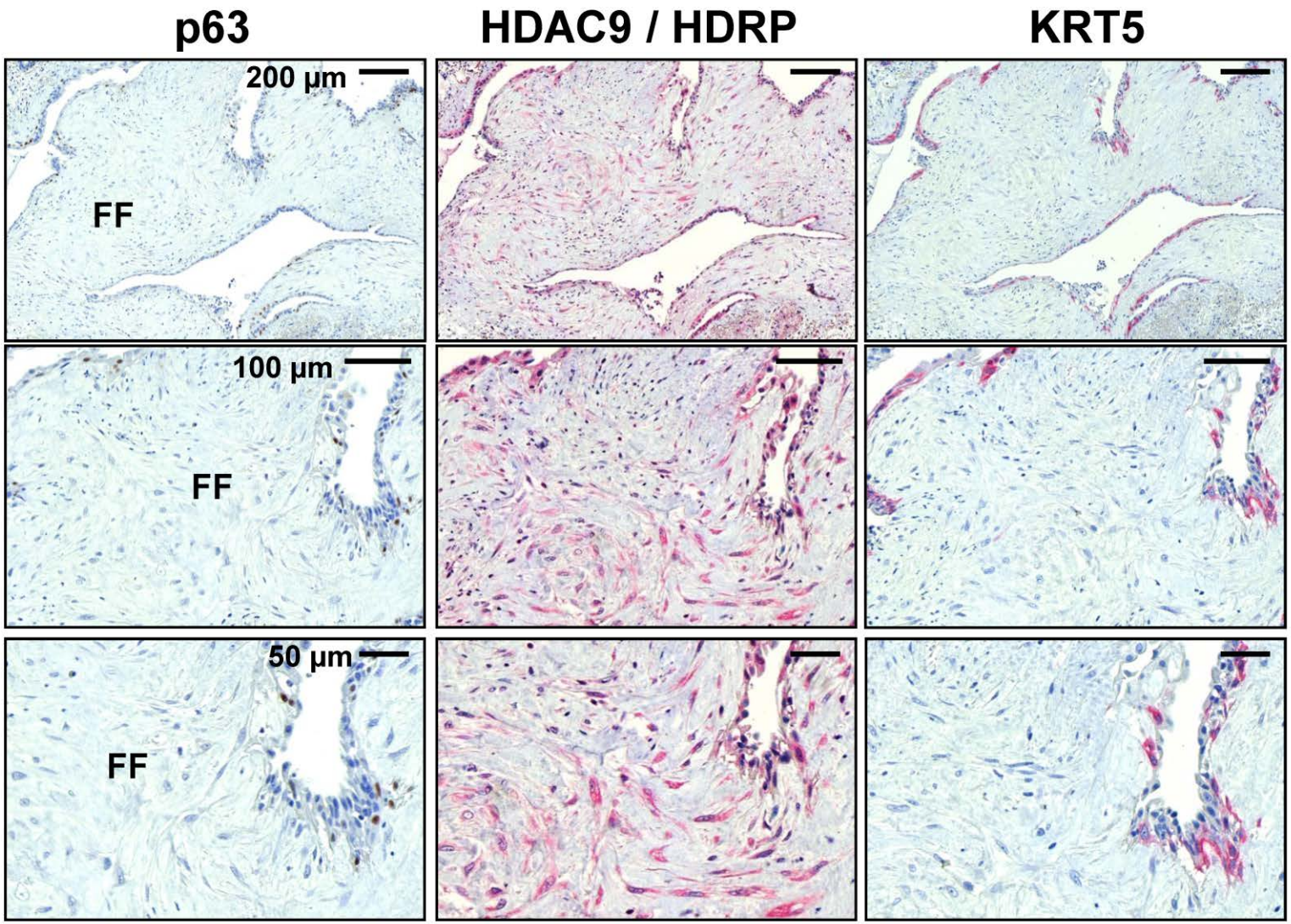

Supplementary-Figure S15: Expression of class-IIa-histone deacetylase HDAC9-isoform HDRP in fibroblast foci and abnormal bronchiolar epithelium of idiopathic pulmonary fibrosis (IPF) lungs.
Representative immunohistochemistry for p63, HDRP, and KRT5 in serial sections of IPF-lung tissue. In IPF, the antibody for HDRP revealed robust cytoplasmic staining of myofibroblasts in fibroblast foci [FF] and in overlying bronchiolar basal cells (indicated by KRT5- and p63-staining).

Korfei et al_Supplementary-Figure S16

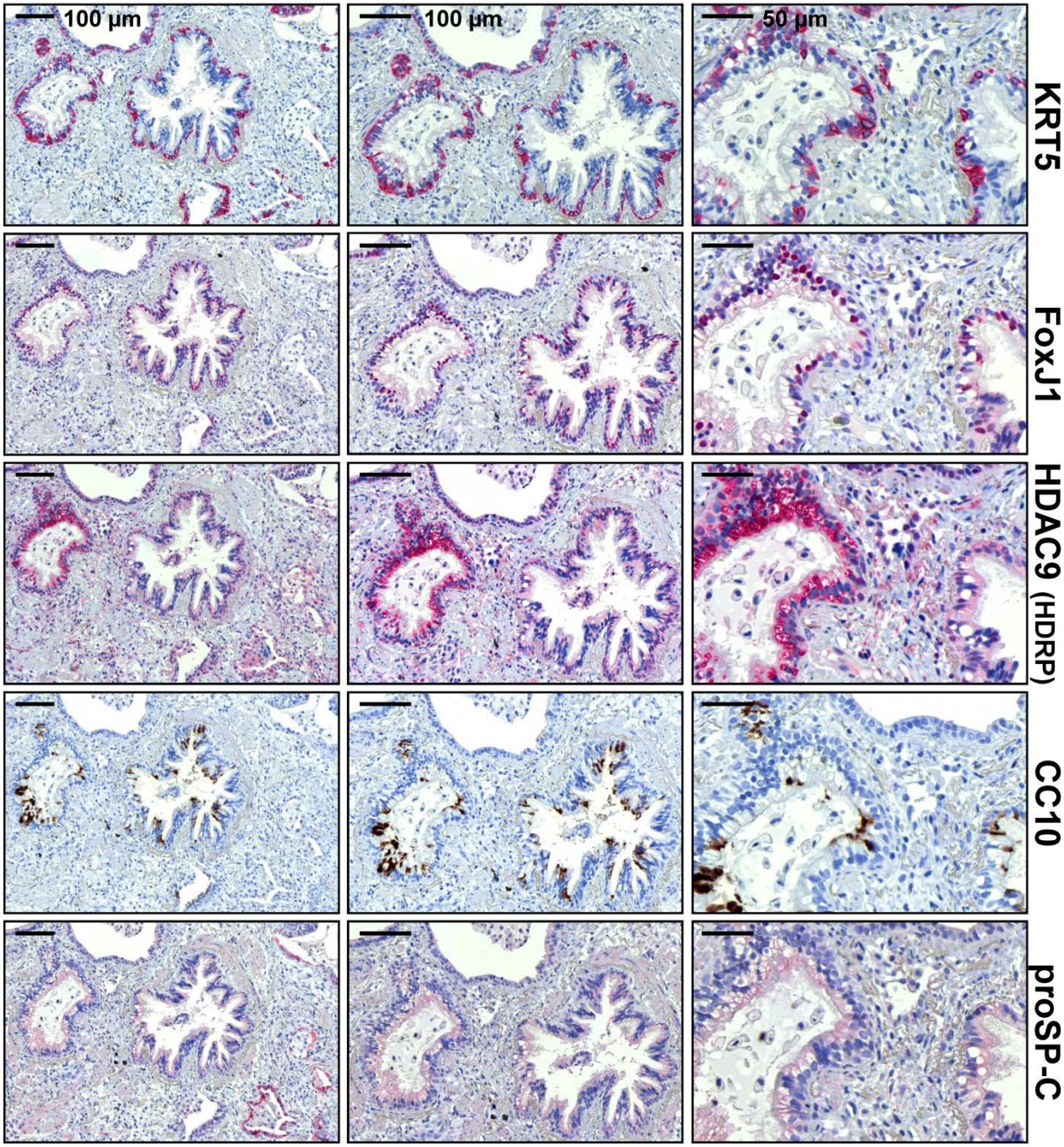

Supplementary-Figure S16: Induction of HDAC9-isoform HDRP in a particular subtyp of bronchial epithelial cells of idiopathic pulmonary fibrosis (IPF)-lungs.

Representative immunohistochemistry for KRT5, FoxJ1, HDRP, CC10 and proSP-C in serial sections of IPF-lung tissue. In IPF, the antibody for HDRP revealed robust cytoplasmic staining of a luminal bronchial cell type which was positive for FoxJ1, but not for CC10, and which could never be observed in normal control-lungs. It has to be noted, that not all FoxJ1-positive ciliated bronchial cells of IPF-lungs revealed significant expression of HDRP.

Korfei et al_Supplementary-Figure S17

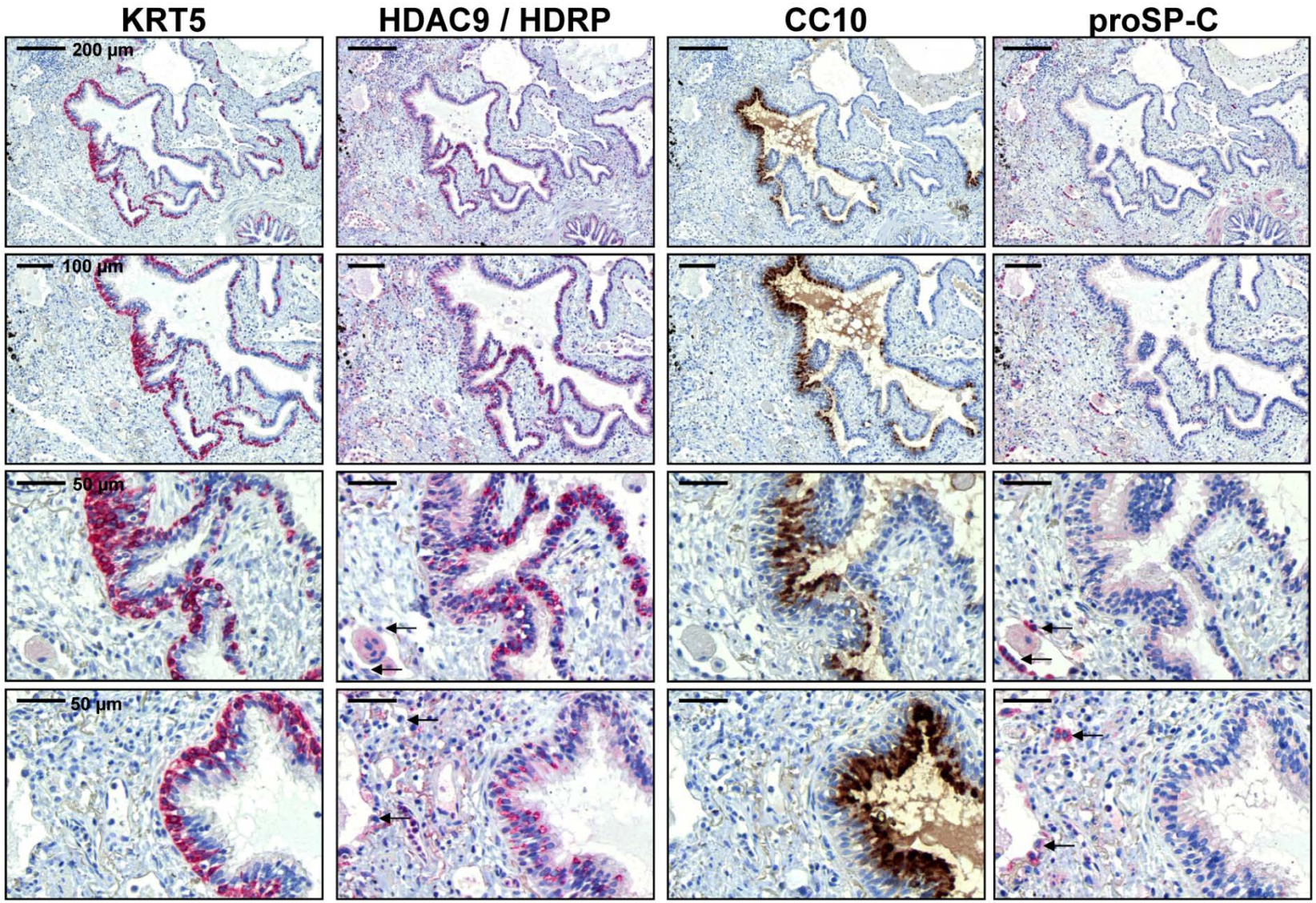

Supplementary-Figure S17: Expression and localization of HDAC9-isoform HDRP in a particular subtyp of bronchial epithelial cells of idiopathic pulmonary fibrosis (IPF)-lungs.

Representative immunohistochemistry for KRT5, HDRP, CC10 and proSP-C in serial sections of IPF-lung tissue. In IPF, the antibody for HDRP revealed robust cytoplasmic staining of a luminal bronchial cell type which could never be observed in normal control-lungs. Clara cells (positive for CC10) did not express HDRP, and also bronchiolar basal cells (positive for KRT5) of normal as well as abnormal bronchioles in IPF revealed no or only weak expression of HDRP. AECII in IPF-lungs (indicated by arrows and proSP-C-staining) showed no significant expression of HDRP.

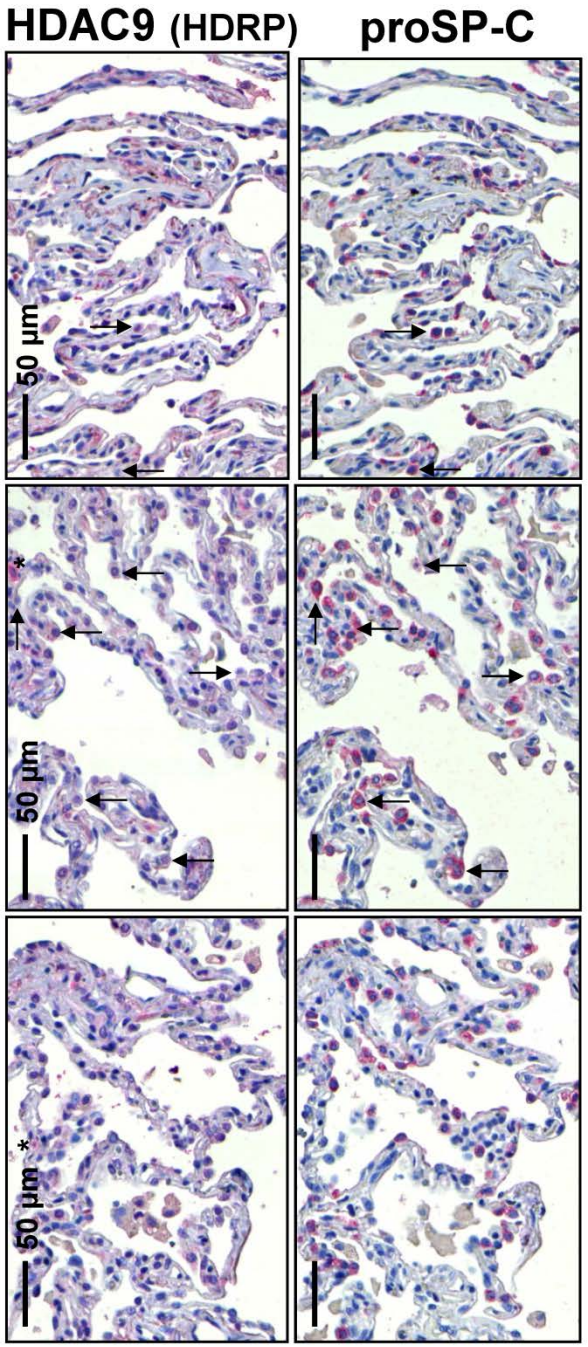

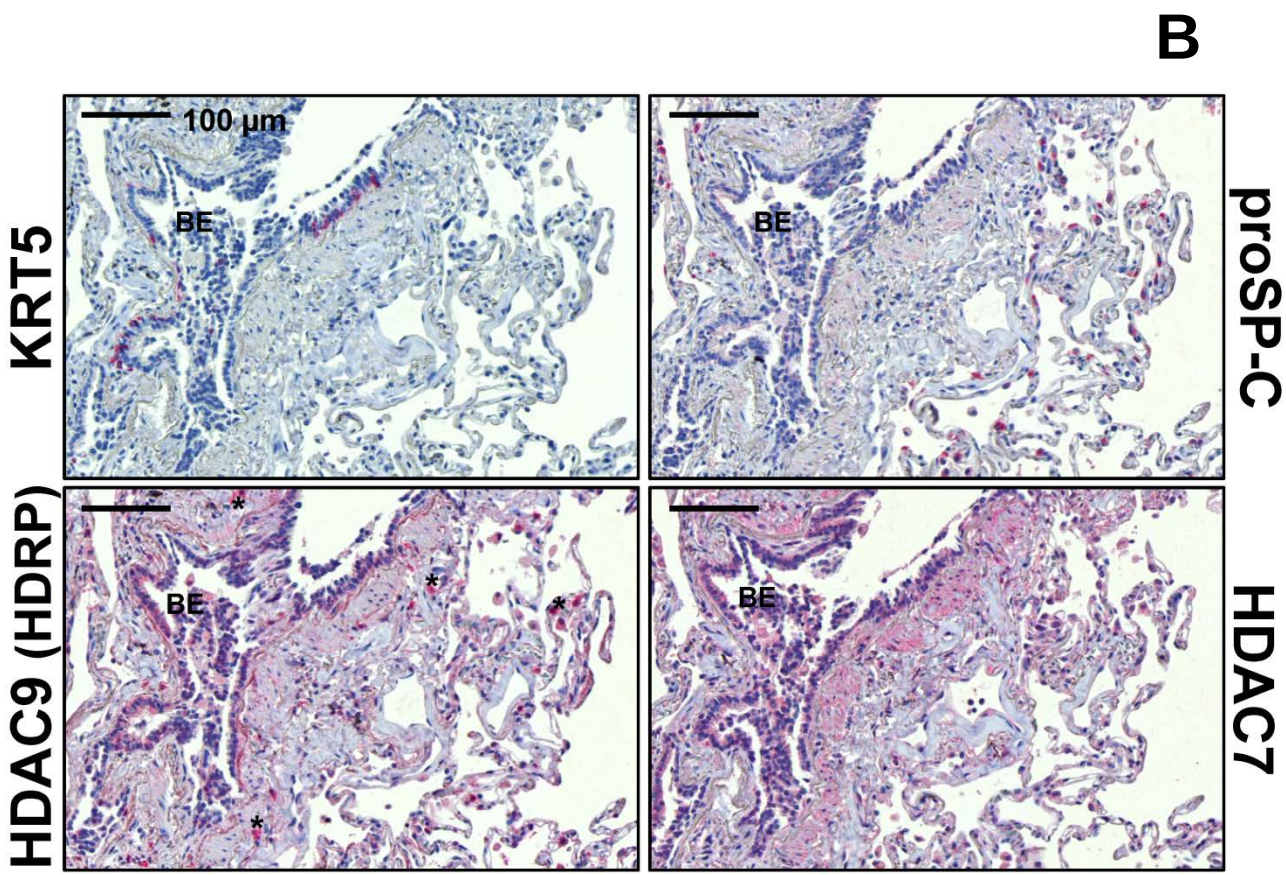

Supplementary-Figure S18: Expression and localization of HDAC9-isoform HDRP in control-lungs.

(**A**) Representative immunohistochemistry for HDRP and proSP-C in serial sections of control-lung tissue. AECII in normal lungs (indicated by arrows and proSP-C-staining) revealed no or only faint expression of HDAC9.

(**B**) Representative immunohistochemistry for KRT5, HDRP, proSP-C and HDAC7 in serial sections of control-lung tissue. HDRP was weakly expressed in bronchial epithelium (BE) of normal control-lungs. Interstitial inflammatory cells (indicated by asterisks) revealed strong HDRP expression.

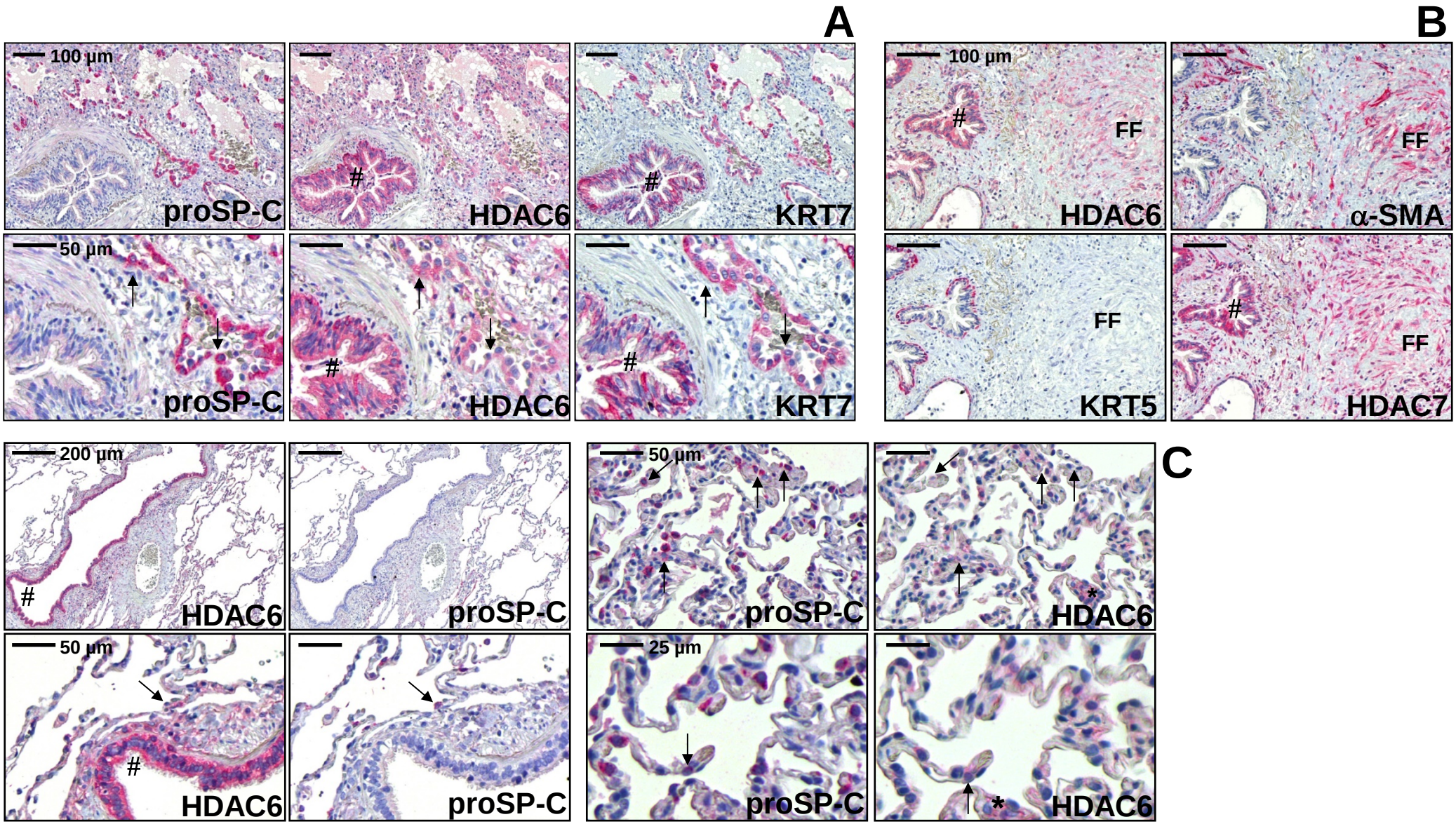

Legend to Supplementary-Figure S19: see next page

Legend to Supplementary-Figure S19: Expression and localization of Class-IIb-histone deacetylase HDAC6 in idiopathic pulmonary fibrosis (IPF) - and non-diseased control-lungs.

(**A**) Representative immunohistochemistry for proSP-C, HDAC6, and cytokeratin-7 (KRT7) in serial sections of IPF-lung tissue. In IPF, robust expression of HDAC6 was observed in type-II alveolar epithelial cells (AECII) surrounded by fibrotic tissue (indicated by arrows and proSP-C-staining); and a very strong staining for HDAC6 was observed in ciliated bronchial epithelial cells (indicated by hashmarks and KRT7-staining).

(**B**) Representative immunohistochemistry for HDAC6, α-SMA, KRT5 and HDAC7 in serial sections of IPF-lung tissue. In IPF, myofibroblasts of fibroblast foci (FF, indicated by α-SMA-staining) revealed moderate expression of HDAC6, in comparison to the very strong HDAC7 expression in FF.

(**C**) Representative immunohistochemistry for HDAC6 and proSP-C in serial sections of control-lung tissue. In control-lungs, no or weak expression of HDAC6 was observed in AECII (indicated by arrows and proSP-C-staining), whereas the ciliated bronchial epithelium (indicated by hashmarks) revealed very strong HDAC6 expression. Basal expression of HDAC6 was also observed in the interstitium of normal lungs (indicated by asterisks).

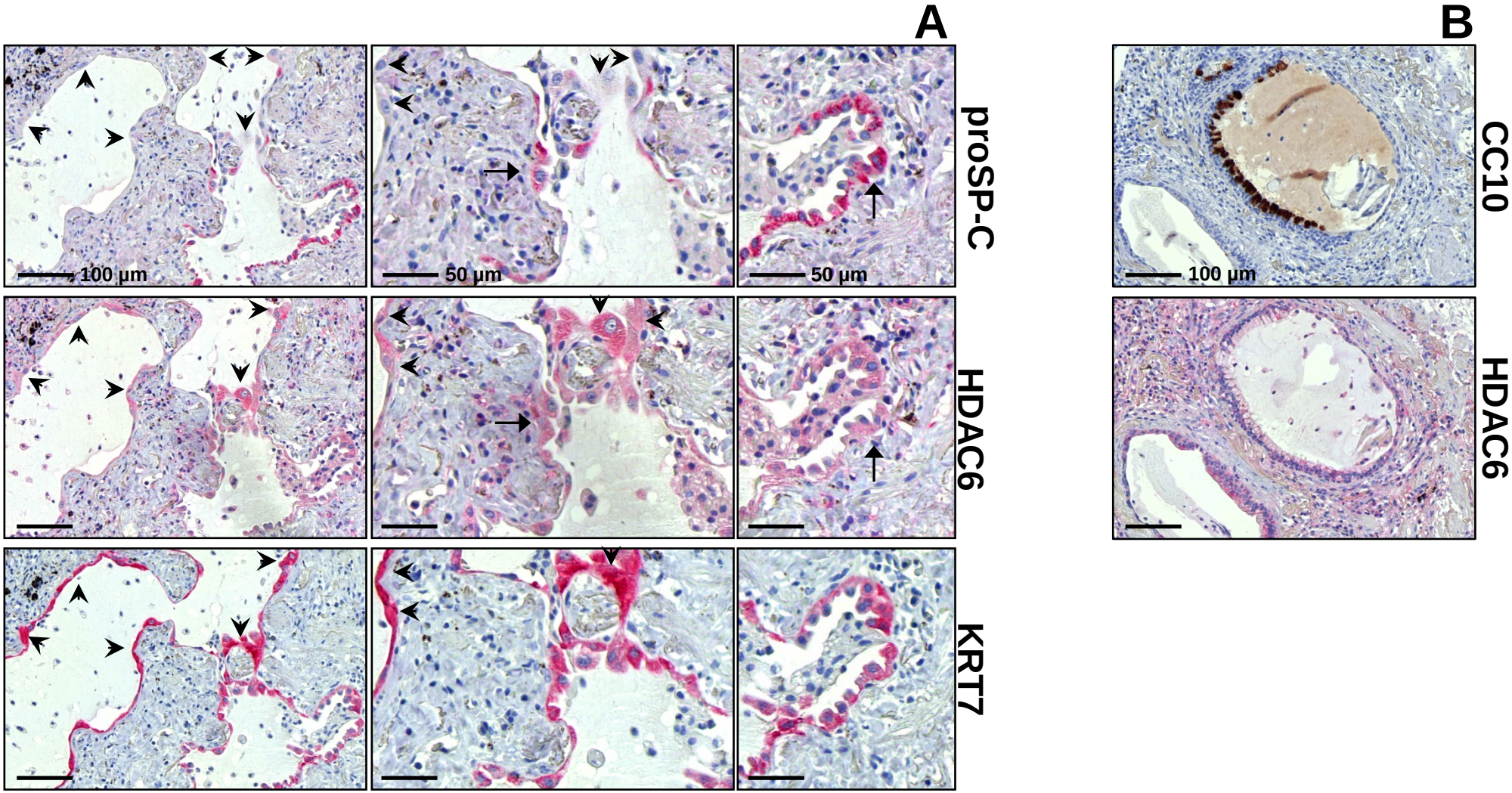

Supplementary-Figure S20: Expression and localization of class-IIb-histone deacetylase HDAC6 in idiopathic pulmonary fibrosis (IPF) lungs.

(**A**) Representative immunohistochemistry for proSP-C, HDAC6, and KRT7 in serial sections of IPF-lung tissue. In IPF, HDAC6 was expressed in the cytoplasm of AECII (indicated by arrows and proSP-C-staining), and in AECII-like cells without proSP-C expression or representing possibly type-I alveolar epithelial cells (indicated by arrowheads and KRT7-staining for indication of simple epithelia).

(**B**) Representative immunohistochemistry for CC10 and HDAC6 in serial sections of IPF-lung tissue. Clara cells (positive for CC10) in IPF- as well as control-lungs did not express HDAC6.

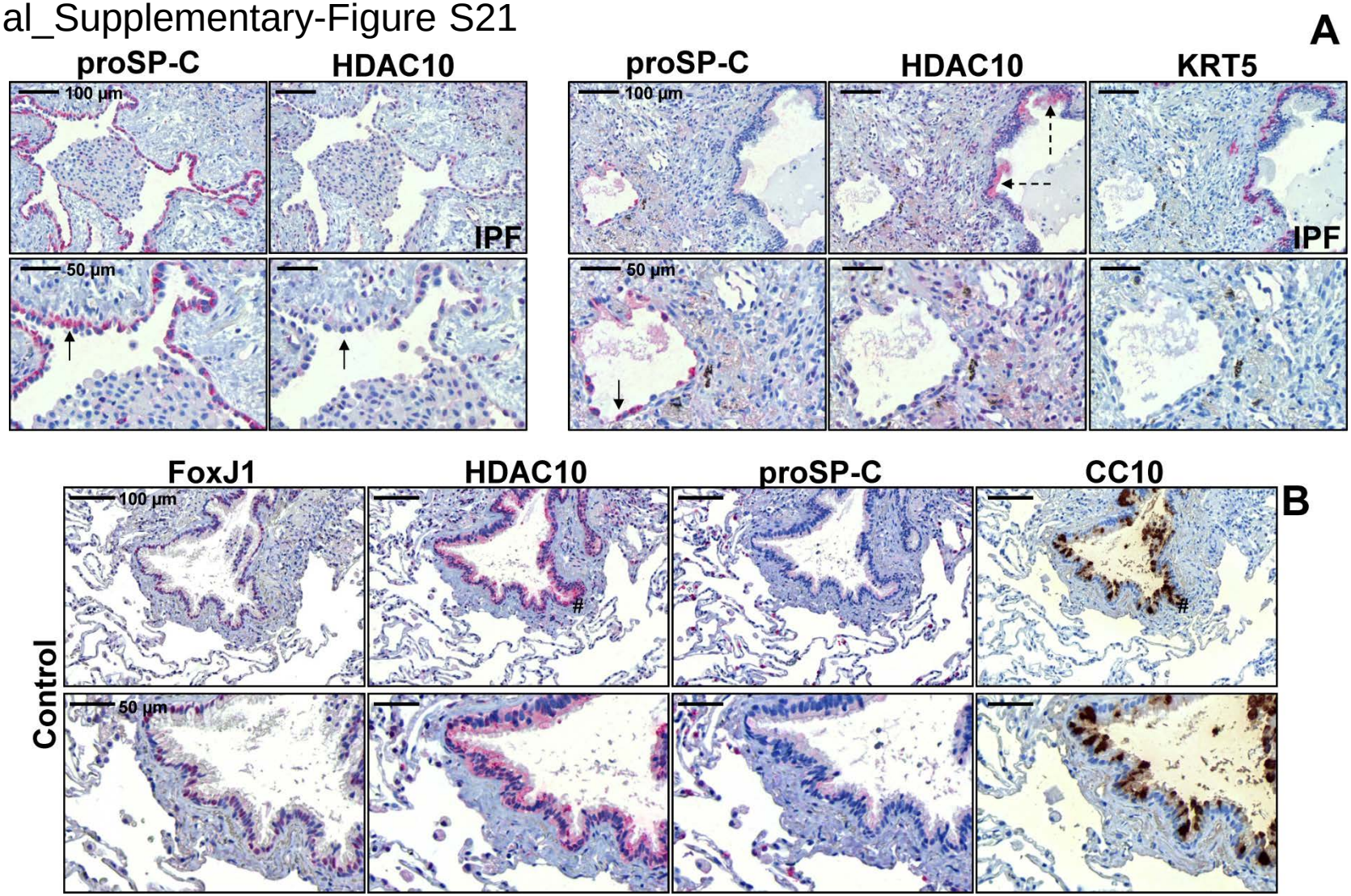

Supplementary-Figure S21: Expression and localization of class-IIb-histone deacetylase HDAC10 in idiopathic pulmonary fibrosis (IPF)- and control-lungs.

(**A**) Representative immunohistochemistry for proSP-C, HDAC10, and KRT5 in serial sections of IPF-lung tissue. AECII in IPF-lungs (indicated by arrows and proSP-C-staining) did not express HDAC10. Instead of that, Clara cells (indicated by dashed arrows) revealed robust cytoplasmic expression of HDAC10. Ciliated bronchial cells indicated weak cytoplasmic HDAC10 expression. (**B**) Representative immunohistochemistry for FoxJ1, HDAC10, proSP-C, and CC10 in serial sections of control-lung tissue. In normal control-lungs, HDAC10 was robustly expressed in non-ciliated Clara cells (indicated by hashmarks and CC10-staining); ciliated bronchial cells (positive for FoxJ1) indicated a weak-to-moderate expression of HDAC10. AECII in control-lungs (indicated by proSP-C-staining) did not indicate a significant HDAC10 expression.

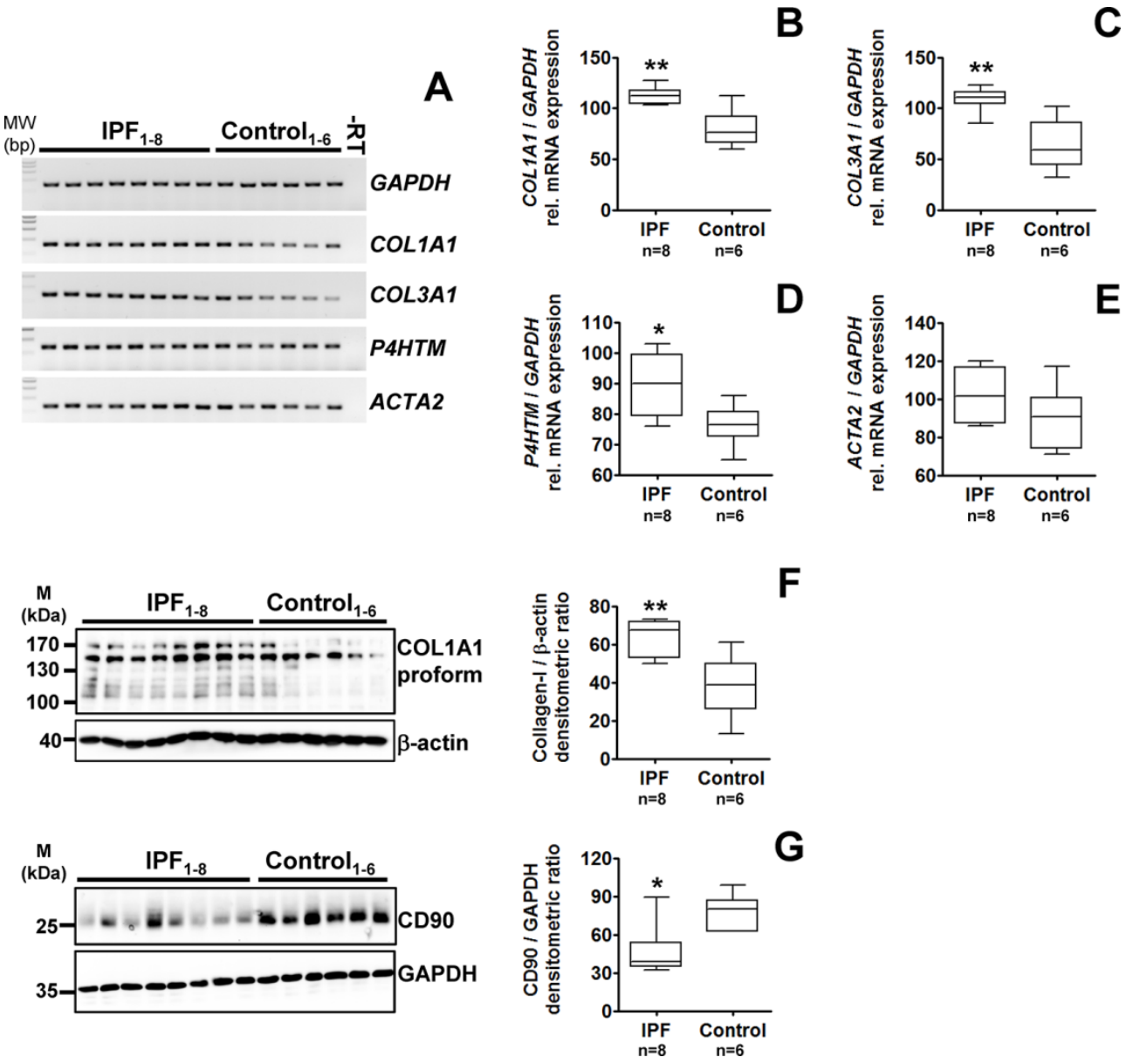

Supplementary-Figure S22: Expression analysis of extracellular matrix (ECM) associated genes in primary fibroblasts isolated from idiopathic pulmonary fibrosis (IPF) - and non-diseased control-lungs.

(**A**-**E**) Representative agarose gels (**A**) and densitometric quantification of reverse transcription-polymerase chain reactions for *COL1A1* (**B**), *COL3A1* (**C**), *P4HTM* (**D**), and *ACTA2* (**E**) of human fibroblasts isolated from peripheral explanted lung tissue of patients with IPF (n=8) and non-diseased control-lungs (control, n=6). Each PCR reaction was performed with 100 ng reverse-transcribed complementary DNA, and *GAPDH* was used as reference gene. -RT control = PCR of a RNA sample without reverse transcriptase. *p<0.05, **p<0.01.

(**F**, **G**) Representative immunoblots and quantitative immunoblot analysis of human fibroblasts isolated from peripheral explanted lung tissue of patients with sporadic IPF (n=8) and non-diseased control-lungs (control, n=6) for COL1A1 (Collagen-I, **F**) and CD90 (**G**), and β-actin or GAPDH as loading control. *p<0.05, **p<0.01.

Densitometric ratios of the respective gene to *GAPDH*, as well as of the respective protein to β-actin or GAPDH are depicted as a box-and whisker diagram (*box* indicates 25th and 75th, *horizontal line* indicates the 50th percentile [median], and extensions above and below reflect extreme values); statistics were performed by Mann Whitney-test.

Korfei et al_Supplementary-Figure S23

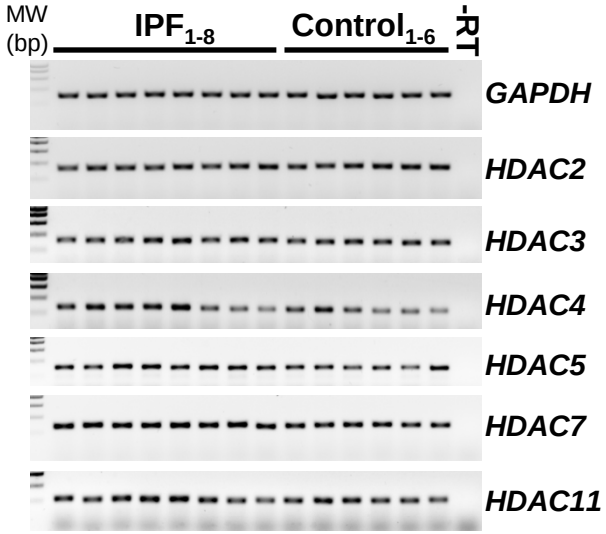

Supplementary-Figure S23: Expression analysis of histone deacetylases in primary fibroblasts isolated from idiopathic pulmonary fibrosis (IPF) - and non-diseased control-lungs (supplemental data to figure 3 of the main manuscript).
Representative agarose gels of reverse transcription-polymerase chain reactions for *HDAC2*, *HDAC3*, *HDAC4*, *HDAC5*, *HDAC7*, and *HDAC11* of human fibroblasts isolated from peripheral explanted lung tissue of patients with IPF (n=8) and non-diseased control-lungs (control, n=6). Each PCR reaction was performed with 100 ng reverse-transcribed complementary DNA, and *GAPDH* was used as reference gene. -RT control = PCR of a RNA sample without reverse transcriptase.

Korfei et al_Supplementary-Figure S24

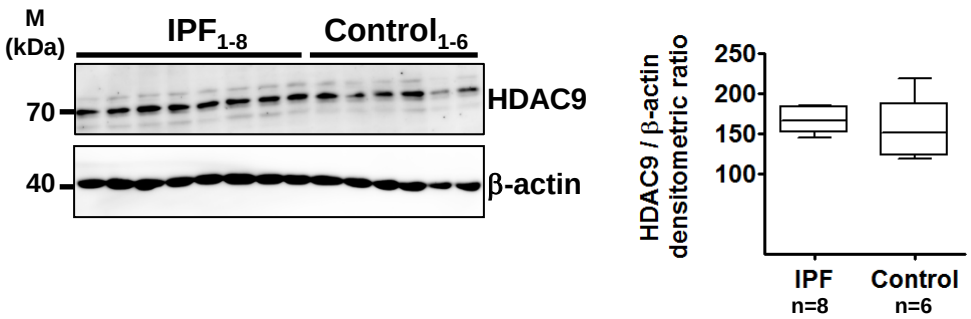

Supplementary-Figure S24: Protein expression analysis of histone deacetylase 9 (HDAC9) in primary fibroblasts isolated from idiopathic pulmonary fibrosis (IPF) - and non-diseased control-lungs.
Representative immunoblot and quantitative immunoblot analysis of human fibroblasts isolated from subpleural lung tissue of patients with sporadic IPF (n=8) and non-diseased control-lungs (control, n=6) for HDAC9, by using β-actin as loading control. No significant difference in HDAC9 protein expression was observed between IPF- and control fibroblasts.
The densitometric ratio of the HDAC9 protein to β-actin is depicted as a box-and whisker diagram (*box* indicates 25th and 75th, *horizontal line* indicates the 50th percentile [median], and extensions above and below reflect extreme values).

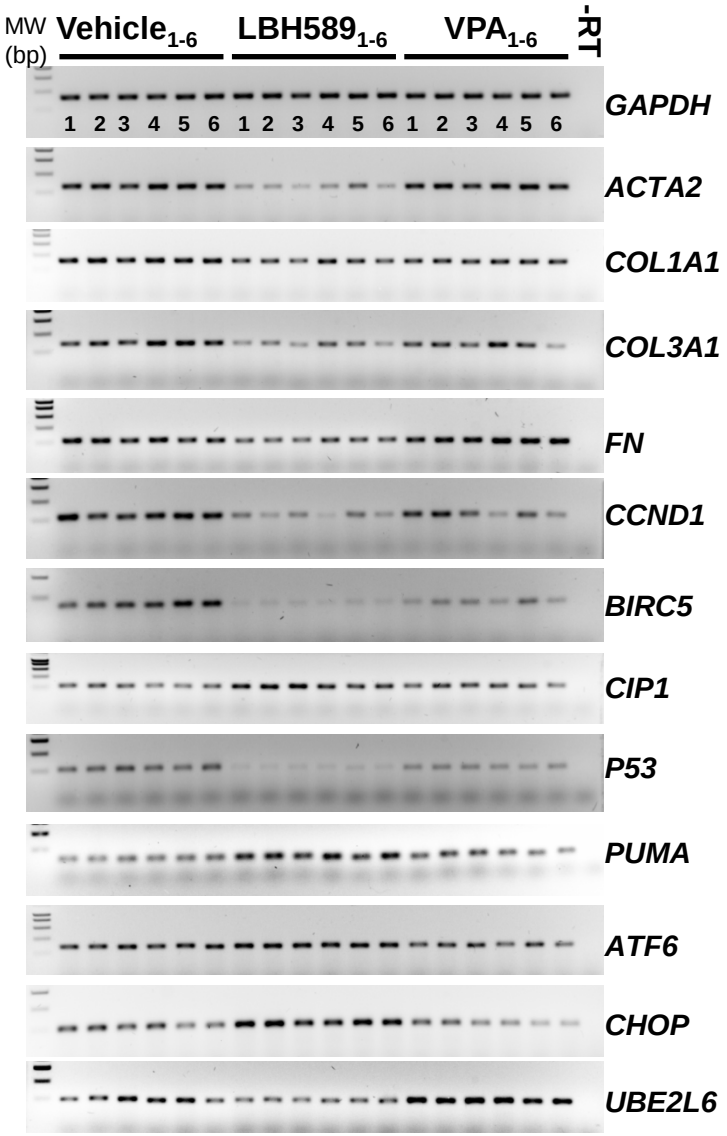

Supplementary-Figure S25: Cellular signalling in primary IPF-fibroblasts in response to treatment with panobinostat or valproic acid (supplemental data to figure 4 of the main manuscript).
Primary IPF-fibroblasts (n=6) were incubated for 30h with vehicle (0.03% DMSO, 0.1% ethanole), panobinostat (LBH589, 85 nmol) or valproic acid (VPA, 1.5 mM). The effects of vehicle - and histone deacetylase inhibitor treatments were analyzed by semiquantitative reverse transcription-polymerase chain reaction (RT-PCR) for indicated genes, and is depicted by representative agarose gels of RT-PCR products for *ACTA2*, *COL1A1*, *COL3A1*, *FN*, *CCND1*, *BIRC5*, *CIP1*, *P53*, *PUMA*, *ATF6*, *CHOP* and *UBE2L6*. Each PCR reaction was performed with 100 ng reverse-transcribed complementary DNA, and *GAPDH* was used as reference gene. -RT control = PCR of a RNA sample without reverse transcriptase.

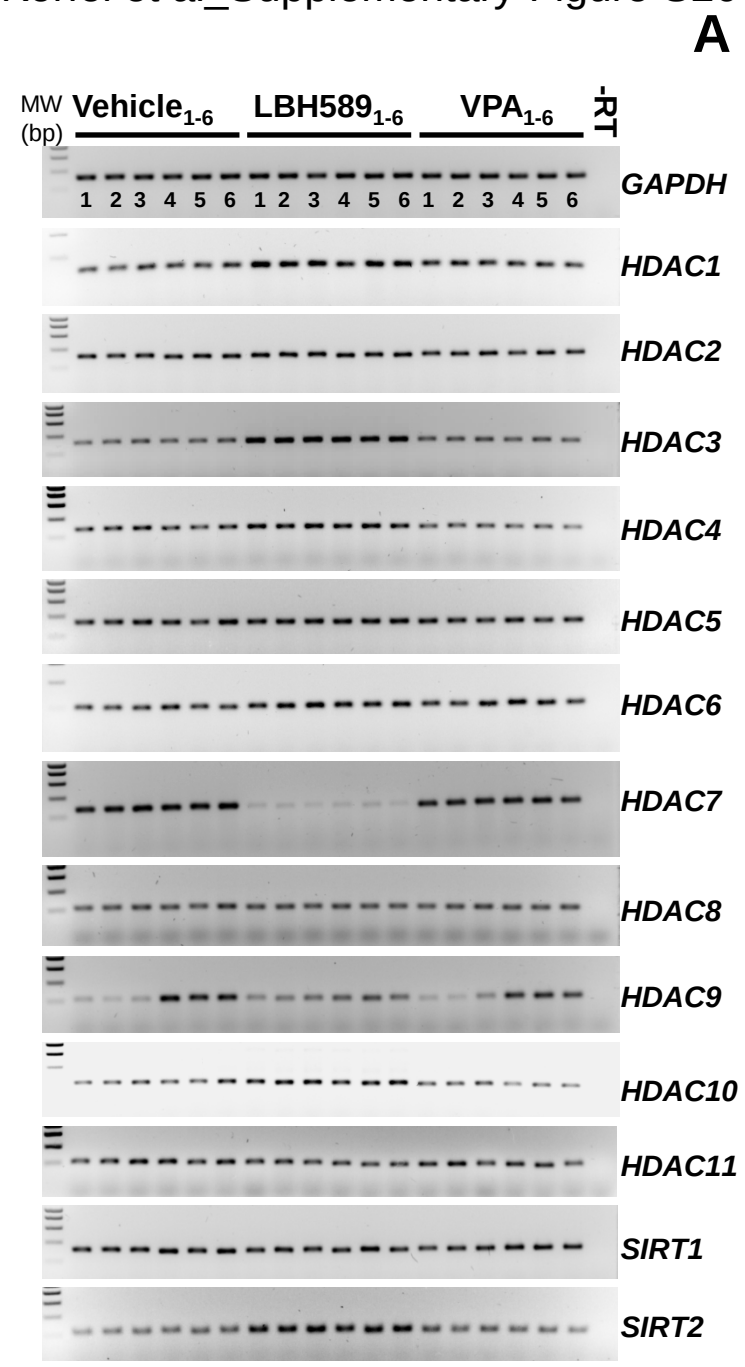

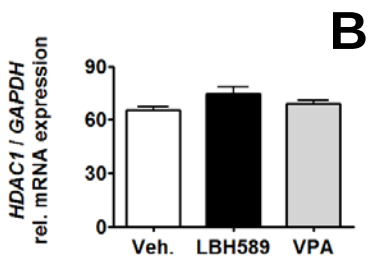

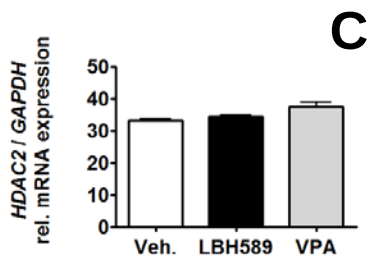

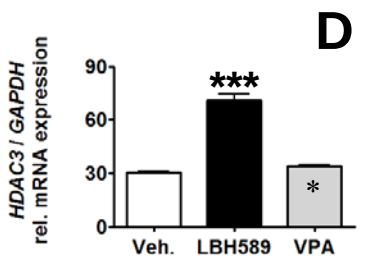

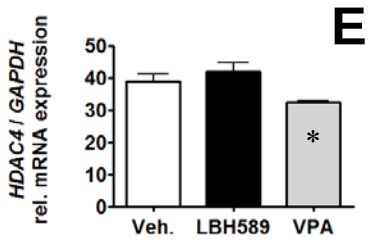

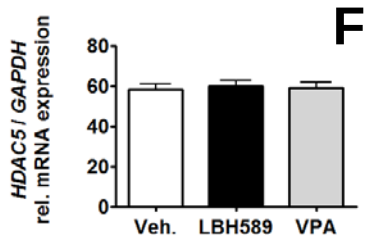

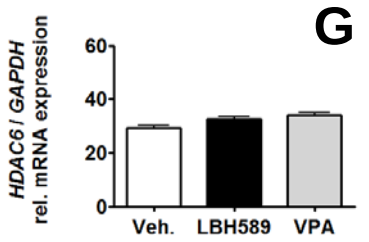

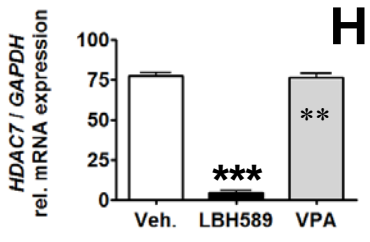

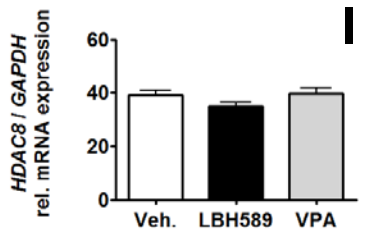

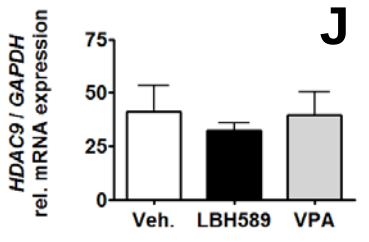

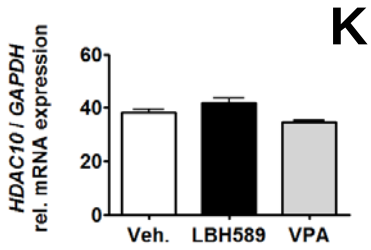

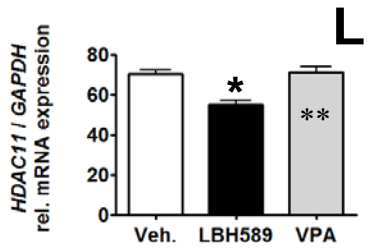

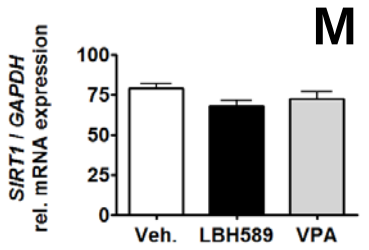

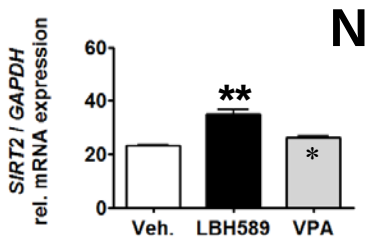

Legend to Supplementary-Figure S26: see next page

Legend to Supplementary-Figure S26: Effects of histone deacetylase inhibitor treatment on histone deacetylase gene expression in primary IPF-fibroblasts.
Primary IPF-fibroblasts (n=6) were incubated for 30h with vehicle (0.03% DMSO, 0.1% ethanole), panobinostat (LBH589, 85 nmol) or valproic acid (VPA, 1.5 mM). Gene expression of histone deacetylases (HDAC) was analyzed by semiquantitative reverse transcription-polymerase chain reaction (RT-PCR), and is depicted by representative agarose gels (**A**) and densitometric quantification of RT-PCR products for *HDAC1* (**B**), *HDAC2* (**C**), *HDAC3* (**D**), *HDAC4* (**E**), *HDAC5* (**F**), *HDAC6* (**G**), *HDAC7* (**H**), *HDAC8* (**I**), *HDAC9* (**J**), *HDAC10* (**K**), *HDAC11* (**L**), *SIRT1* (**M**), and *SIRT2* (**N**). Each PCR reaction was performed with 100 ng reverse-transcribed complementary DNA, and *GAPDH* was used as reference gene. Data are presented as mean ± SEM of the individual values of different treatments. -RT control = PCR of a RNA sample without reverse transcriptase. *p<0.05, **p<0.01, ***p<0.001, LBH589 vs. vehicle; ∗p<0.05, ∗∗p<0.01 VPA vs. LBH589; by Dunn´s multiple comparison test.

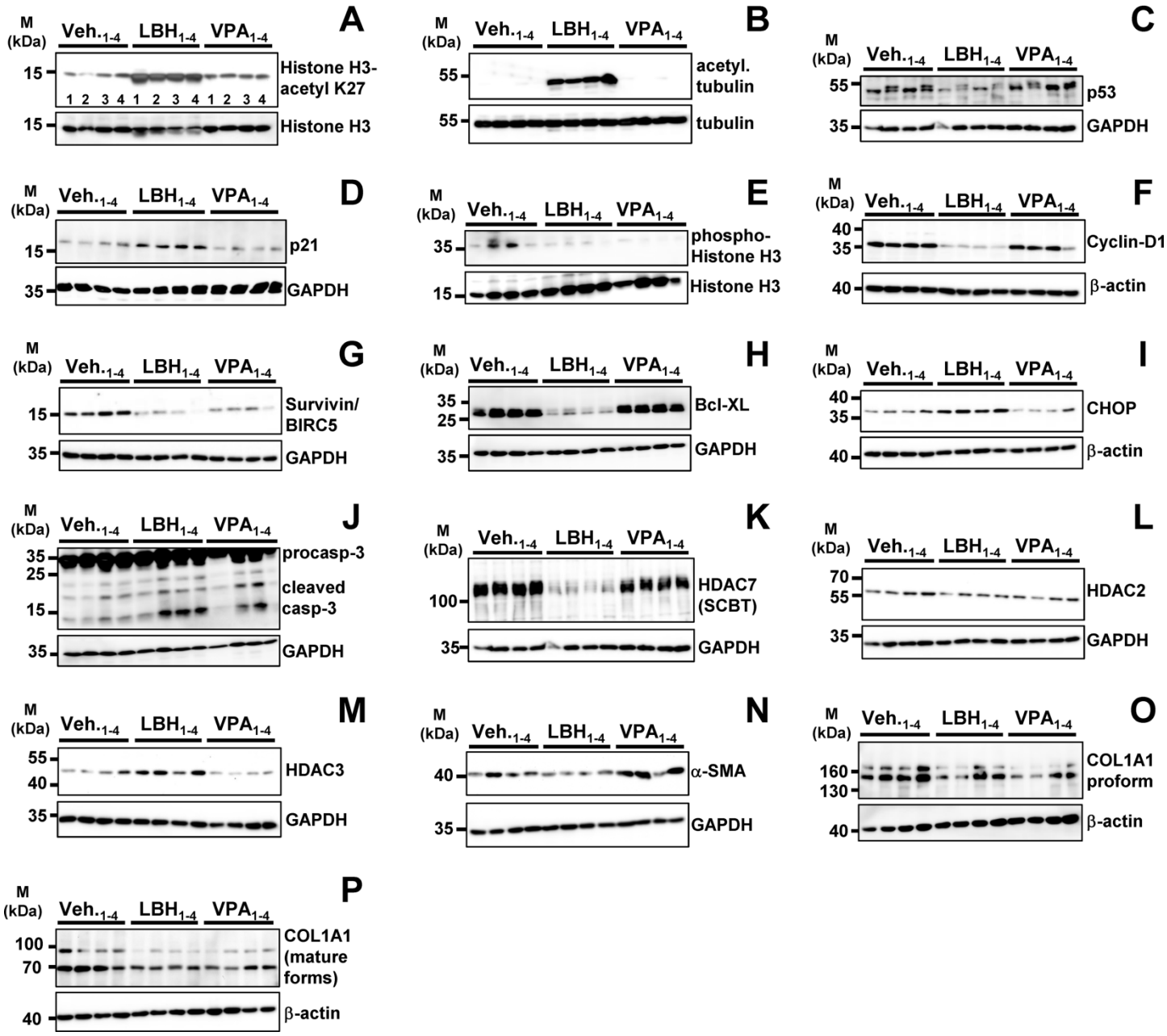

Supplementary-Figure S27: Analysis of acetylation status, apoptotic signalling, and profibrotic protein expression in primary IPF-fibroblasts in response to treatment with panobinostat or valproic acid (supplemental data to figure 5 of the main manuscript).

Primary IPF-fibroblasts (n=4) were incubated for 30h with vehicle (0.03% DMSO, 0.1% ethanole), panobinostat (LBH589, 85 nmol) or valproic acid (VPA, 1.5 mM). Status of acetylation, apoptosis, HDAC protein expression, and profibrotic protein expression was analyzed by quantitative immuno-blotting. In dependency of research target, histone H3, GAPDH, β-actin, or tubulin served as loading control. (**A**) Histone H3-acetyl K27, (**B**) acetylated tubulin, (**C**) p53, (**D**) p21, (**E**) phospho-histone H3, (**F**) Cyclin D1, (**G**) Survivin, (**H**) Bcl-Xl, (**I**) CHOP, (**J**) caspase-3, (**K**) HDAC7 (antibody from Santa Cruz B. I.), (**L**) HDAC2, (**M**) HDAC3, (**N**) α-SMA, (**O**) COL1A1 (pro-form), and (**P**) COL1A1 (mature form).

Korfei et al_Supplementary-Figure S28

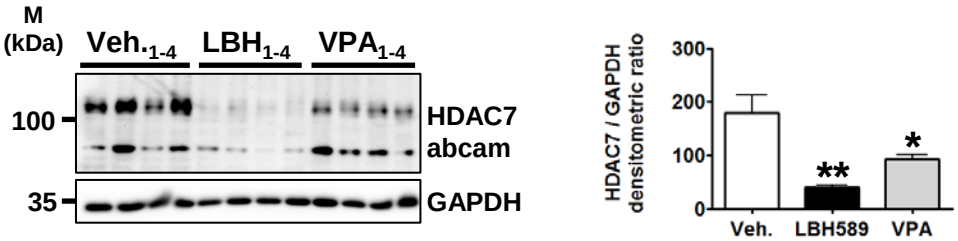

Supplementary-Figure S28: Analysis of HDAC7-protein expression in primary IPF-fibroblasts in response to treatment with panobinostat or valproic acid by immunoblotting with use of a specific antibody directed against human HDAC7 from Abcam (ab137366).

Primary IPF-fibroblasts (n=4) were incubated for 30h with vehicle (0.03% DMSO, 0.1% ethanole), panobinostat (LBH589, 85 nmol) or valproic acid (VPA, 1.5 mM), followed by lysis of fibroblastic cells and quantitative immunoblot-analysis for HDAC7.

Data are presented as mean ± SEM of the individual values of different treatments. *p<0.05, **p<0.01, LBH589 or VPA vs. vehicle; by Dunn´s multiple comparison test.